Supplementary Information for:

Control of triplet state generation in heavy atom-free BODIPY-anthracene dyads by media polarity and structural factors

Mikhail A. Filatov,[a*] Safakath Karuthedath,[b] Pavel M. Polestshuk,[c] Susan Callaghan,[a] Keith J. Flanaghan,[a] Maxime Telitchko,[a] Thomas Wiesner,[a] Frédéric Laquai[b] and Mathias O. Senge[a*]

[a] School of Chemistry, SFI Tetrapyrrole Laboratory, Trinity Biomedical Sciences Institute, 152-160 Pearse Street, Trinity College Dublin, The University of Dublin, Dublin 2, Ireland

[b] King Abdullah University of Science and Technology (KAUST), KAUST Solar Center (KSC), Physical Sciences and Engineering Division (PSE), Material Science and Engineering Program (MSE), Thuwal 23955-6900, Kingdom of Saudi Arabia

[c] Department of Chemistry, M.V. Lomonosov Moscow State University, Leninskie Gory, 1/3 Moscow 119991, Russia

Content: Page

A. General Procedures

The handling of all air/water sensitive materials was carried out using standard high vacuum techniques. Dried toluene, DCM and THF was obtained by passing through alumina under N_2 in the solvent purification systems and then further dried over activated molecular sieves. Dry DMF was purchased from Aldrich. Unless specified otherwise all other solvents were used as commercially supplied. Where mixtures of solvents were used, ratios are reported by volume. Analytical thin layer chromatography was performed using silica gel 60 (fluorescence indicator F254, pre-coated sheets, 0.2 mm thick, 20 cm × 20 cm; Merck) plates and visualized by UV irradiation (λ = 254 nm). Column chromatography was carried out using Fluka Silica Gel 60 (230–400 mesh).

UV-Vis spectra were recorded in solutions using a Specord 250 spectrophotometer from Analytic Jena (1 cm path length quartz cell). Emission, excitation spectra and lifetimes were measured using a Cary Eclipse G9800A fluorescence spectrophotometer and Horiba Jobin Yvon Fluorolog 4 instruments. Emission quantum yields of the compounds were measured relative to the fluorescence of fluorescein in 0.1 M NaOH (φ_f = 0.95).[1] Sample concentrations were chosen to obtain an absorbance of 0.03-0.07, at least three measurements were performed for each sample.

For TRPL experiments samples were excited with the wavelength-tunable output of an OPO (Radiantis Inspire HF-100), pumped by the fundamental of a Ti:Sa fs-oscillator (Spectra Physics MaiTai eHP) at 820 nm. The repetition rate of the fs pulses was adjusted by a pulse picker (APE Pulse Select). Typical pulse energies were in the range of several nanojoules (nJ). The samples in 1 mm quartz cuvettes (Hellma Analytics) were excited at 370 nm under nitrogen atmosphere. The PL of the samples was collected by an optical telescope (consisting of two plano-convex lenses) and focused on the slit of a spectrograph (PI Spectra Pro SP2300) and detected with a Streak Camera (Hamamatsu C10910) system with a temporal resolution of 1.4 ps. The data was acquired in photon counting mode using the Streak Camera software (HPDTA) and exported to Origin Pro 2015 for further analysis.

The singlet oxygen quantum yield measurements were performed according to previously described procedure.[2] Solutions of the $^1O_2$ trap, 1,3-diphenylisobenzofuran (DPBF), with an optical density of 1.0 in air-saturated ethanol and hexane were employed. Corresponding BAD was added to the cuvette, and its absorbance was adjusted to around 0.01 at wavelength of irradiation. The solutions in the cuvette were irradiated with 532 nm laser light at the same power density of 10 $mWcm^{-2}$. The absorption spectra of the solutions were measured every 15 s. The slope of plots of absorbance of DPBF at 414 nm *vs.* irradiation time for each photosensitizer was calculated.

NMR spectra were recorded on a Bruker Advance III 400 MHz, a Bruker DPX400 400 MHz or an Agilent 400 spectrometer. Accurate mass measurements (HRMS) were carried out using a Bruker microTOF-Q™ ESI-TOF mass spectrometer. Mass spectrometry was performed with a Q-Tof Premier Waters MALDI quadrupole time-of-flight (Q-TOF) mass spectrometer equipped with Z-spray electrospray ionization (ESI) and matrix assisted laser desorption ionization (MALDI) sources in positive mode with *trans*-2-[3-(4-*tert*-butylphenyl)-2-methyl-2-propenylidene]malononitrile (DCTB) as the matrix. Melting points were measured using an automated melting point meter SMP50 (Stuart) and are uncorrected.

Single crystal X-ray diffraction data for all compounds were collected on a Bruker APEX 2 DUO CCD diffractometer by using graphite-monochromated MoK_α (λ = 0.71073 Å) radiation or Incoatec IμS CuK_α (λ = 1.54178 Å) radiation. Crystals were grown by slow evaporation of CH_2Cl_2–MeOH or toluene solutions of the dyads. Crystals were mounted on a MiTeGen MicroMount and collected at 100(2) K by using an Oxford Cryosystems Cobra low-temperature device. Data was collected by using omega and phi scans and were corrected for Lorentz and polarization effects by using the APEX software suite.[3] Using Olex2, the structure was solved with the XT structure solution program, using the intrinsic phasing solution method and refined against $|F^2|$ with XL using least-squares minimization.[4] Hydrogen atoms were generally placed in geometrically calculated positions and refined using a riding model. Details of data refinements are given in Table S2. All images were prepared by using Olex2. CCDC 1585148–1585154 contain the supplementary crystallographic data for this paper. These data can be obtained free of charge from The Cambridge Crystallographic Data Centre via www.ccdc.cam.ac.uk/data_request/cif.

B. Steady-state optical spectroscopy

Table S1. Absorption, emission and excitation spectra of the dyads in dichloromethane.

Compound	Absorption spectrum	Emission and excitation spectra
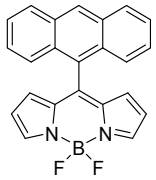	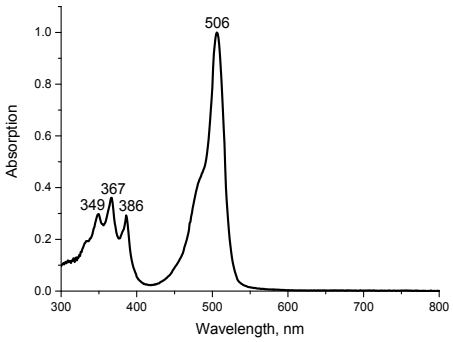	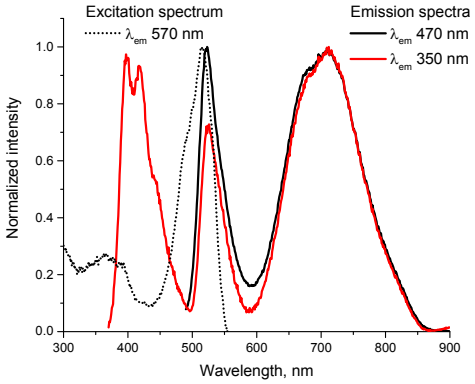
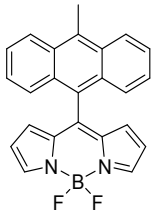	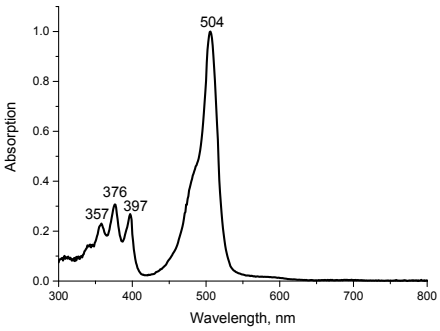	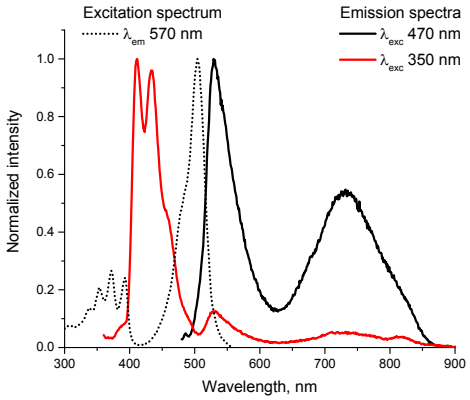
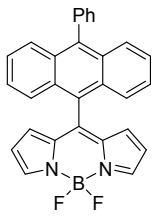	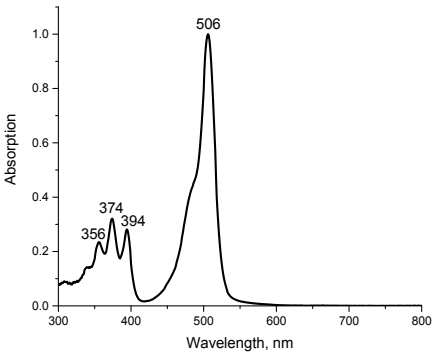	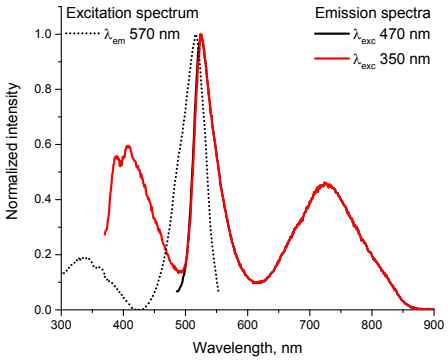

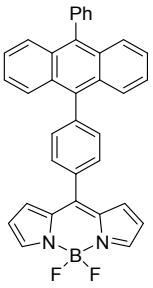
Ph
N
B
N
F
F

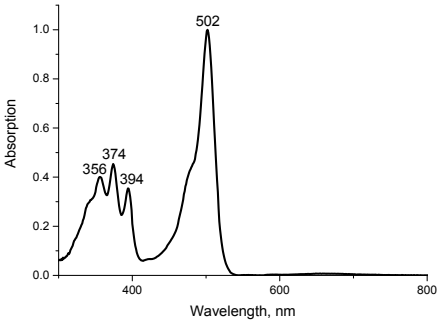
Absorption
Wavelength, nm
502
374
356
394

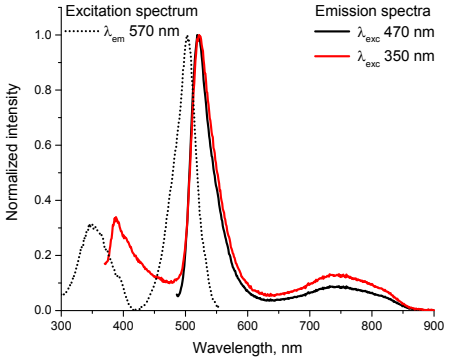
Excitation spectrum
λem 570 nm
Emission spectra
λexc 470 nm
λexc 350 nm
Normalized intensity
Wavelength, nm

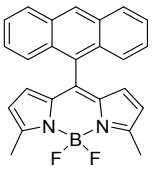
N
B
N
F
F

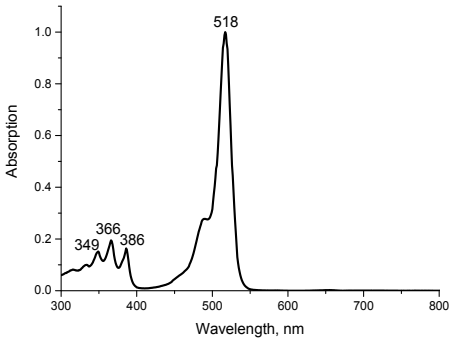
Absorption
Wavelength, nm
518
366
349
386

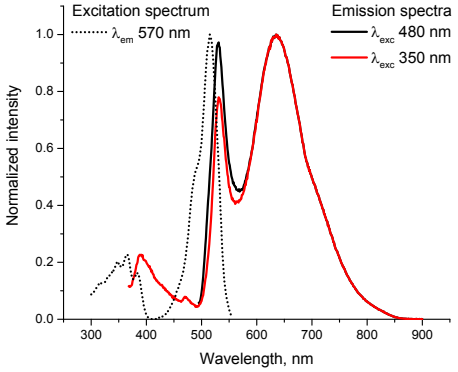
Excitation spectrum
λem 570 nm
Emission spectra
λexc 480 nm
λexc 350 nm
Normalized intensity
Wavelength, nm

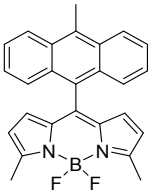
N
B
N
F
F

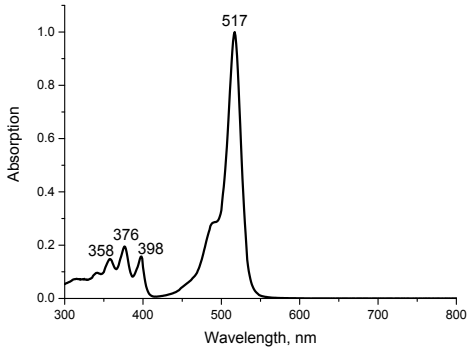
Absorption
Wavelength, nm
517
376
358
398

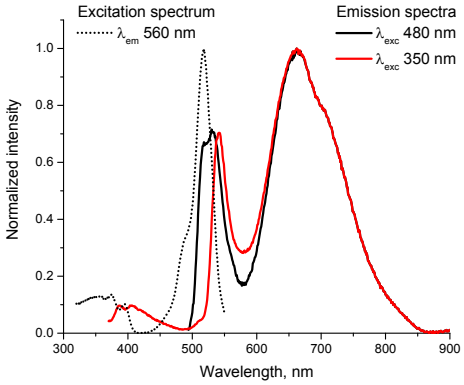
Excitation spectrum
λem 560 nm
Emission spectra
λexc 480 nm
λexc 350 nm
Normalized intensity
Wavelength, nm

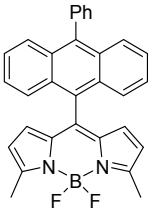
Ph
N
B
N
F
F

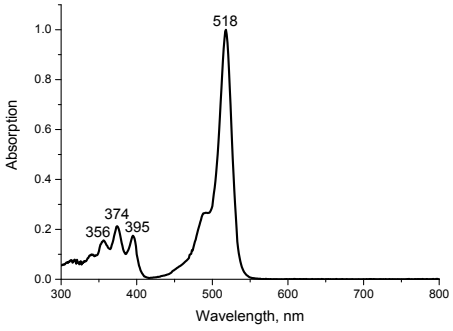
Absorption
Wavelength, nm
518
374
356
395

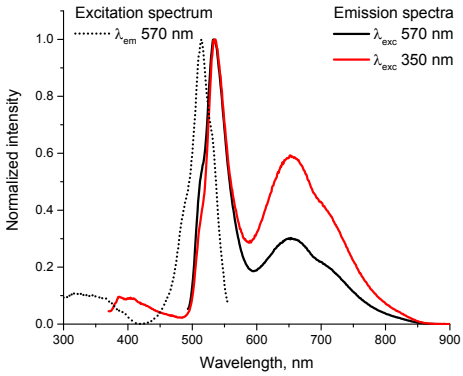
Excitation spectrum
λem 570 nm
Emission spectra
λexc 570 nm
λexc 350 nm
Normalized intensity
Wavelength, nm

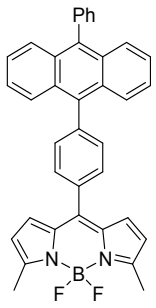
Ph
N
B
F
F

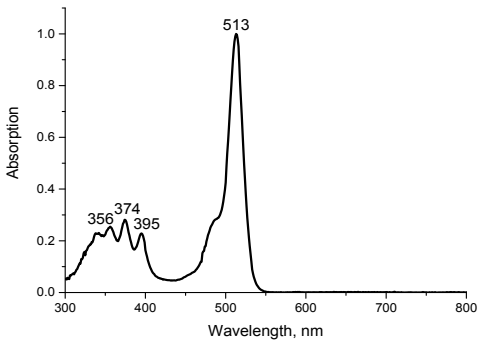
Absorption
Wavelength, nm
513
356
374
395

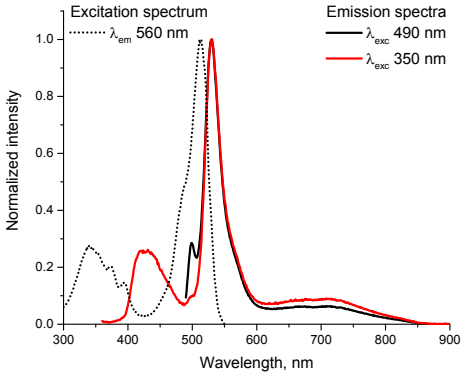
Excitation spectrum
λem 560 nm
Emission spectra
λexc 490 nm
λexc 350 nm
Normalized intensity
Wavelength, nm

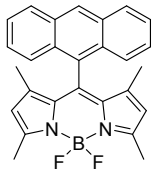
N
B
F
F

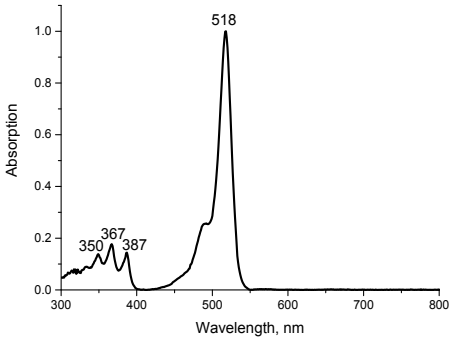
Absorption
Wavelength, nm
518
350
367
387

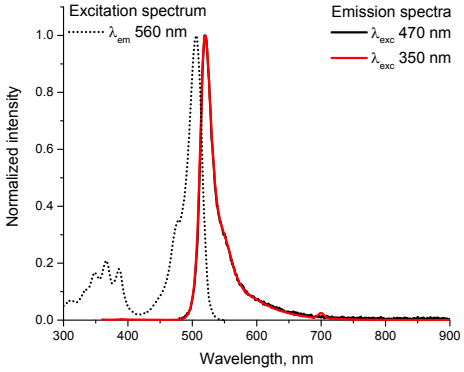
Excitation spectrum
λem 560 nm
Emission spectra
λexc 470 nm
λexc 350 nm
Normalized intensity
Wavelength, nm

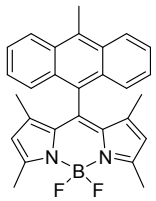
N
B
F
F

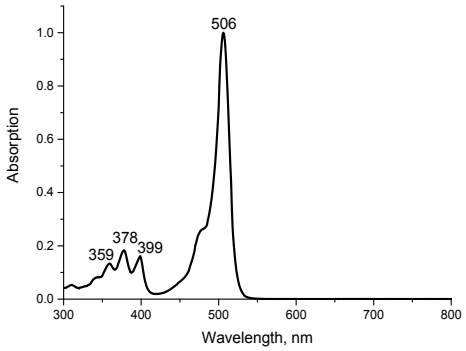
Absorption
Wavelength, nm
506
359
378
399

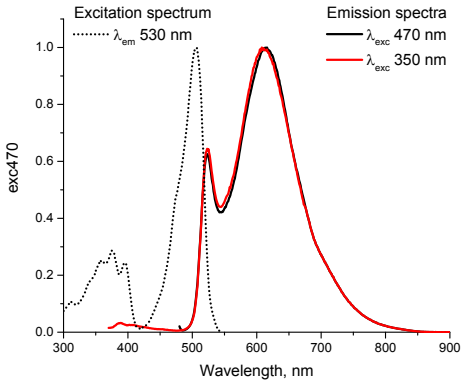
Excitation spectrum
λem 530 nm
Emission spectra
λexc 470 nm
λexc 350 nm
exc470
Wavelength, nm

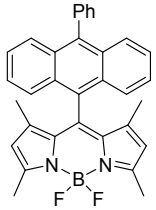
Ph
N
B
F
F

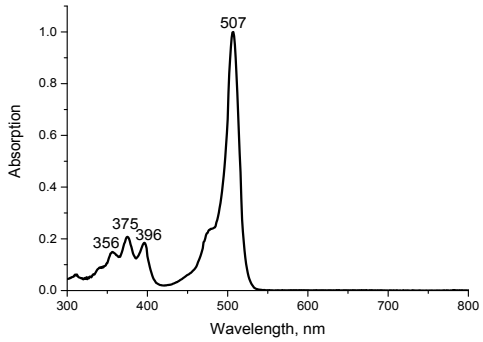
Absorption
Wavelength, nm
507
356
375
396

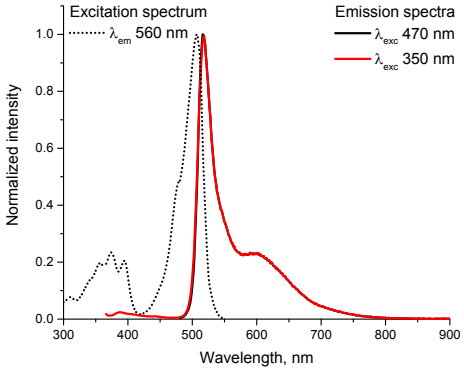
Excitation spectrum
λem 560 nm
Emission spectra
λexc 470 nm
λexc 350 nm
Normalized intensity
Wavelength, nm

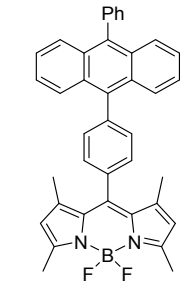
Ph
N
B
N
F
F

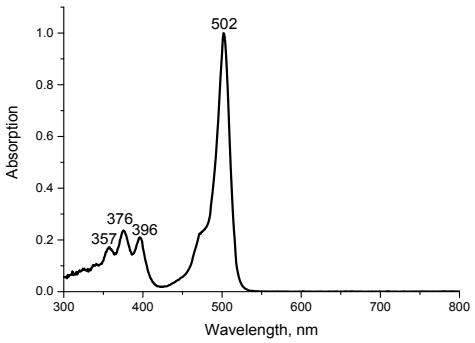
Absorption
Wavelength, nm
502
376
357
396

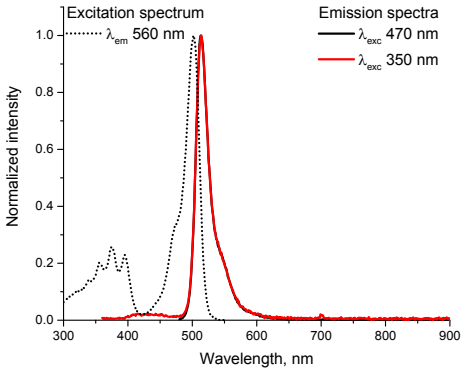
Excitation spectrum
λem 560 nm
Emission spectra
λexc 470 nm
λexc 350 nm
Normalized intensity
Wavelength, nm

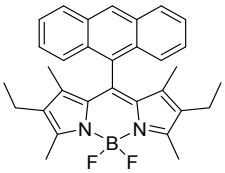
N
B
N
F
F

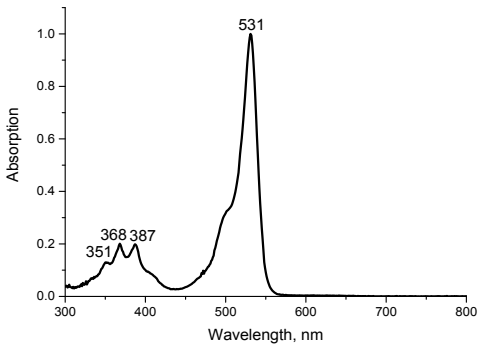
Absorption
Wavelength, nm
531
368
387
351

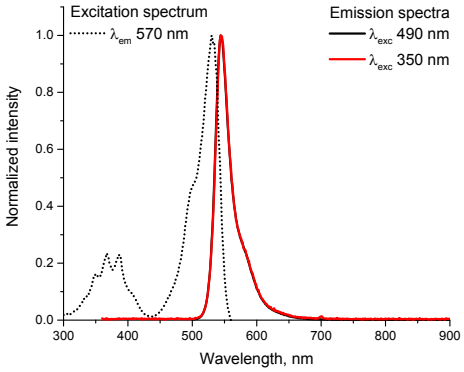
Excitation spectrum
λem 570 nm
Emission spectra
λexc 490 nm
λexc 350 nm
Normalized intensity
Wavelength, nm

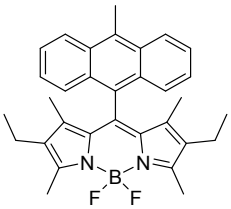
N
B
N
F
F

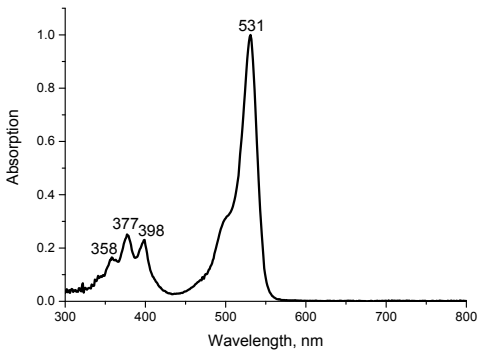
Absorption
Wavelength, nm
531
377
398
358

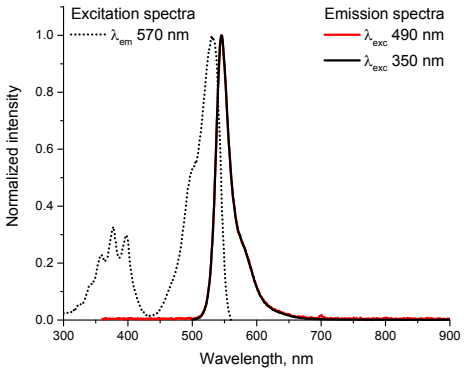
Excitation spectra
λem 570 nm
Emission spectra
λexc 490 nm
λexc 350 nm
Normalized intensity
Wavelength, nm

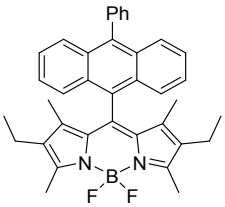
Ph
N
B
N
F
F

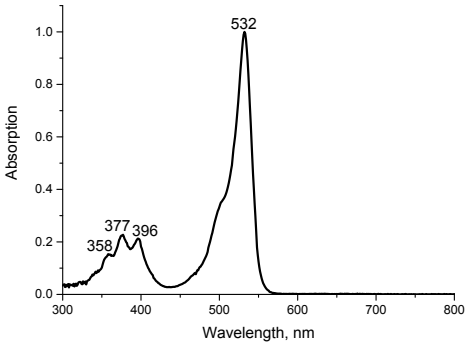
Absorption
Wavelength, nm
532
377
396
358

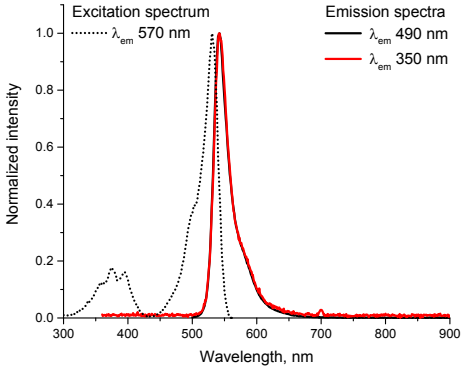
Excitation spectrum
λem 570 nm
Emission spectra
λem 490 nm
λem 350 nm
Normalized intensity
Wavelength, nm

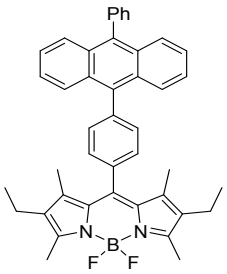
Ph
N
B
N
F
F

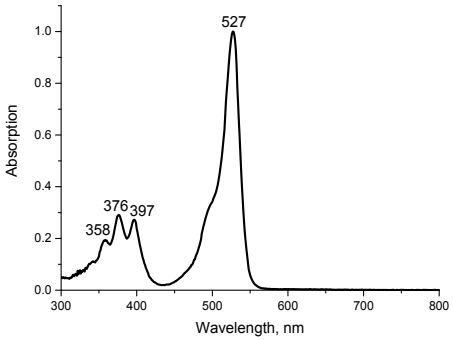
Absorption
Wavelength, nm
527
376
397
358

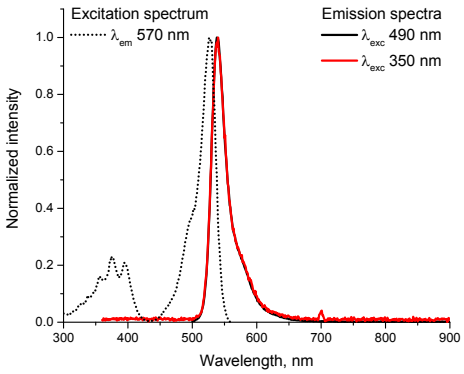
Excitation spectrum
λem 570 nm
Emission spectra
λexc 490 nm
λexc 350 nm
Normalized intensity
Wavelength, nm

C. Time-resolved optical spectroscopy

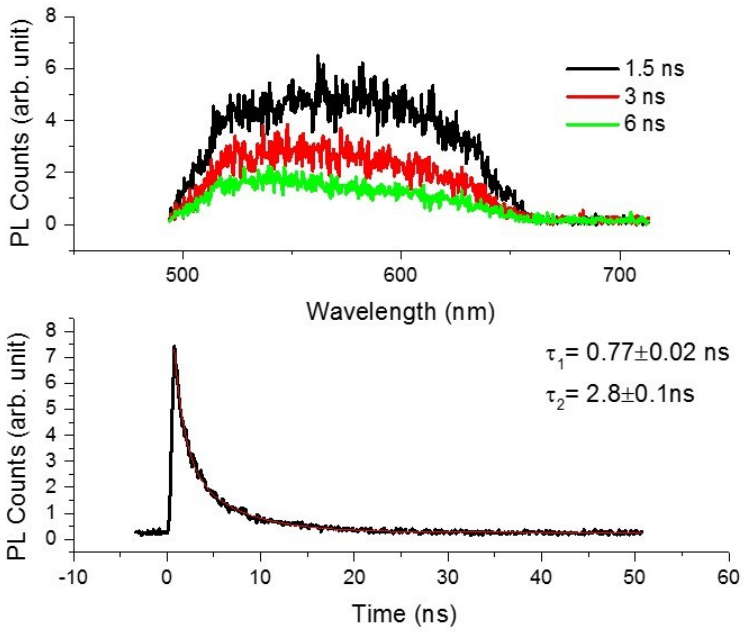

Figure S1: Time-resolved photoluminescence spectra of compound **2** in DMF.

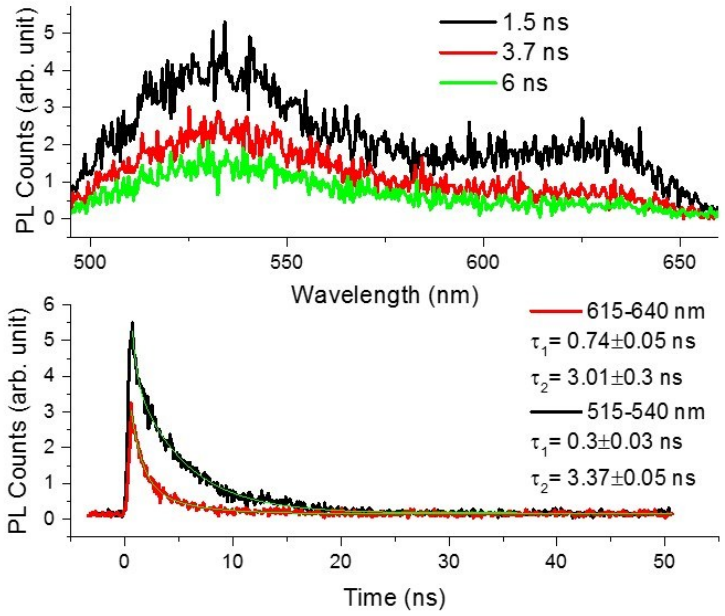

Figure S2: Time-resolved photoluminescence spectra of compound **6** in DMF.

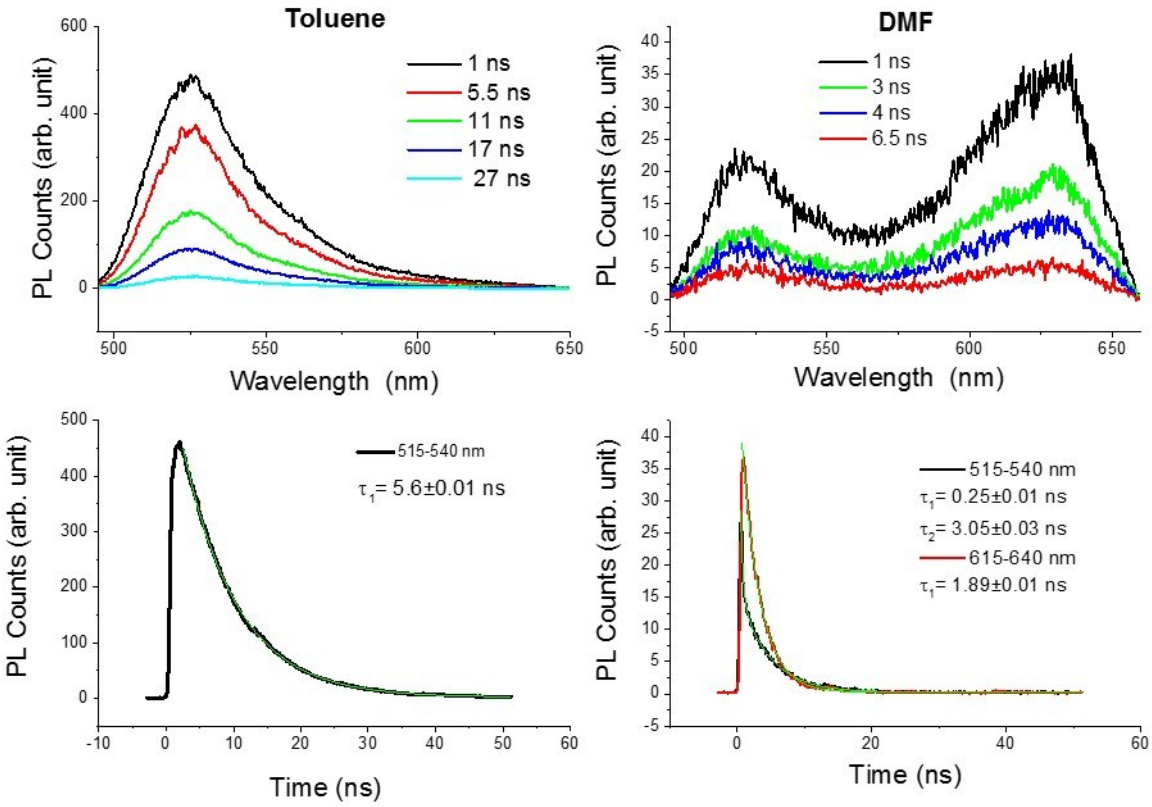

Figure S3: Time-resolved photoluminescence spectra of compound **10** in DMF and toluene.

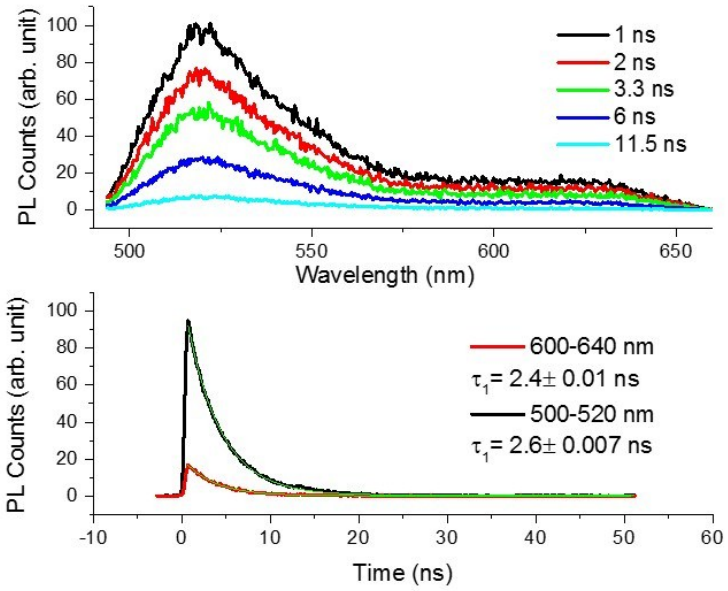

Figure S4: Time-resolved photoluminescence spectra of compound **11** in DMF.

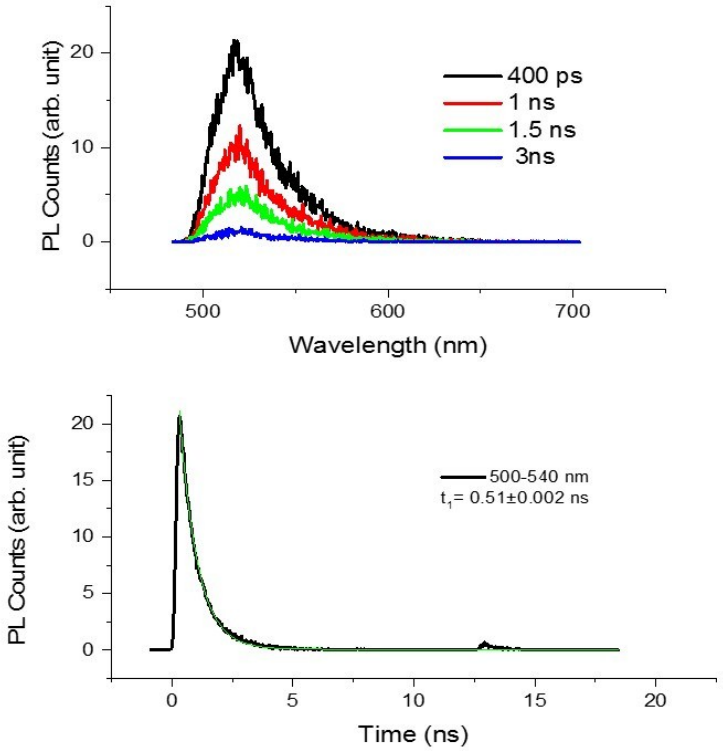

Figure S5: Time-resolved photoluminescence spectra of compound **12** in DMF.

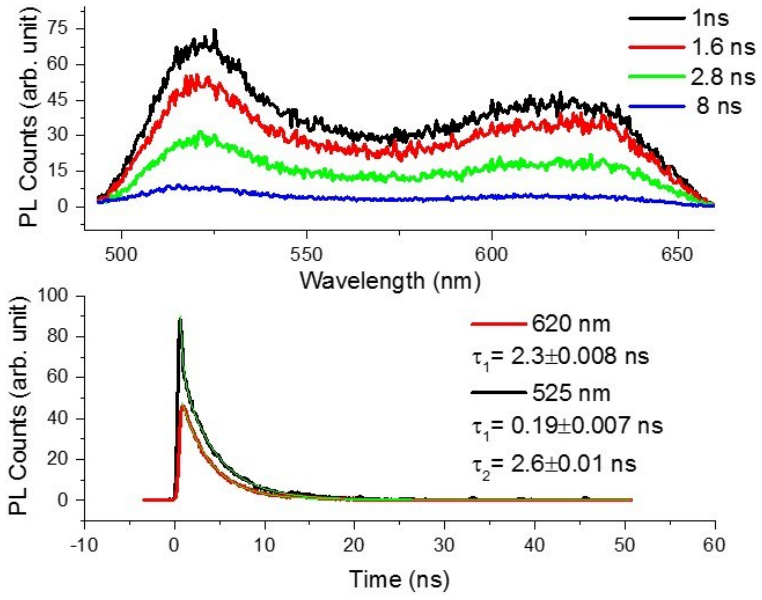

Figure S6: Time-resolved photoluminescence spectra of compound **9** in DMF.

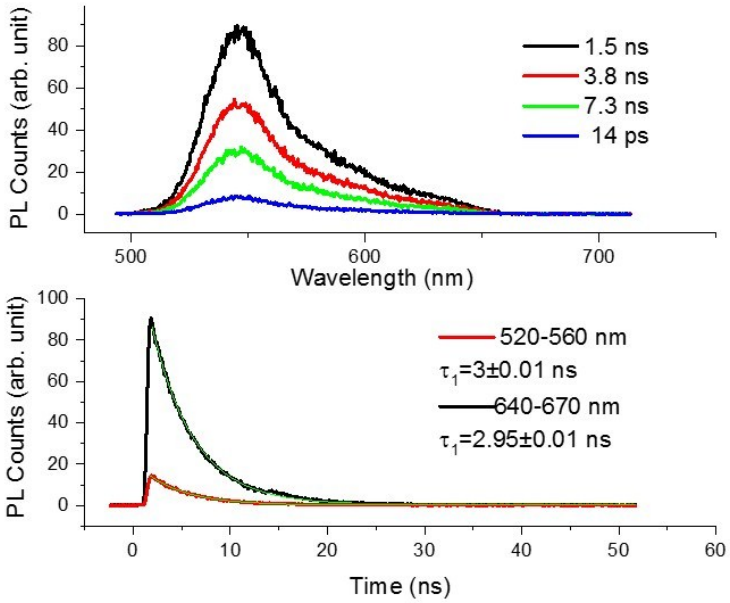

Figure S7: Time-resolved photoluminescence spectra of compound **14** in DMF.

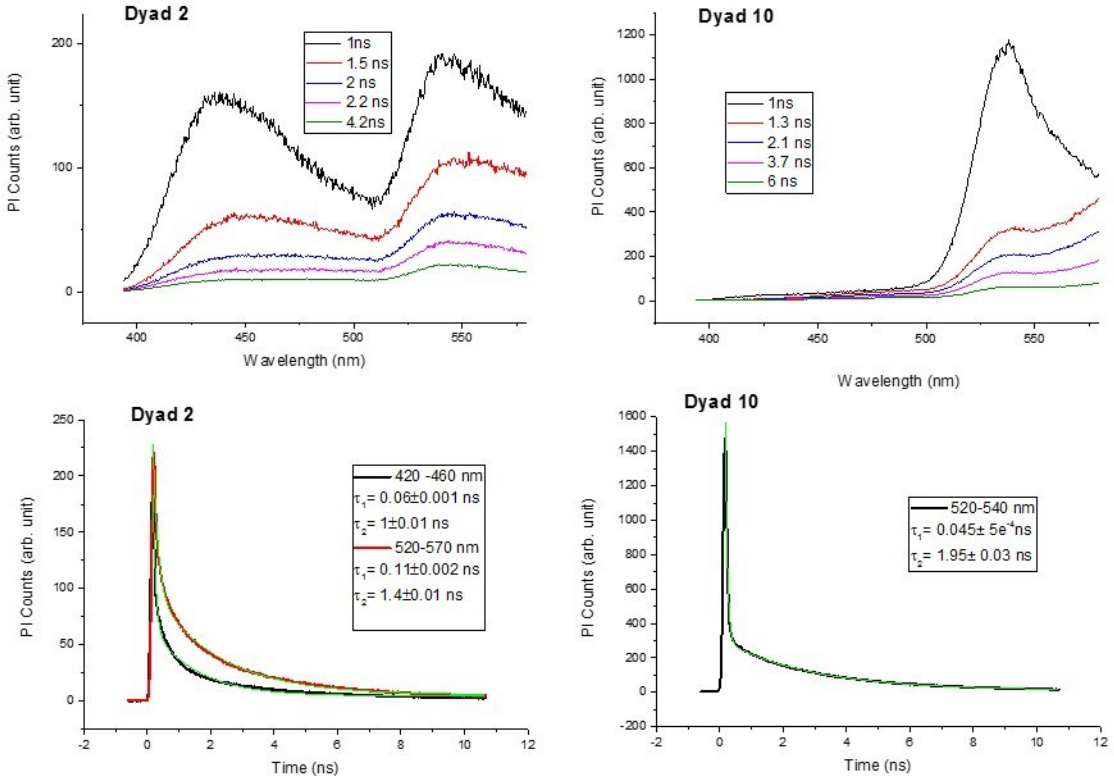

Figure S8: Time-resolved photoluminescence spectra of compounds **2** and **10** in DMF comparing the band peaking at 420 nm.

D. Transient absorption spectroscopy

Transient absorption (TA) spectroscopy measurements were carried out using a home-built pump-probe setup. Two different configurations of the setup were used for either short delay, namely 100 fs to 8 ns experiments, or long delay, namely 1 ns to 300 μs delays, as described below:

The output of a titanium:sapphire amplifier (Coherent LEGEND DUO, 4.5 mJ, 3 kHz, 100 fs) was split into three beams (2 mJ, 1 mJ, and 1.5 mJ). Two of them were used to separately pump two optical parametric amplifiers (OPA) (Light Conversion TOPAS Prime). The TOPAS 1 generates tunable pump pulses, while the TOPAS 2 generates signal (1300 nm) and idler (2000 nm) only. For measuring TA whole visible range, we used 1300 nm (signal) of TOPAS 2 to produce white-light super continuum from 350 to 1100 nm. For short delay TA measurements, we used the TOPAS 1 for producing pump pulses while the probe pathway length to the sample was kept constant at approximately 5 meters between the output of the TOPAS1 and the sample, the pump pathway length was varied between 5.12 and 2.6 m with a broadband retroreflector mounted on automated mechanical delay stage (Newport linear stage IMS600CCHA controlled by a Newport XPS motion controller), thereby generating delays between pump and probe from -400 ps to 8 ns.

For the 1 ns to 300 μs delay (long delay) TA measurement, the same probe white-light supercontinuum as for the 100 fs to 8 ns delays was used. The excitation light (pump pulse) was provided by an actively Q-switched Nd:YVO4 laser (InnoLas picolo AOT) frequency-doubled (tripled) to provide pulses at 355 nm, and triggered by an electronic delay generator (Stanford Research Systems DG535), itself triggered by the TTL sync from the Legend DUO, allowing control of the delay between pump and probe with a jitter of roughly 100 ps.

Pump and probe beams were focused on the sample with the aid of proper optics. The transmitted fraction of the white light was guided to a custom-made prism spectrograph (Entwicklungsbüro Stresing) where it was dispersed by a prism onto a 512 pixel NMOS linear image sensor (Hamamatsu S8381-512). The probe pulse repetition rate was 3 kHz, while the excitation pulses were mechanically chopped to 1.5 kHz (100 fs to 8 ns delays) or directly generated at 1.5 kHz frequency (1 ns to 300 μs delays), while the detector array was read out at 3 kHz. Adjacent diode readings corresponding to the transmission of the sample after excitation and in the absence of an excitation pulse were used to calculate $\Delta T/T$. Measurements were averaged over several thousand shots to obtain a good signal-to-noise ratio.

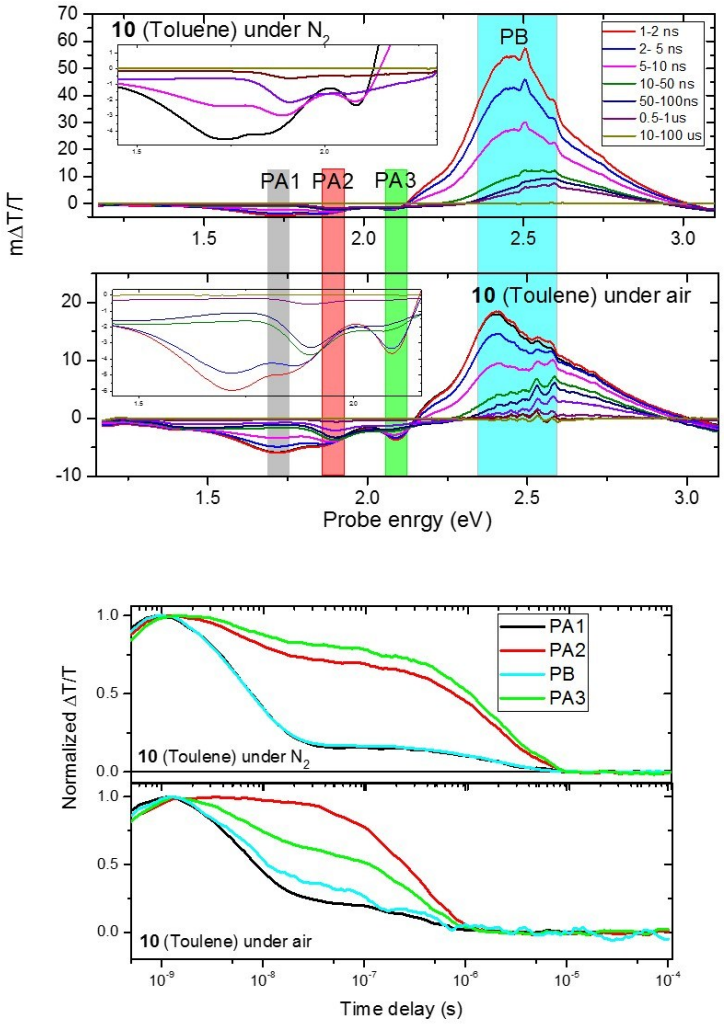

Figure S9: ns-µs Transient absorption spectra (top panel) and kinetics (bottom panel) of **10** (in toluene) under nitrogen and air saturated atmosphere.

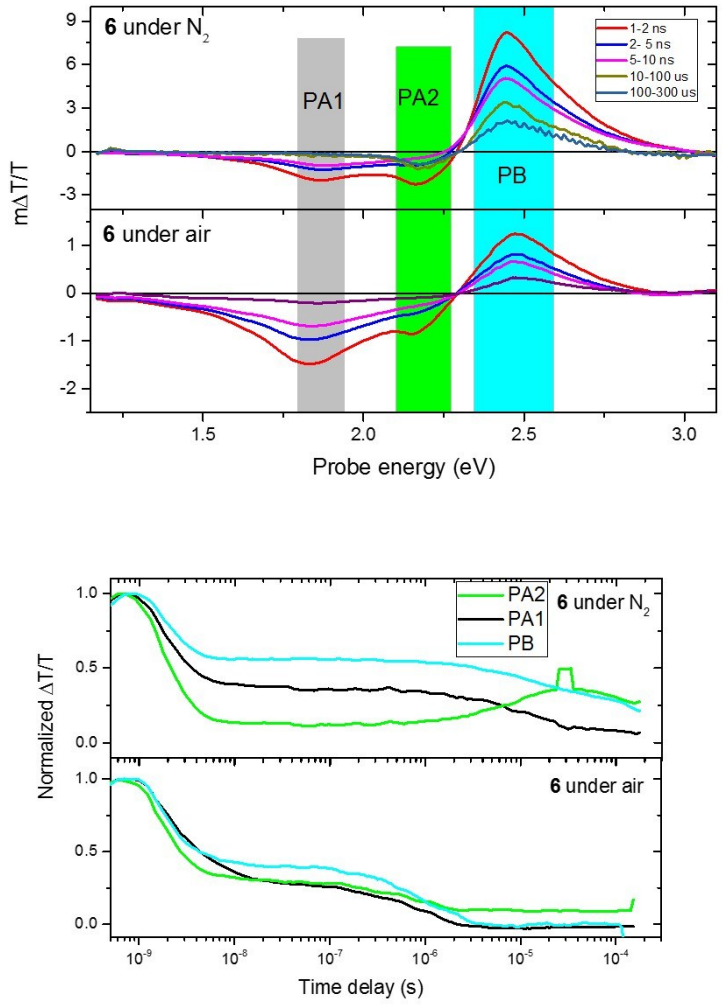

Figure S10: ns-µs Transient absorption spectra (top panel) and kinetics (bottom panel) of compound **6** in DMF under nitrogen and air saturated atmosphere.

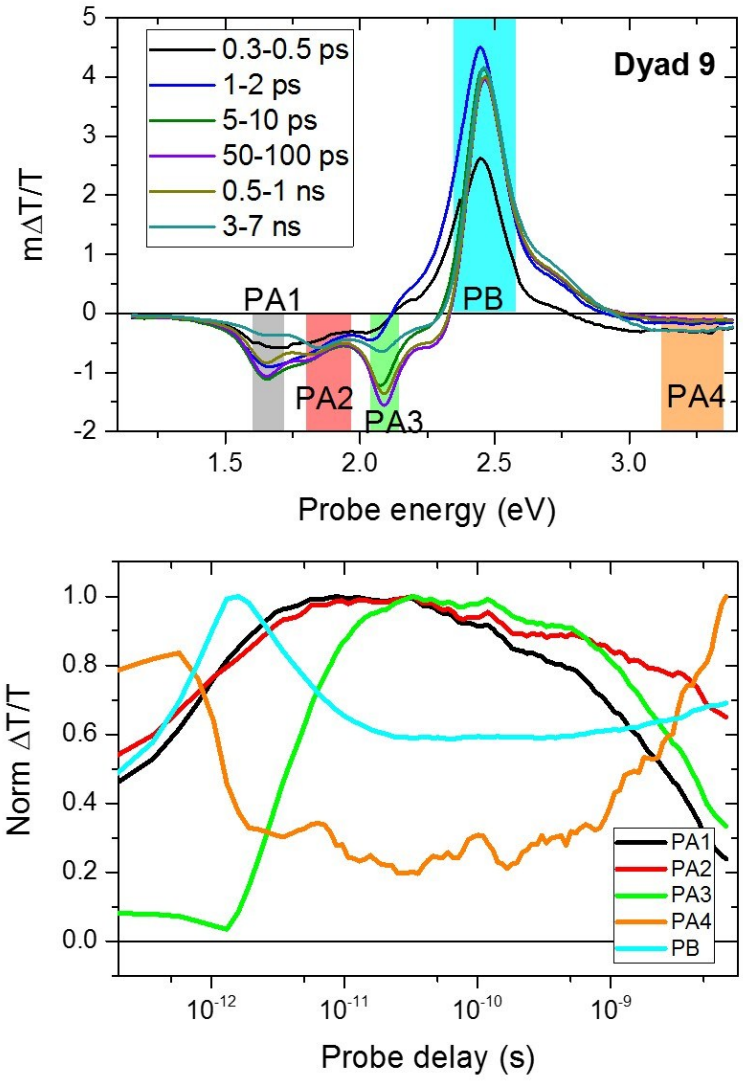

Figure S11: ps-ns Transient absorption spectra and kinetics of **9** in DMF.

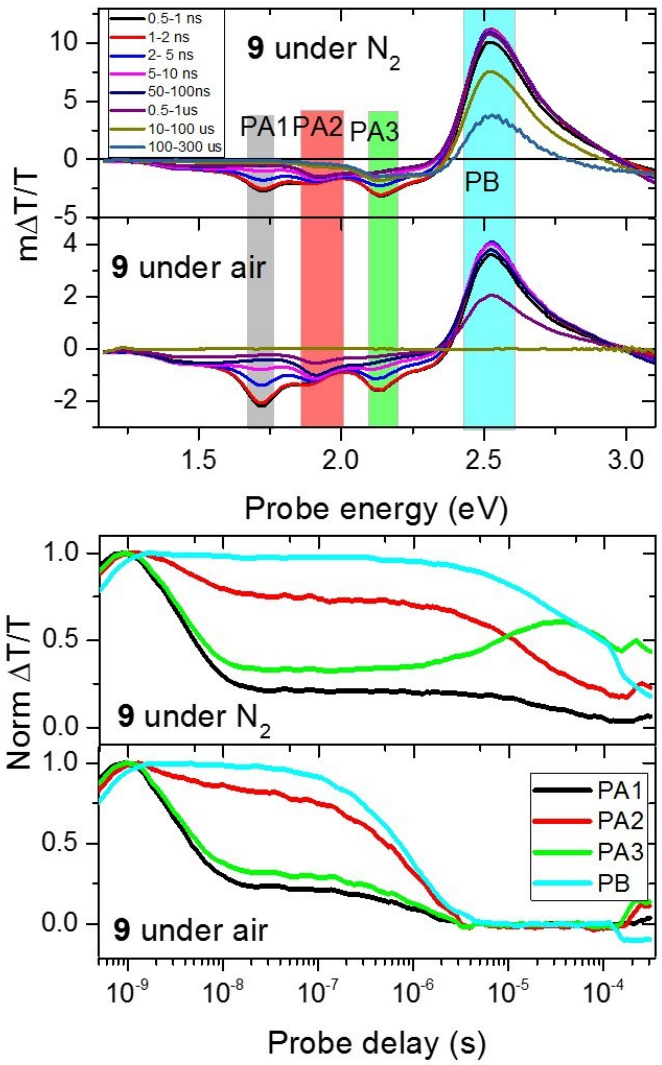

Figure S12: ns-µs TA spectra and kinetics of **9** in DMF in air and nitrogen atmosphere.

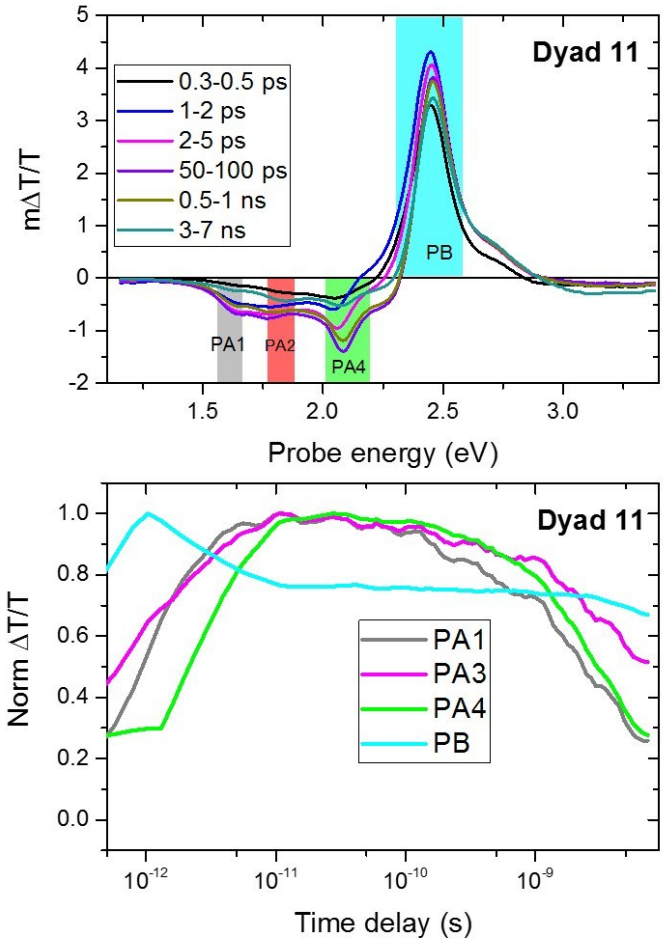

Figure S13: ps-ns Transient absorption spectra and kinetics of **11** in DMF.

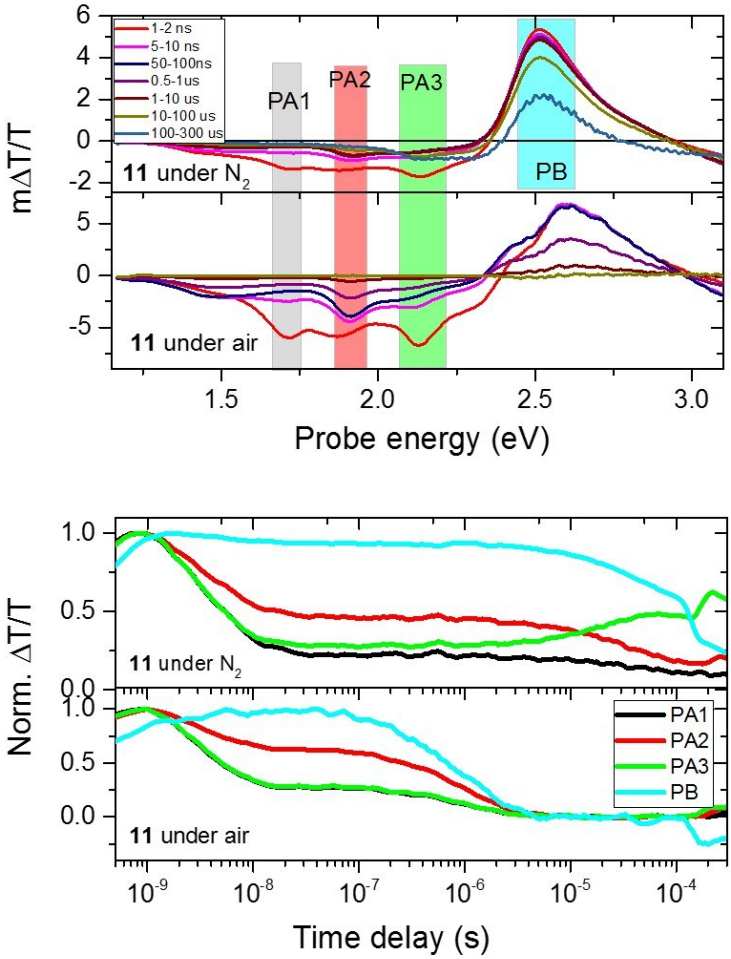

Figure S14: ns-µs Transient absorption spectra and kinetics of **11** in DMF under air and nitrogen atmosphere.

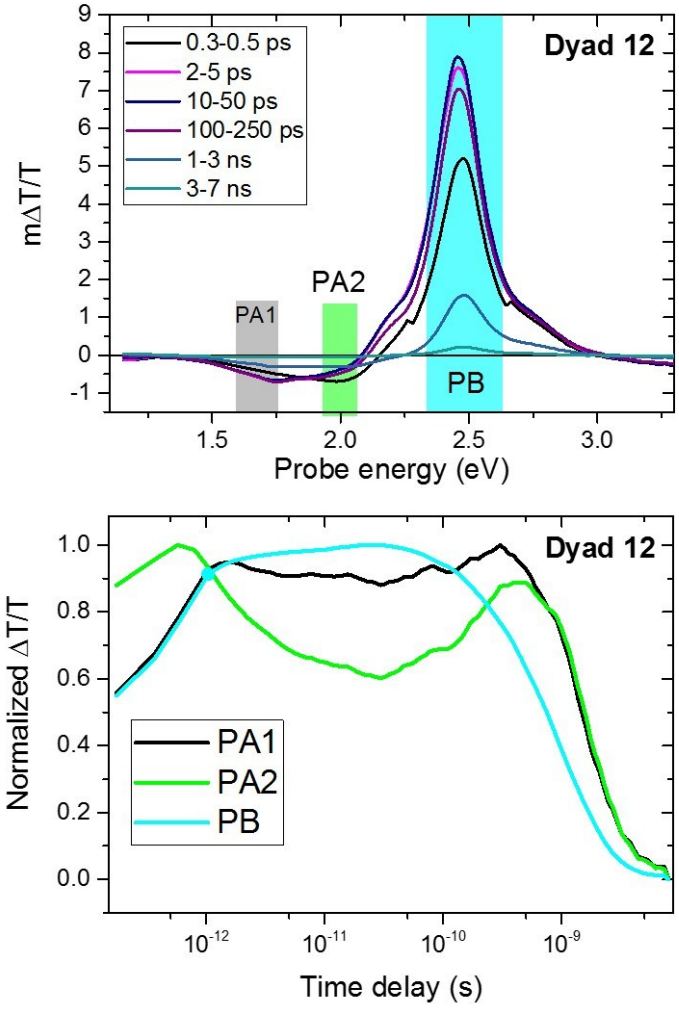

Figure S15: ps-ns Transient absorption spectra and kinetics of **12** in DMF.

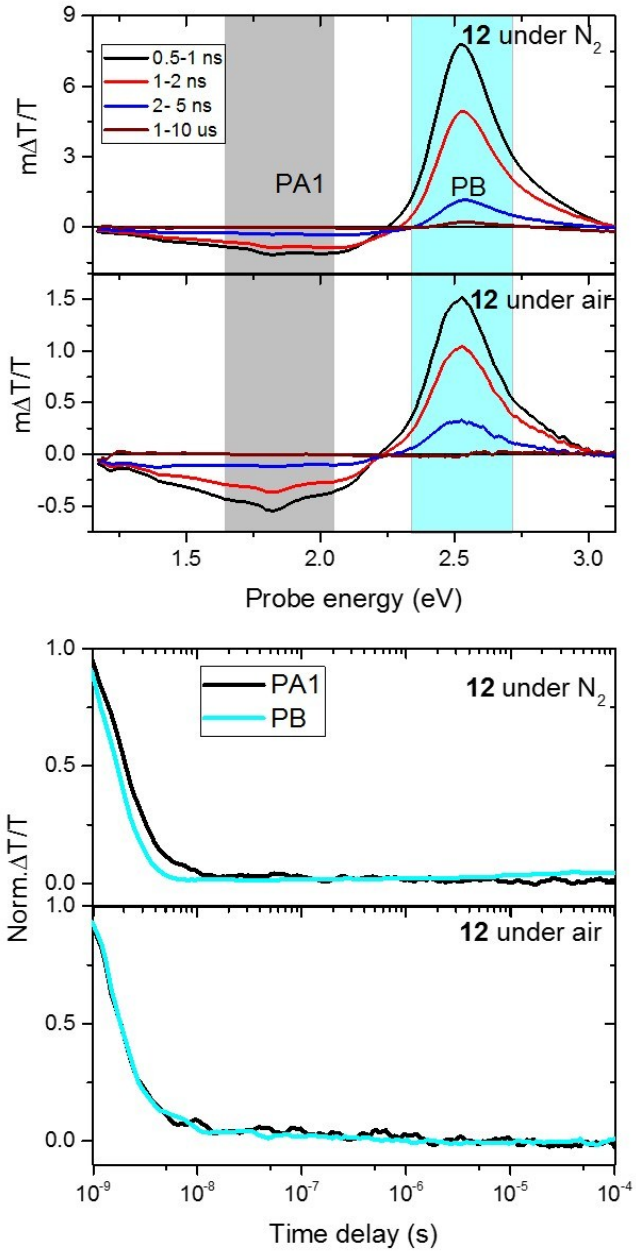

Figure S16: ns-µs Transient absorption spectra and kinetics of **12** in DMF in air and nitrogen atmosphere.

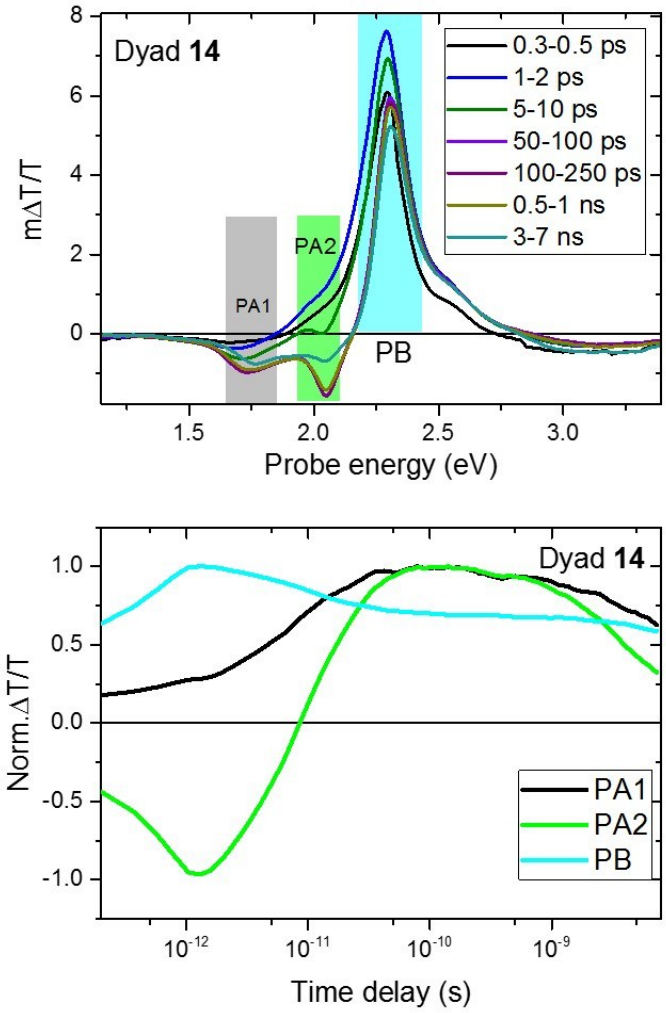

Figure S17: ps–ns Transient absorption spectra and kinetics of **14** in DMF.

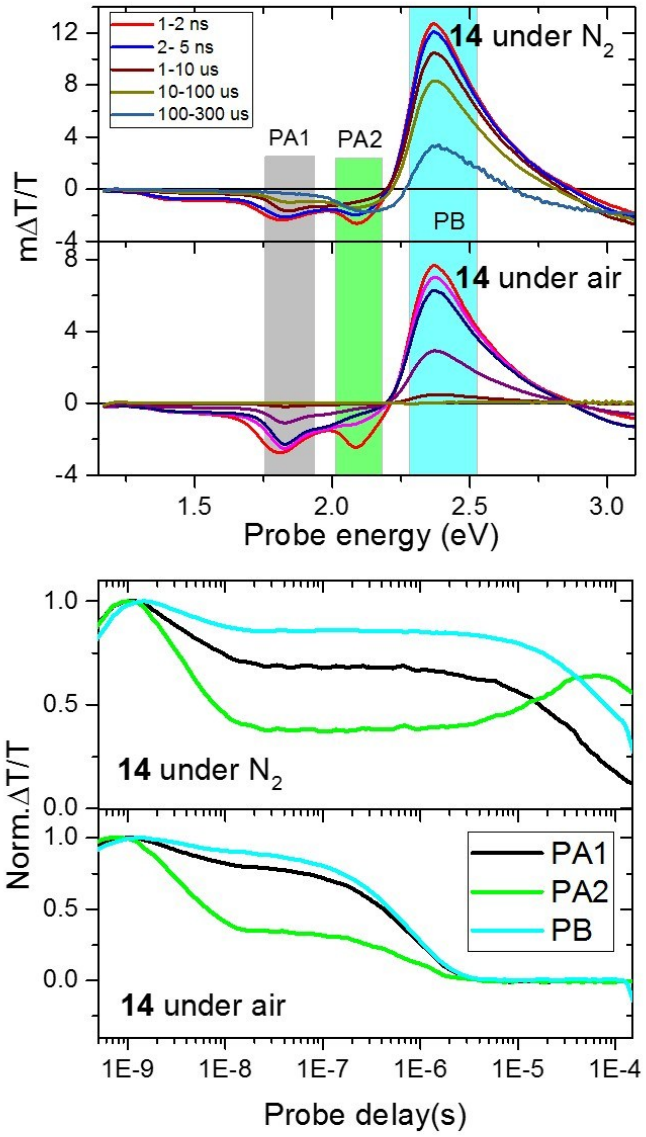

Figure S18: ns-µs Transient absorption spectra and kinetics of **14** in DMF in air and nitrogen atmosphere.

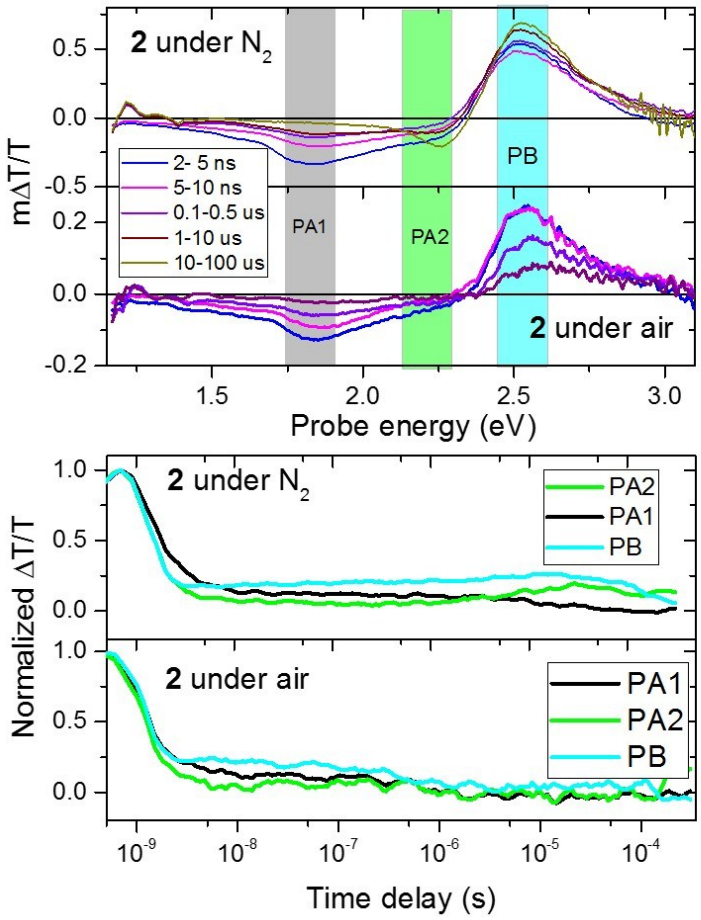

Figure S19: ns-µs Transient absorption spectra and kinetics of **2** in DMF in air and nitrogen atmosphere.

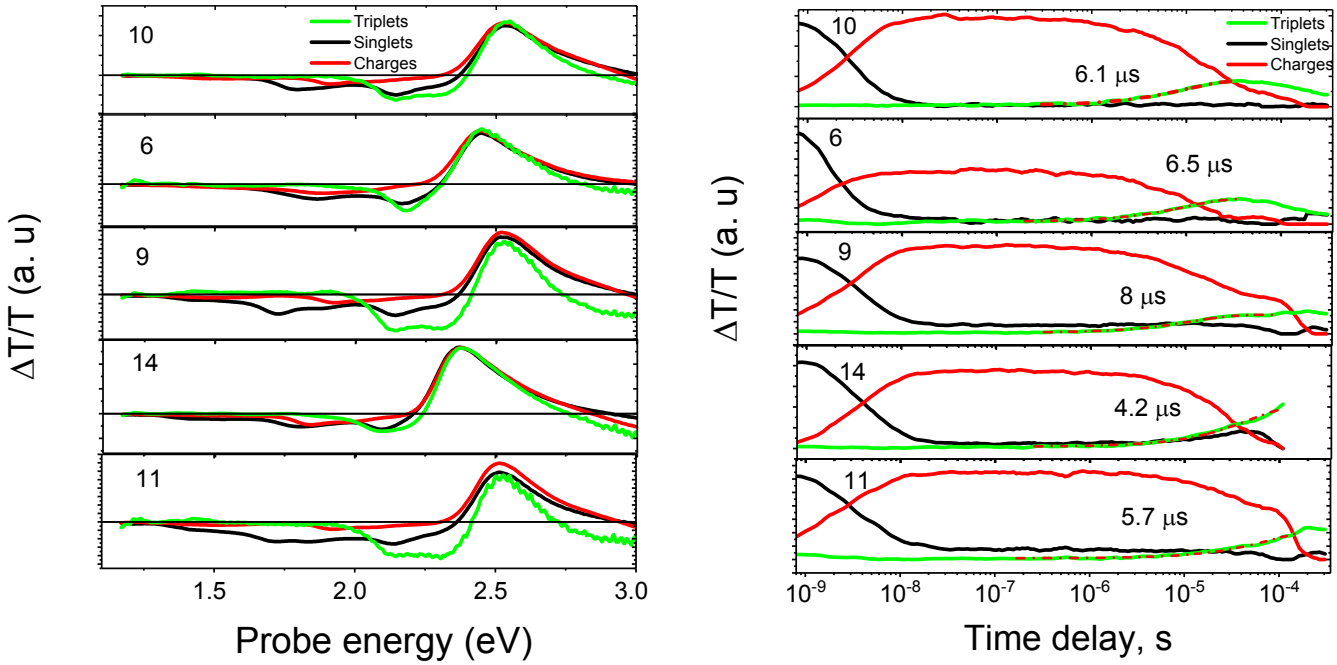

Figure S20: The component spectra and kinetics of singlets (black), charges (red), and triplets (green) obtained by multivariate curve resolution of ns-μsTA data of all compounds studied in this paper in DMF except for 2 and 12 where most of the excited states were decayed in ns-ps timescale. The red dashed line in denotes a fitted single-exponential rise of the triplet population.

E. X-ray Crystallography

Table S2: Details of XRD data refinement

Compound	**2**	**5**	**6**	**7**	**8**
Empirical formula	$C_{24}H_{17}BF_2N_2$	$C_{26}H_{20}BCl_3F_2N_2$	$C_{26}H_{21}BF_2N_2$	$C_{31}H_{23}BF_2N_2$	$C_{37}H_{27}BF_2N_2$
Formula weight	382.20	515.60	410.26	472.32	548.41
Temperature/K	99.99	100.0	100.0	100.01	100.0
Crystal system	monoclinic	monoclinic	monoclinic	triclinic	Triclinic
Space group	$P2_1/n$	P2/c	C2/c	$P\bar{1}$	$P\bar{1}$
a/Å	14.2177(13)	14.2315(15)	13.2502(6)	8.9484(18)	10.3605(16)
b/Å	13.2738(11)	11.3053(12)	12.7869(6)	9.6443(19)	13.301(2)
c/Å	19.7784(17)	15.4276(16)	12.8459(6)	17.849(4)	21.611(4)
α/°	90	90	90	87.62(3)	76.897(3)
β/°	95.067(2)	93.737(2)	114.6660(10)	77.07(3)	82.836(6)
γ/°	90	90	90	68.24(3)	73.801(5)
Volume/Å³	3718.1(6)	2476.9(5)	1977.88(16)	1392.9(6)	2779.5(8)
Z	8	4	4	2	4
$D_{calc}g/cm^3$	1.366	1.383	1.378	1.126	1.311
μ/mm^{-1}	0.094	0.403	0.093	0.075	0.680
F(000)	1584.0	1056.0	856.0	492.0	1144.0
Crystal size/mm³	0.3 × 0.12 × 0.12	0.28 × 0.2 × 0.06	0.291 × 0.154 × 0.14	0.18 × 0.09 × 0.02	0.26 × 0.1 × 0.03
Radiation	MoKα	MoKα	MoKα	MoKα	CuKα
Wavelength/Å	λ = 0.71073	λ = 0.71073	λ = 0.71073	λ = 0.71073	λ = 1.54178
2θ/°	3.39 to 55.04	3.602 to 50.98	4.646 to 55.996	2.344 to 50.498	4.206 to 136.41
Reflections collected	61492	30226	31215	35555	54487
Independent reflections	8548	4620	2391	5051	10075
R_{int}	0.0521	0.0633	0.0312	0.0872	0.0617
R_{sigma}	0.0349	0.0395	0.0130	0.0667	0.0420
Restraints	0	307	0	0	0
Parameters	525	421	144	328	761
GooF	1.011	1.013	1.055	1.029	1.054
R_1 *[I> 2σ (I)]*	0.0418	0.0480	0.0404	0.0796	0.0473
wR_2 *[I> 2σ (I)]*	0.0918	0.1102	0.1058	0.1817	0.1227
R_1 *[all data]*	0.0681	0.0849	0.0481	0.1378	0.0645
wR_2 *[all data]*	0.1042	0.01289	0.1105	0.2092	0.1347
Largest peak/e Å⁻³	0.30	0.37	0.40	0.77	0.17
Deepest hole/e Å⁻³	-0.24	-0.45	-0.22	-0.34	-0.29
Flack parameter	--	--	--	--	--

Compound	**14**	**10**
Empirical formula	$C_{32}H_{33}BF_2N_2$	$C_{63}H_{58}B_2F_4N_4$
Formula weight	494.41	968.75
Temperature/K	100.0	100.0
Crystal system	monoclinic	triclinic
Space group	$P2_1/c$	$P\bar{1}$
a/Å	15.836(6)	8.5680(10)
b/Å	20.573(7)	9.7581(11)
c/Å	7.781(3)	15.2034(18)
α/°	90	101.961(2)
β/°	101.878(8)	91.811(2)
γ/°	90	99.856(2)
Volume/Å³	2480.7(15)	1222.2(2)
Z	4	1
D_{calc} *g/cm³*	1.324	1.316
μ/mm⁻¹	0.087	0.087
F(000)	1048.0	510.0
Crystal size/mm³	0.6 × 0.05 × 0.05	0.529 × 0.428 × 0.235
Radiation	MoKα	MoKα
Wavelength/Å	λ = 0.71073	λ = 0.71073
2θ/°	3.29 to 51	4.34 to 62.358
Reflections collected	58475	36115
Independent reflections	4627	7861
R_{int}	0.1328	0.0519
R_{sigma}	0.0715	0.0488
Restraints	0	165
Parameters	341	355
GooF	1.013	1.031
R_1 *[I>=2σ (I)]*	0.0483	0.0644
wR_2 *[I>=2σ (I)]*	0.0937	0.1717
R_1 *[all data]*	0.1076	0.1073
wR_2 *[all data]*	0.1125	0.2011
Largest peak/e Å⁻³	0.19	0.84
Deepest hole/e Å⁻³	-0.23	-0.52
Flack parameter	--	--

Crystal Data for 2: $C_{24}H_{17}BF_2N_2$ (M =382.20 g/mol): monoclinic, space group $P2_1/n$ (no. 14), a = 14.2177(13) Å, b = 13.2738(11) Å, c = 19.7784(17) Å, β = 95.067(2)°, V = 3718.1(6) Å^3, Z = 8, T = 99.99 K, μ(MoK_α) = 0.094 mm^{-1}, D_{calc} = 1.366 g/cm^3, 61492 reflections measured (3.39° ≤ 2θ ≤ 55.04°), 8548 unique (R_{int} = 0.0521, R_{sigma} = 0.0349) which were used in all calculations. The final R_1 was 0.0418 (I > 2σ(I)) and wR_2 was 0.1042 (all data).

Crystal Data for 5: $C_{26}H_{20}BCl_3F_2N_2$ (M =515.60 g/mol): monoclinic, space group P2/c (no. 13), a = 14.2315(15) Å, b = 11.3053(12) Å, c = 15.4276(16) Å, β = 93.737(2)°, V = 2476.9(5) Å^3, Z = 4, T = 100.0 K, μ(MoK_α) = 0.403 mm^{-1}, D_{calc} = 1.383 g/cm^3, 30226 reflections measured (3.602° ≤ 2θ ≤ 50.98°), 4620 unique (R_{int} = 0.0633, R_{sigma} = 0.0395) which were used in all calculations. The final R_1 was 0.0480 (I > 2σ(I)) and wR_2 was 0.1289 (all data). Solvent chloroform molecules were modelled over four positions and fixed using restraints (SADI, DFIX, and ISOR) in a 50:27:13:10 % occupancy.

Crystal Data for 6: $C_{26}H_{21}BF_2N_2$ (M =410.26 g/mol): monoclinic, space group C2/c (no. 15), a = 13.2502(6) Å, b = 12.7869(6) Å, c = 12.8459(6) Å, β = 114.6660(10)°, V = 1977.88(16) Å^3, Z = 4, T = 100.0 K, μ(MoK_α) = 0.093 mm^{-1}, D_{calc} = 1.378 g/cm^3, 31215 reflections measured (4.646° ≤ 2θ ≤ 55.996°), 2391 unique (R_{int} = 0.0312, R_{sigma} = 0.0130) which were used in all calculations. The final R_1 was 0.0404 (I > 2σ(I)) and wR_2 was 0.1105 (all data).

Crystal Data for 7: $C_{31}H_{23}BF_2N_2$ (M =472.32 g/mol): triclinic, space group $P\bar{1}$ (no. 2), a = 8.9484(18) Å, b = 9.6443(19) Å, c = 17.849(4) Å, α = 87.62(3)°, β = 77.07(3)°, γ = 68.24(3)°, V = 1392.9(6) Å^3, Z = 2, T = 100.01 K, μ(MoK_α) = 0.075 mm^{-1}, D_{calc} = 1.126 g/cm^3, 35555 reflections measured (2.344° ≤ 2θ ≤ 50.498°), 5051 unique (Rint = 0.0872, Rsigma = 0.0667) which were used in all calculations. The final R1 was 0.0796 (I > 2σ(I)) and wR2 was 0.2092 (all data). Solvent molecules (DCM and MeOH) were squeezed from solution using a solvent mask in OLEX2 as no reliable solution could be modelled.

Crystal Data for 8: $C_{37}H_{27}BF_2N_2$ (M =548.41 g/mol): triclinic, space group $P\bar{1}$ (no. 2), a = 10.3605(16) Å, b = 13.301(2) Å, c = 21.611(4) Å, α = 76.897(3)°, β = 82.836(6)°, γ = 73.801(5)°, V = 2779.5(8) Å^3, Z = 4, T = 100.0 K, μ(CuK_α) = 0.680 mm^{-1}, D_{calc} = 1.311 g/cm^3, 54487 reflections measured (4.206° ≤ 2θ ≤ 136.41°), 10075 unique (R_{int} = 0.0617, R_{sigma} = 0.0420) which were used in all calculations. The final R_1 was 0.0473 (I > 2σ(I)) and wR_2 was 0.1347 (all data).

Crystal Data for 14: $C_{32}H_{33}BF_2N_2$ (M =494.41 g/mol): monoclinic, space group $P2_1/c$ (no. 14), a = 15.836(6) Å, b = 20.573(7) Å, c = 7.781(3) Å, β = 101.878(8)°, V = 2480.7(15) Å^3, Z = 4, T = 100.0 K, μ(MoK_α) = 0.087 mm^{-1}, D_{calc} = 1.324 g/cm^3, 58475 reflections measured (3.29° ≤ 2θ ≤ 51°), 4627 unique (R_{int} = 0.1328, R_{sigma} = 0.0715) which were used in all calculations. The final R_1 was 0.0483 (I > 2σ(I)) and wR_2 was 0.1125 (all data).

Crystal Data for 10: $C_{63}H_{58}B_2F_4N_4$ (M =968.75 g/mol): triclinic, space group P-1 (no. 2), a = 8.5680(10) Å, b = 9.7581(11) Å, c = 15.2034(18) Å, α = 101.961(2)°, β = 91.811(2)°, γ = 99.856(2)°, V = 1222.2(2) Å^3, Z = 1, T = 100.0 K, μ(MoK_α) = 0.087 mm^{-1}, *Dcalc* = 1.316 g/cm^3, 36115 reflections measured (4.34° ≤ 2θ ≤ 62.358°), 7861 unique (R_{int} = 0.0519, R_{sigma} = 0.0488) which were used in all calculations. The final R_1 was 0.0644 (I > 2σ(I)) and wR_2 was 0.2011 (all data). The structure was modelled containing one toluene molecule that was projected over symmetry in a 50:50 % occupancy. This toluene molecule was fixed using restraints (ISOR, DFIX, SADI, FLAT, RIGU, and SIMU).

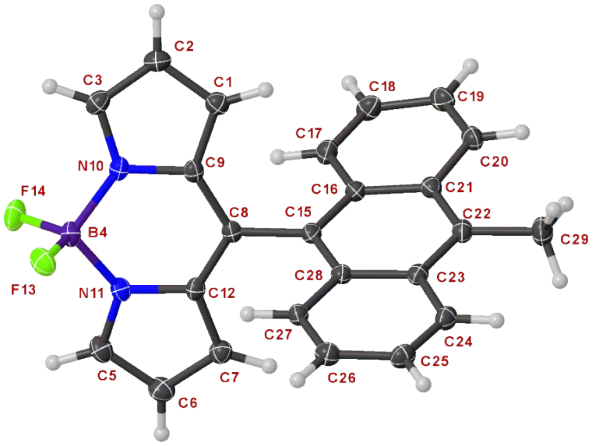

Figure S21: Molecular structure of **2** (thermal displacement 50%).

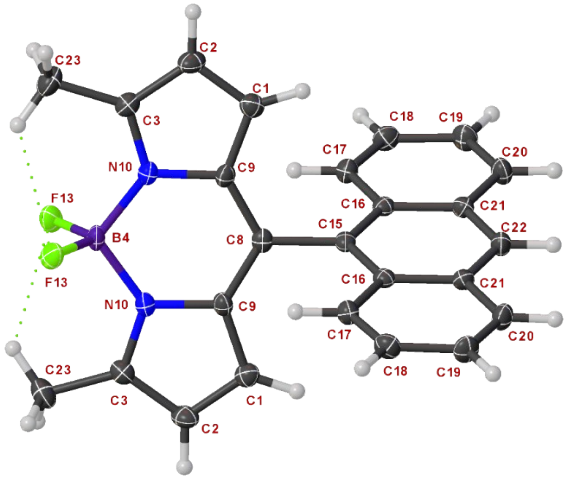

Figure S22: Molecular structure of **5** (thermal displacement 50%).

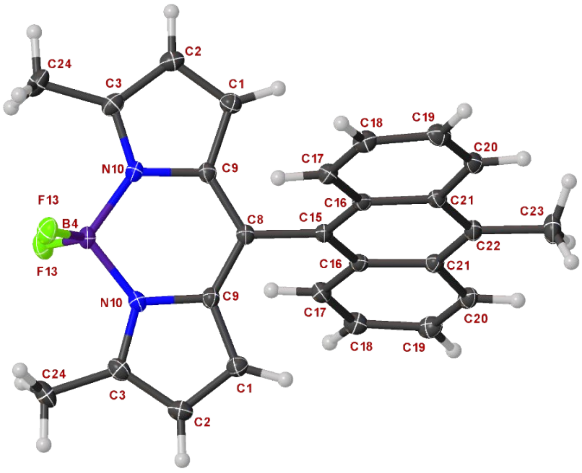

Figure S23: Molecular structure of **6** (thermal displacement 50%).

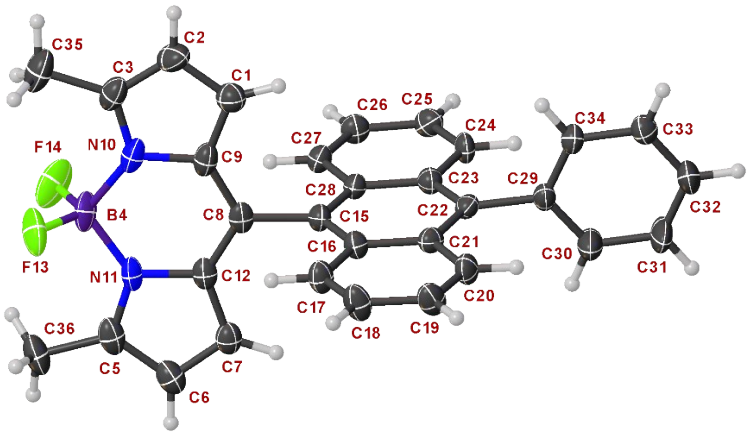

Figure S24: Molecular structure of **7** (thermal displacement 50%).

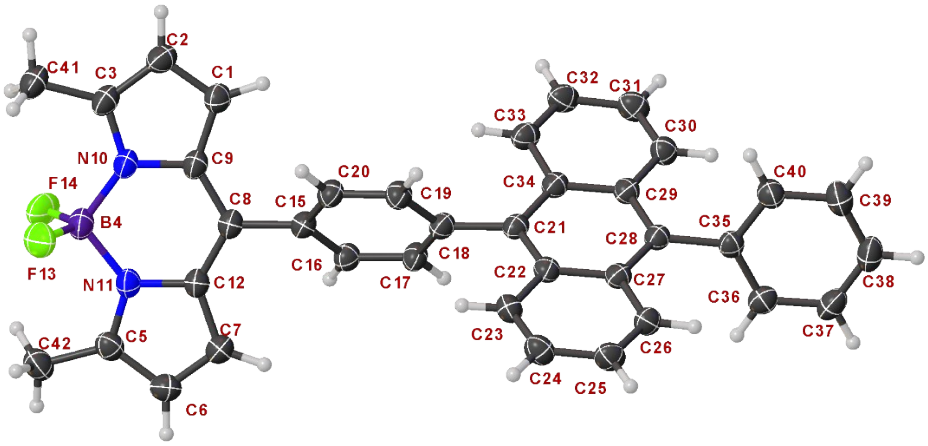

Figure S25: Molecular structure of **8** (thermal displacement 50%).

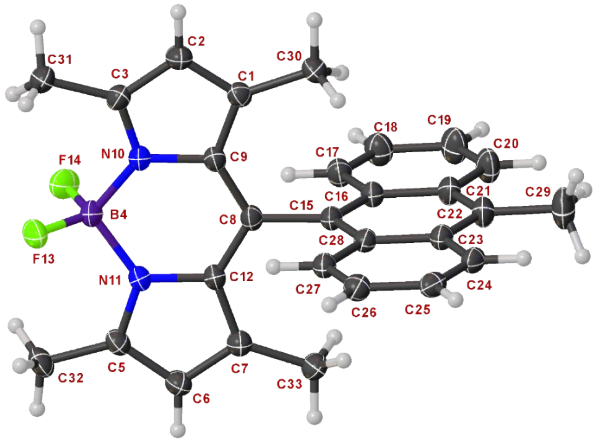

Figure S26: Molecular structure of **10** (thermal displacement 50%).

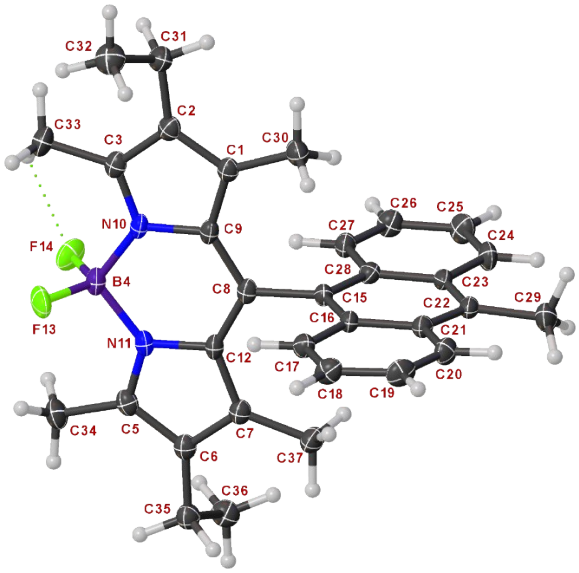

Figure S27: Molecular structure of **14** (thermal displacement 50%).

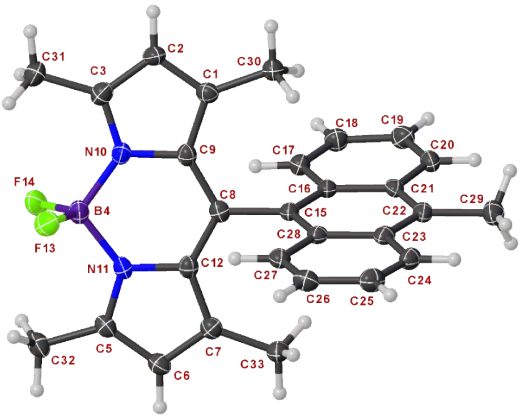

Figure S28: Molecular structure of **10** (thermal displacement 50%).

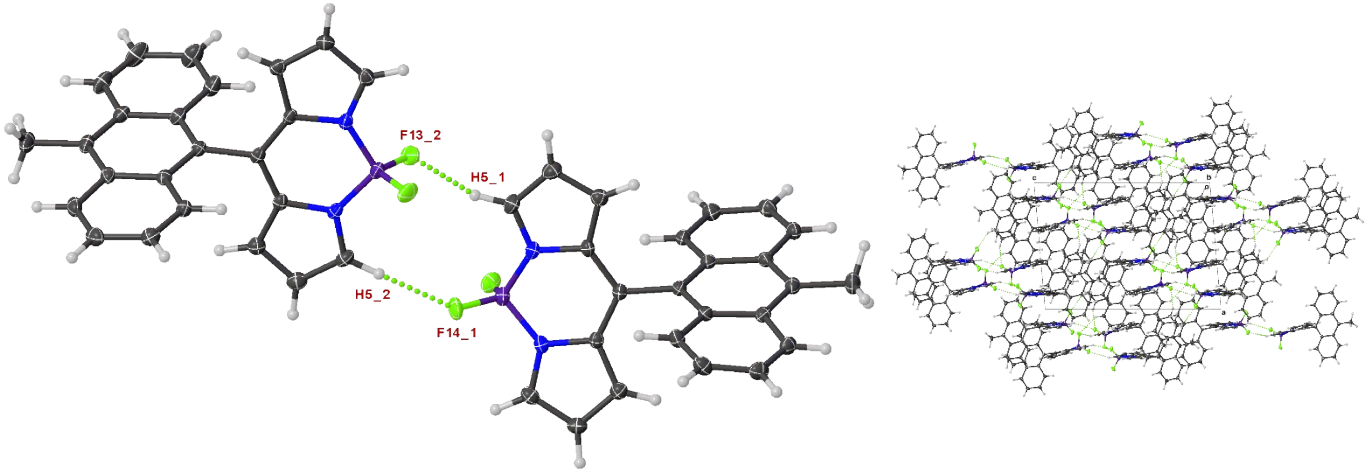

Figure S29: Left: Expanded structure of **2** displaying the H···F close contacts present in the structure (thermal displacement 50%). Atoms involved in the H···F have been labelled. Right: Moiety packing of **2** looking down the b-axis showing the repeating head-to-head interactions between individual molecules within the unit cell.

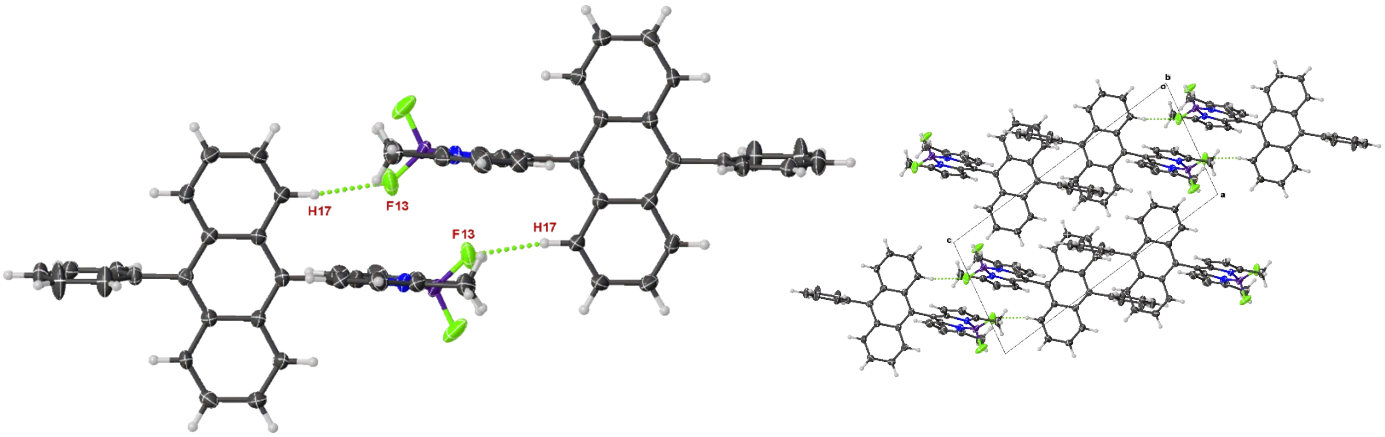

Figure S30: Left: Expanded structure of **7** displaying the H···F close contacts present in the structure (thermal displacement 50%). Atoms involved in the H···F have been labelled. Right: Moiety packing of **7** looking down the b-axis showing the repeating head-to-head interactions between individual molecules within the unit cell.

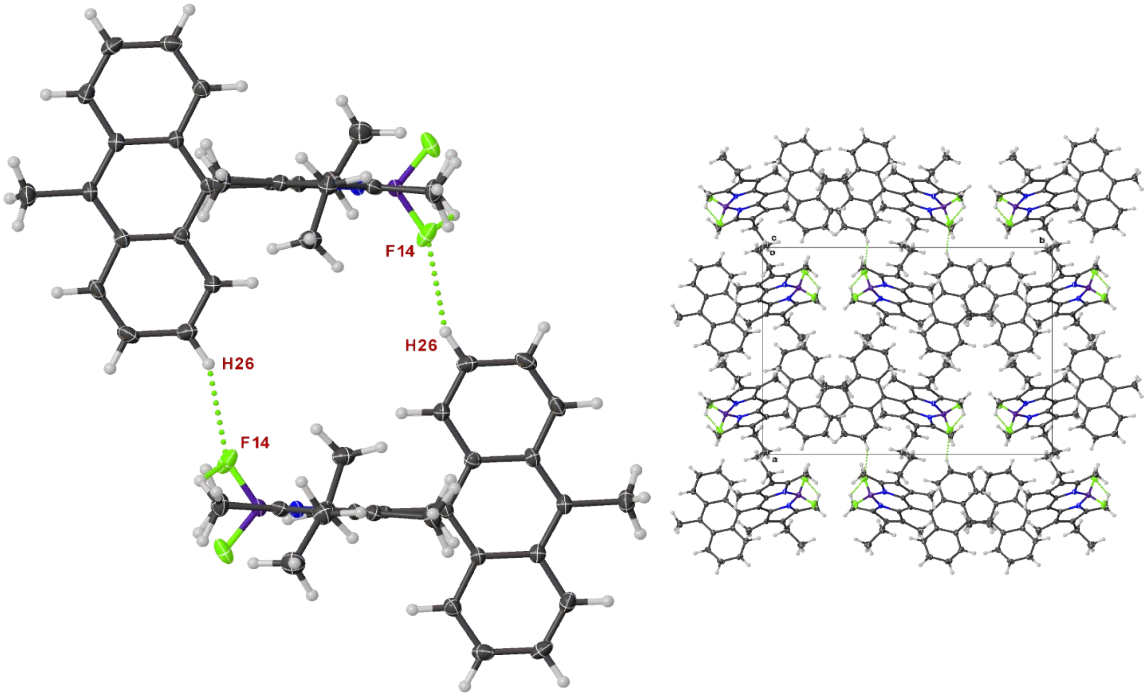

Figure S31: Left: Expanded structure of **14** displaying the H···F close contacts present in the structure (thermal displacement 50%). Atoms involved in the H···F have been labelled. Right: Moiety packing of **14** looking down the a-axis showing the repeating head-to-head interactions between individual molecules within the unit cell.

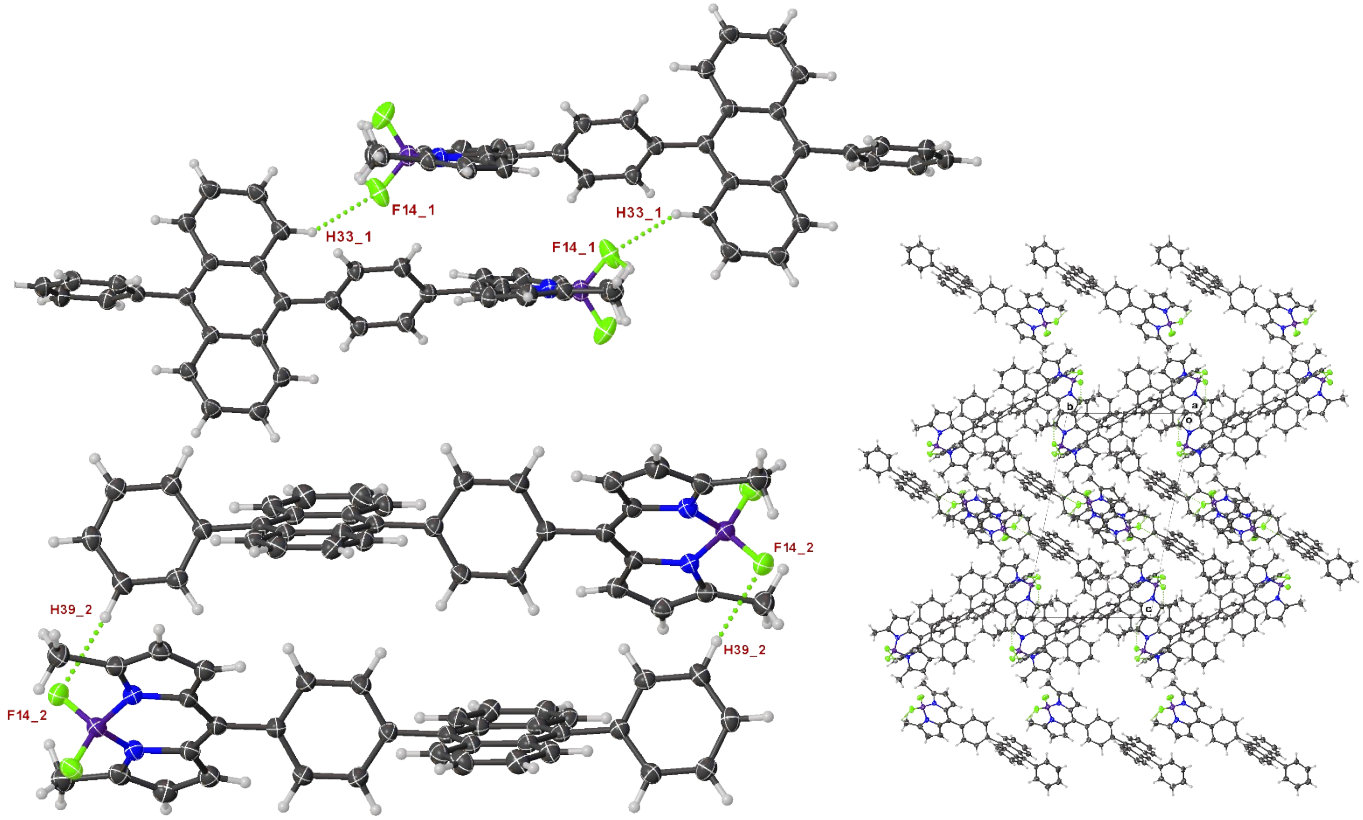

Figure S32: Left: Expanded structure of **8** displaying both independent molecules and the H···F close contacts present in each motif (thermal displacement 50%). Atoms involved in the H···F have been labelled. Right: Moiety packing of **8** looking down the a-axis showing the repeating head-to-head interactions between individual molecules within the unit cell.

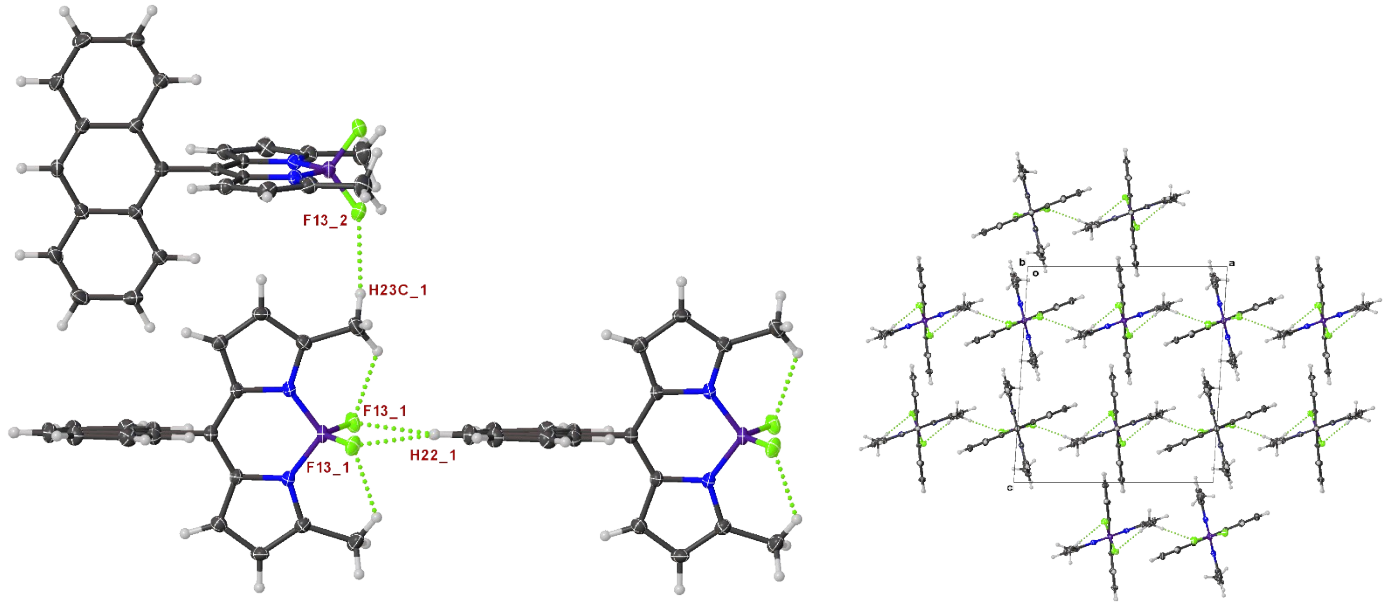

Figure S33: Left: Expanded structure of **5** displaying the H···F close contacts present in the structure (thermal displacement 50%). Atoms involved in the H···F have been labelled. Right: Moiety packing of **5** looking down the b-axis showing an interesting alternation intra- to intermolecular halogen bonded network.

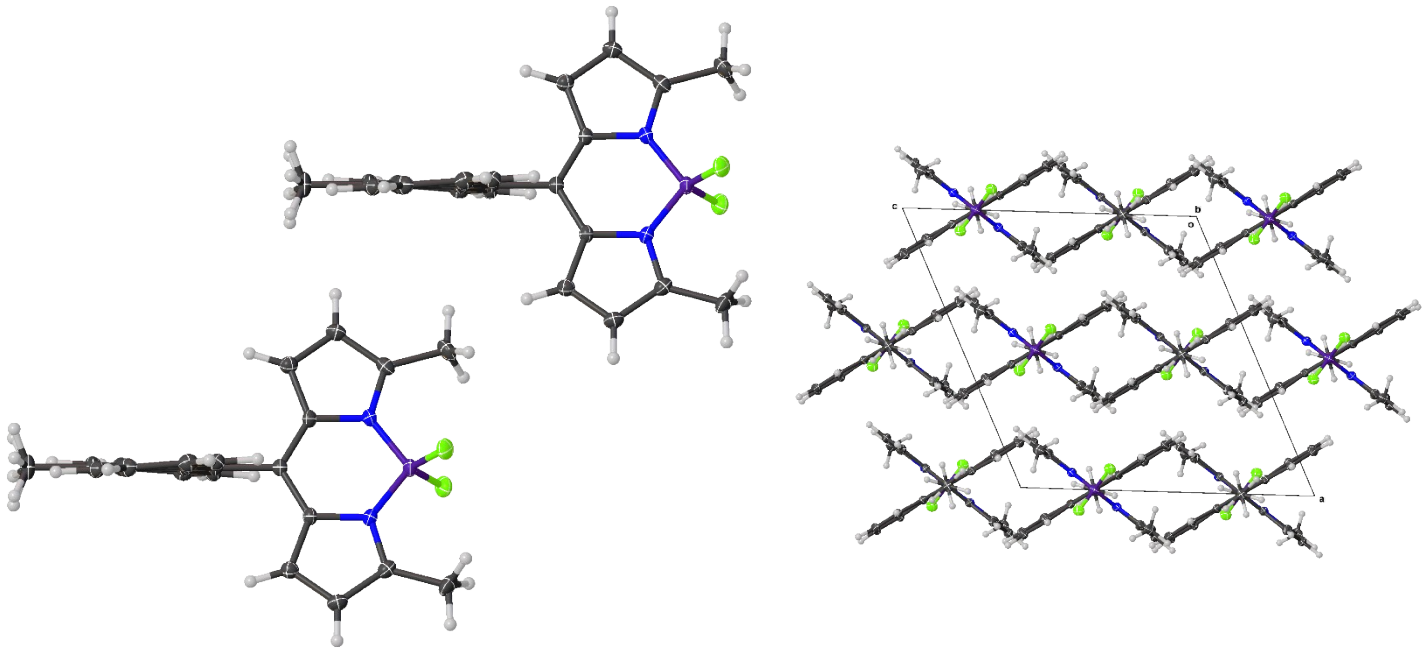

Figure S34: Left: Expanded structure of **6** displaying the absence of any H···F close contacts present in the structure (thermal displacement 50%). Right: Moiety packing of **6** looking down the b-axis showing stacking between individual BODIPY and anthracene subunits.

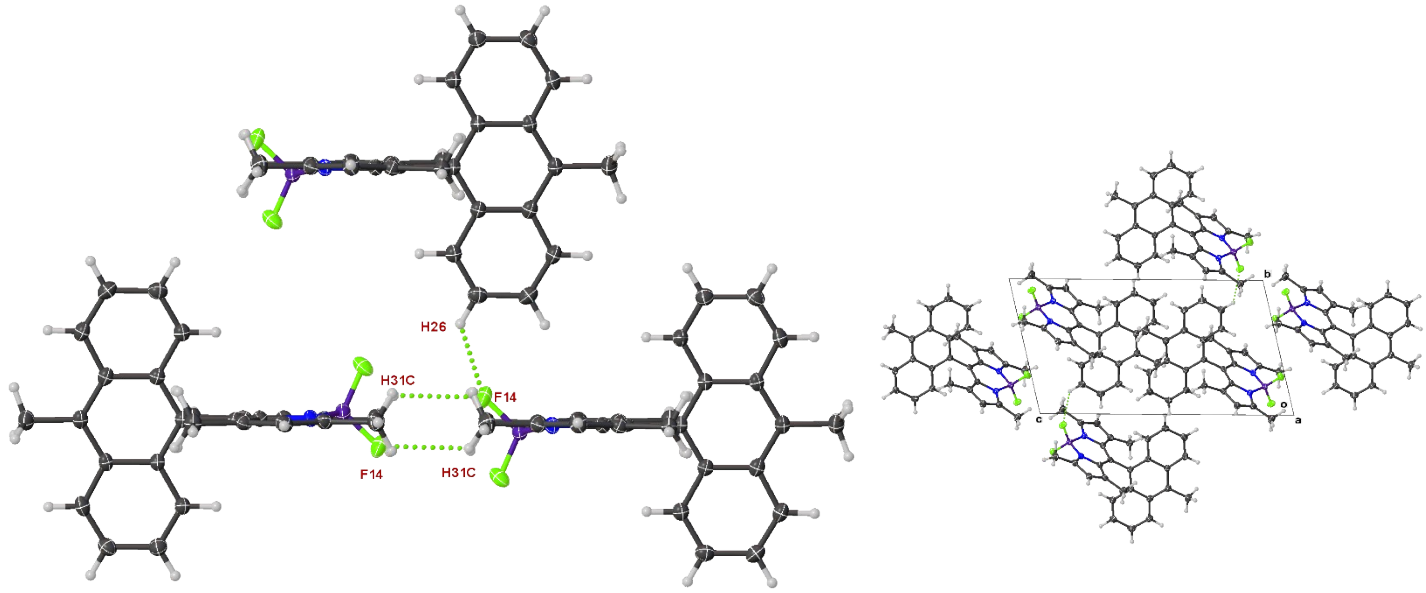

Figure S35: Left: Expanded structure of **10** displaying the H···F close contacts present in the structure (thermal displacement 50%). Atoms involved in the H···F have been labelled. Right: Moiety packing of **D10** looking down the a-axis showing the repeating head-to-head interactions between individual molecules within the unit cell.

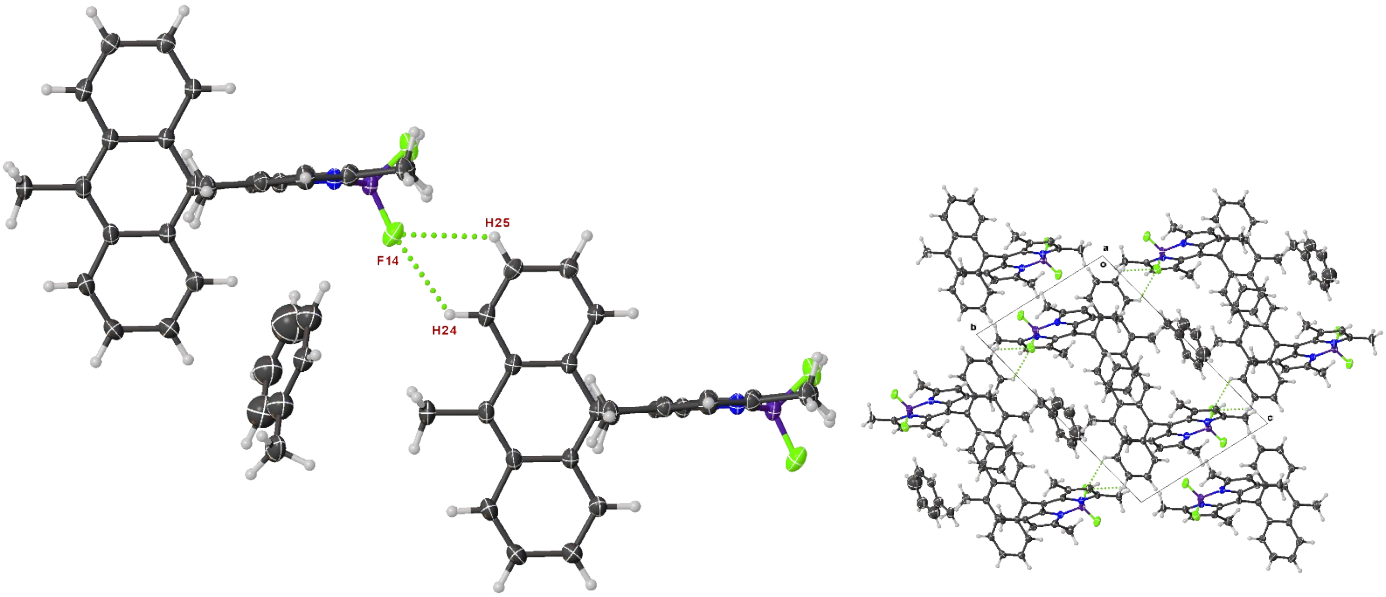

Figure S36: Left: Expanded structure of **10** displaying the H···F close contacts present in the structure (thermal displacement 50%). Atoms involved in the H···F have been labelled. Right: Moiety packing of **10** looking down the a-axis showing the repeating head-to-tail interactions between individual molecules within the unit cell.

F. Computational Details

All calculations were performed using GAMESS quantum chemistry package[5] in spin unrestricted formalism using M06-2X meta-GGA functional[6] with 54% of Hartree-Fock exchange part. This method is referred to as DFT-SCF. The Karlsruhe valence triple-zeta KTZV basis set[7] incorporated in GAMESS quantum chemistry package was employed. Solvent was modeled using iterative isotropic polarizable continuum model (PCM)[8] calculation with parameters corresponding to ethanol. Ground electronic state geometry of the dyads **1**, **5**, **9**, **13** and **2**, **6**, **10**, **14** were optimized in C_{2v} and C_s symmetry, respectively. Using optimized geometries, vertical excitation energies were evaluated within the DFT-SCF/(PCM) models separately for BODIPY local excited states and charge-transfer state.

All the involved excited states have been computed in both singlet and triplet spin states. In a single determinant DFT-SCF formalism singlet excited states have been converged from respective triplet orbital vectors which were chosen as an initial guess. In some difficult cases the convergence was achieved using the orbitals generated for cation-radical doublet state.

Symmetry reduction due to the twisting of BODIPY and anthracene fragments breaks the SCF stage convergence for excited states thus precluding the evaluation of excitation energies by means of DFT-SCF. Thus, the minimal multireference complete active space (CASSCF) approach[9] with four electrons and four orbitals (two HOMO/LUMO pairs on the anthracene BODIPY fragments, was used in frozen scan calculations for dyad **1** within C_2 symmetry. Additionally, calculation using Nakano's MRMP perturbative method[10] on state-specific converged CASSCF(4/4) orbitals for molecule **1** were made in order to check the quality of DFT-SCF excitation energies. These data showed the good consistence of the results within 0.15 eV.

Table S3: Atomic coordinates (Å) for optimized structure of **BADs**.

Dyad 1			Dyad 2			Dyad 5		
C	-3.64856	0.00000	-3.21050	C	0.11947	-5.21575	0.00000	C	-3.65615	0.00000	2.09571
C	3.64856	-0.00000	-3.21050	C	2.52459	3.11018	0.00000	C	3.65615	0.00000	2.09571
C	-3.65650	0.00000	-1.78295	C	-2.51225	3.11149	0.00000	C	-3.64844	0.00000	3.52334
C	3.65650	0.00000	-1.78295	C	3.37130	1.97958	0.00000	C	3.64844	0.00000	3.52334
C	-0.00000	-2.54781	0.66059	C	-3.35937	1.98129	0.00000	C	-0.00000	-3.36217	-1.46677
C	-0.00000	2.54781	0.66059	C	0.05143	-3.70592	0.00000	C	-0.00000	3.36217	-1.46677
C	-0.00000	-3.36561	1.78150	C	-0.02985	-3.66248	-2.49115	C	-0.00000	-2.91434	-4.04875
C	-0.00000	3.36561	1.78150	C	-0.02985	-3.66248	2.49115	C	0.00000	2.91434	-4.04875
C	-0.00000	-2.51839	2.91178	C	0.01301	-2.99800	-1.21874	C	-0.00000	-2.52575	-2.61154
C	-0.00000	2.51839	2.91178	C	0.01301	-2.99800	1.21874	C	-0.00000	2.52575	-2.61154
C	-2.46896	0.00000	-3.88872	C	-0.06444	-2.96576	-3.66048	C	-0.00000	-2.54465	-0.34812
C	2.46896	-0.00000	-3.88872	C	-0.06444	-2.96576	3.66048	C	-0.00000	2.54465	-0.34812
C	-2.49041	0.00000	-1.07968	C	2.55294	0.85894	0.00000	C	-2.48983	0.00000	1.39283
C	2.49041	-0.00000	-1.07968	C	-2.54138	0.86026	0.00000	C	2.48983	0.00000	1.39283
C	-0.00000	-1.20636	1.11907	C	1.21188	1.31783	0.00000	C	-2.46891	0.00000	4.20168
C	-0.00000	1.20636	1.11907	C	-1.20026	1.31861	0.00000	C	2.46891	-0.00000	4.20168
C	-1.21789	0.00000	-3.19150	C	-0.00061	-1.56037	-1.22033	C	-0.00000	-1.20513	-0.80796
C	1.21789	-0.00000	-3.19150	C	-0.00061	-1.56037	1.22033	C	-0.00000	1.20513	-0.80796
C	-1.22526	0.00000	-1.75584	C	-0.05322	-1.54171	-3.65391	C	-1.22458	0.00000	2.06889
C	1.22526	0.00000	-1.75584	C	-0.05322	-1.54171	3.65391	C	1.22458	-0.00000	2.06889
C	0.00000	0.00000	-3.87020	C	0.00566	-0.86964	0.00000	C	-1.21765	0.00000	3.50460
C	0.00000	0.00000	-1.06789	C	-0.02416	-0.86421	-2.47477	C	1.21765	0.00000	3.50460
C	0.00000	0.00000	0.42320	C	-0.02416	-0.86421	2.47477	C	-0.00000	0.00000	-0.11228
H	-4.58763	0.00000	-3.74476	C	0.00567	0.62147	0.00000	C	-0.00000	0.00000	1.37934
H	4.58763	-0.00000	-3.74476	H	-0.87916	-5.65947	0.00000	C	-0.00000	0.00000	4.18367
H	-0.00000	-4.43931	1.80641	H	0.64969	-5.59026	-0.87089	H	-4.60190	0.00000	1.57311
H	0.00000	4.43931	1.80641	H	0.64969	-5.59026	0.87089	H	4.60190	-0.00000	1.57311
H	-4.60226	0.00000	-1.26046	H	2.77832	4.15611	0.00000	H	-4.58758	0.00000	4.05759
H	4.60226	0.00000	-1.26046	H	-2.76552	4.15753	0.00000	H	4.58758	-0.00000	4.05759
H	-0.00000	-2.84171	-0.37450	H	4.44501	2.00409	0.00000	H	-0.00000	-4.43672	-1.49363
H	-0.00000	2.84171	-0.37450	H	-4.43307	2.00618	0.00000	H	-0.00000	4.43672	-1.49363
H	-0.00000	-2.77164	3.95783	H	-0.05385	-4.74012	-2.52334	H	-0.00000	-3.99685	-4.14483
H	-0.00000	2.77164	3.95783	H	-0.05385	-4.74012	2.52334	H	0.00000	3.99685	-4.14483
H	-2.44985	0.00000	-4.97055	H	-0.10339	-3.49184	-4.60360	H	-0.00000	-2.83631	0.68778
H	2.44985	0.00000	-4.97055	H	-0.10339	-3.49184	4.60360	H	0.00000	2.83631	0.68778
H	-2.50709	0.00000	0.00130	H	-2.83476	-0.17498	0.00000	H	-0.87706	-2.50794	-4.55375
H	2.50709	-0.00000	0.00130	H	2.84608	-0.17634	0.00000	H	0.87706	-2.50794	-4.55375
H	-0.00000	0.00000	-4.95358	H	-0.07366	-1.00346	-4.59051	H	-0.87706	2.50794	-4.55375
N	-0.00000	-1.23480	2.51903	H	-0.07366	-1.00346	4.59051	H	0.87706	2.50794	-4.55375
N	0.00000	1.23480	2.51903	H	-0.02314	0.21673	-2.47018	H	-2.50465	0.00000	0.31192
B	-0.00000	0.00000	3.43941	H	-0.02314	0.21673	2.47018	H	2.50465	-0.00000	0.31192
F	-1.15093	0.00000	4.25974	N	1.24081	2.71792	0.00000	H	-2.44994	0.00000	5.28357
F	1.15093	0.00000	4.25974	N	-1.22857	2.71863	0.00000	H	2.44994	0.00000	5.28357
				B	0.00635	3.63880	0.00000	H	-0.00000	0.00000	5.26709
				F	0.00662	4.45920	-1.15107	N	-0.00000	-1.23684	-2.20974
				F	0.00662	4.45920	1.15107	N	0.00000	1.23684	-2.20974
								B	-0.00000	0.00000	-3.11984
								F	-1.15159	0.00000	-3.95271
								F	1.15159	-0.00000	-3.95271

Dyad 6			Dyad 9			Dyad 10		
C	-3.65615	0.00000	C	-3.64850	0.00000	C	5.47773	0.13010
C	3.65615	0.00000	C	3.64850	0.00000	C	-4.30732	2.90244
C	-3.64844	0.00000	C	-3.65450	0.00000	C	-4.31820	-2.88266
C	3.64844	0.00000	C	3.65450	-0.00000	C	3.96809	0.05605
C	-0.00000	-3.36217	C	-0.00000	-3.36036	C	3.92287	-0.02757
C	-0.00000	3.36217	C	-0.00000	3.36036	C	3.92287	-0.02757
C	-0.00000	-2.91434	C	-0.00000	-3.07082	C	-1.73275	3.36514
C	0.00000	2.91434	C	-0.00000	3.07082	C	-2.86698	2.52426
C	-0.00000	-2.52575	C	-0.00000	-2.89241	C	-2.87639	-2.51000
C	-0.00000	2.52575	C	-0.00000	2.89241	C	-1.74548	-3.35510
C	-0.00000	-2.54465	C	-0.00000	-2.56793	C	3.25941	0.01454
C	-0.00000	2.54465	C	-0.00000	2.56793	C	3.25941	0.01454
C	-2.48983	0.00000	C	-2.48669	0.00000	C	0.81844	3.06869
C	2.48983	0.00000	C	2.48669	0.00000	C	0.80674	-3.06908
C	-2.46891	0.00000	C	-2.46996	0.00000	C	3.22439	-0.06562
C	2.46891	-0.00000	C	2.46996	0.00000	C	3.22439	-0.06562
C	-0.00000	-1.20513	C	-0.00000	-2.51703	C	-0.59278	2.57005
C	-0.00000	1.20513	C	0.00000	2.51703	C	-0.60235	-2.56432
C	-1.22458	0.00000	C	-1.21776	0.00000	C	1.82202	-0.00319
C	1.22458	-0.00000	C	1.21776	0.00000	C	1.82202	-0.00319
C	-1.21765	0.00000	C	-1.22311	0.00000	C	1.80014	-0.05877
C	1.21765	0.00000	C	1.22311	0.00000	C	1.80014	-0.05877
C	-0.00000	0.00000	C	-0.00000	-1.21185	C	-1.04872	1.21517
C	-0.00000	0.00000	C	0.00000	1.21185	C	-1.05300	-1.20783
C	-0.00000	0.00000	C	0.00000	0.00000	C	1.13031	0.00210
H	-4.60190	0.00000	C	0.00000	0.00000	C	1.12364	-0.03004
H	4.60190	-0.00000	C	0.00000	0.00000	C	1.12364	-0.03004
H	-4.58758	0.00000	H	-4.59962	0.00000	C	-0.36108	0.00259
H	4.58758	-0.00000	H	4.59962	0.00000	H	5.84999	0.66191
H	-0.00000	-4.43672	H	-4.58842	0.00000	H	5.84999	0.66191
H	-0.00000	4.43672	H	4.58842	0.00000	H	-4.41061	3.98441
H	-0.00000	-3.99685	H	-0.00000	-4.43589	H	-4.42561	-3.96423
H	0.00000	3.99685	H	0.00000	4.43589	H	5.92604	-0.86650
H	-0.00000	-2.83631	H	-0.00000	-4.15922	H	-4.80931	2.49203
H	0.00000	2.83631	H	0.00000	4.15922	H	-4.80931	2.49203
H	-0.87706	-2.50794	H	-0.00000	-3.97416	H	-4.81865	-2.47037
H	0.87706	-2.50794	H	-0.00000	3.97416	H	-4.81865	-2.47037
H	-0.87706	2.50794	H	-0.87835	-2.72861	H	5.00065	-0.04831
H	0.87706	2.50794	H	0.87835	-2.72861	H	5.00065	-0.04831
H	-2.50465	0.00000	H	-0.87835	2.72861	H	-1.76130	4.44073
H	2.50465	-0.00000	H	0.87835	2.72861	H	-1.77803	-4.43058
H	-2.44994	0.00000	H	-2.49837	0.00000	H	0.82281	4.15711
H	2.44994	0.00000	H	2.49837	-0.00000	H	0.80615	-4.15751
H	-0.00000	0.00000	H	-0.87680	-2.48105	H	3.74946	-0.10411
N	-0.00000	-1.23684	H	0.87680	-2.48105	H	3.74946	-0.10411
N	0.00000	1.23684	H	-0.87680	2.48105	H	1.36630	2.72414
B	-0.00000	0.00000	H	0.87680	2.48105	H	1.36630	2.72414
F	-1.15159	0.00000	H	-2.45296	0.00000	H	1.35587	-2.72708
F	1.15159	-0.00000	H	2.45296	-0.00000	H	1.35587	-2.72708
			H	-0.00000	0.00000	H	1.26093	-0.08219
			N	-0.00000	-1.23399	H	1.26093	-0.08219
			N	0.00000	1.23399	H	0.04269	-0.03230
			B	-0.00000	0.00000	H	0.04269	-0.03230
			F	-1.15120	0.00000	N	-2.45445	1.24035
			F	1.15120	-0.00000	N	-2.45886	-1.22761
						B	-3.36246	0.00800

						F	-4.20037	0.00951 -1.15143
						F	-4.20037	0.00951 1.15143
						H	-1.35236	-0.08380 4.58767
						H	-0.13436	-0.03331 -2.46124

Dyad 13			**Dyad 14**		
C	-4.87357	0.00000 -1.48010	C	4.21973	2.87882 0.00000
C	4.87357	0.00000 -1.48010	C	1.65211	4.87815 0.00000
C	-0.00000	-3.65423 2.11673	C	-5.56977	0.12681 0.00000
C	-0.00000	3.65423 2.11673	C	1.67371	-4.86868 0.00000
C	-0.00000	-3.64847 3.54452	C	4.23225	-2.85812 0.00000
C	0.00000	3.64847 3.54452	C	-4.01455	-0.02997 -2.49163
C	-3.37512	0.00000 -1.46194	C	-4.01455	-0.02997 2.49163
C	3.37512	0.00000 -1.46194	C	-4.06007	0.05336 0.00000
C	-3.06525	0.00000 1.08729	C	2.77177	2.52654 0.00000
C	3.06525	0.00000 1.08729	C	1.63834	3.37961 0.00000
C	-2.86885	0.00000 -4.04174	C	1.65319	-3.37022 0.00000
C	2.86885	-0.00000 -4.04174	C	2.78271	-2.51223 0.00000
C	-0.00000	-2.48617 1.41542	C	-3.31590	-0.06781 -3.65995
C	-0.00000	2.48617 1.41542	C	-3.31590	-0.06781 3.65995
C	-0.00000	-2.47006 4.22530	C	-3.35122	0.01233 -1.21837
C	0.00000	2.47006 4.22530	C	-3.35122	0.01233 1.21837
C	-2.51925	0.00000 -2.59318	C	-0.91040	3.06204 0.00000
C	2.51925	-0.00000 -2.59318	C	-0.89693	-3.06454 0.00000
C	-2.56717	0.00000 -0.32440	C	0.50284	2.56862 0.00000
C	2.56717	0.00000 -0.32440	C	0.51396	-2.56422 0.00000
C	-0.00000	-1.22277 2.09474	C	-1.89163	-0.06047 -3.65164
C	-0.00000	1.22277 2.09474	C	-1.89163	-0.06047 3.65164
C	-0.00000	-1.21766 3.53012	C	-1.91387	-0.00471 -1.21790
C	-0.00000	1.21766 3.53012	C	-1.91387	-0.00471 1.21790
C	-1.21248	0.00000 -0.77491	C	0.95666	1.21529 0.00000
C	1.21248	0.00000 -0.77491	C	0.96169	-1.20900 0.00000
C	0.00000	0.00000 -0.08635	C	-1.21530	-0.03140 -2.47098
C	0.00000	0.00000 1.40511	C	-1.21530	-0.03140 2.47098
C	0.00000	0.00000 4.21010	C	-1.22157	0.00092 0.00000
N	-1.23453	0.00000 -2.17743	C	0.26988	0.00185 0.00000
N	1.23453	0.00000 -2.17743	N	2.35921	1.24077 0.00000
B	0.00000	0.00000 -3.08124	N	2.36438	-1.22825 0.00000
F	-0.00000	-1.15132 -3.92167	B	3.26563	0.00816 0.00000
F	-0.00000	1.15132 -3.92167	F	4.10587	0.00996 -1.15161
H	-5.27819	-0.88091 -0.97834	F	4.10587	0.00996 1.15161
H	5.27819	-0.88091 -0.97834	H	4.35773	3.95602 0.00000
H	-5.27819	0.88091 -0.97834	H	2.66934	5.26382 0.00000
H	5.27819	0.88091 -0.97834	H	2.69272	-5.24962 0.00000
H	-5.25649	0.00000 -2.49835	H	4.37495	-3.93472 0.00000
H	5.25649	-0.00000 -2.49835	H	-5.94224	0.65852 -0.87105
H	-0.00000	-4.59928 1.59278	H	-5.94224	0.65852 0.87105
H	-0.00000	4.59928 1.59278	H	-6.01800	-0.86983 0.00000
H	-0.00000	-4.58851 4.07731	H	4.71222	2.45613 -0.87641
H	-0.00000	4.58851 4.07731	H	4.71222	2.45613 0.87641
H	-4.15368	0.00000 1.09843	H	1.14918	5.28131 -0.88091
H	4.15368	-0.00000 1.09843	H	1.14918	5.28131 0.88091
H	-3.94580	0.00000 -4.18180	H	1.17265	-5.27417 -0.88092
H	3.94580	-0.00000 -4.18180	H	1.17265	-5.27417 0.88092
H	-2.72108	-0.87816 1.63575	H	4.72290	-2.43333 -0.87642
H	2.72108	-0.87816 1.63575	H	4.72290	-2.43333 0.87642
H	-2.72108	0.87816 1.63575	H	-5.09234	-0.05113 -2.52555
H	2.72108	0.87816 1.63575	H	-5.09234	-0.05113 2.52555

H	-2.44547	-0.87641	-4.53366	H	-0.92536	4.15044	0.00000
H	2.44547	-0.87641	-4.53366	H	-0.90635	-4.15300	0.00000
H	-2.44547	0.87641	-4.53366	H	-3.84091	-0.10649	-4.60379
H	2.44547	0.87641	-4.53366	H	-3.84091	-0.10649	4.60379
H	-0.00000	-2.45338	5.30727	H	-1.45766	2.71533	-0.87794
H	-0.00000	2.45338	5.30727	H	-1.45766	2.71533	0.87794
H	-0.00000	-2.49679	0.33431	H	-1.44562	-2.72067	-0.87817
H	-0.00000	2.49679	0.33431	H	-1.44562	-2.72067	0.87817
H	0.00000	0.00000	5.29358	H	-1.35236	-0.08380	-4.58767

G. Synthetic Procedures and Characterization

Anthracene-9-carbaldehyde, 10-methylanthracene-9-carbaldehyde, pyrene-1-carbaldehyde, pyrrole, 2,4-dimethylpyrrole and 3-ethyl-2,4-dimethylpyrrole were purchased from Sigma-Aldrich. 2-Methylpyrrole,[11] 10-phenylanthracene-9-carbaldehyde,[12] 4-(10-phenylanthracen-9-yl)benzaldehyde[13] were prepared according to reported procedures.

BADs **5-16** were prepared according to a previously described general procedure.[2] BADs **1-4** were prepared according to a previously reported procedure.[14]

8-(Anthracen-9-yl)-4,4-difluoro-4-bora-3a,4a-diaza-s-indacene (1). Obtained in 17% yield. Orange solid, m.p. > 300 °C. R_f: 0.32 (DCM-hexane, 1:1). ^{1}H NMR (400 MHz, $CDCl_3$): δ 8.61 (s, 1H), 8.06 (d, *J* = 8.5 Hz, 2H), 7.99 (s, 2H), 7.79 (dt, *J* = 4.7, 2.4 Hz, 2H), 7.51 – 7.45 (m, 2H), 7.40 (ddd, *J* = 8.6, 6.5, 1.3 Hz, 2H), 6.36 (d, *J* = 5.3 Hz, 4H). ^{13}C NMR (100 MHz, $CDCl_3$): δ 144.63, 131.24, 130.77, 129.10, 128.29, 126.77, 125.95, 125.56, 118.84. UV-vis (DCM): λ_{max} [nm] (log *ε*) = 349 (4.11), 367 (4.23), 386 (4.16), 506 (4.55). HRMS (ESI): *m/z* found 369.1343, calcd for $[M+H]^+$ $C_{23}H_{16}BF_2N_2$ 369.1373.	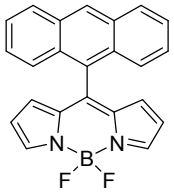
8-(10-Methylanthracen-9-yl)-4,4-difluoro-4-bora-3a,4a-diaza-s-indacene (2). Obtained in 41% yield. Brown solid, m.p. > 300 °C. R_f: 0.20 (DCM-hexane, 1:1). ^{1}H NMR (400 MHz, $CDCl_3$): δ 8.37 (d, *J* = 8.9 Hz, 2H), 8.00 (s, 2H), 7.83 (d, *J* = 8.7 Hz, 2H), 7.57 – 7.49 (m, 2H), 7.44 – 7.37 (m, 2H), 6.38 (s, 4H), 3.22 (s, 3H). ^{13}C NMR (100 MHz, $CDCl_3$): δ 146.46, 144.66, 137.34, 133.47, 131.44, 130.60, 129.47, 127.01, 126.35, 125.60, 125.20, 124.89, 119.00, 14.61. UV–vis (DCM): λ_{max} [nm] (log ε) = 357 (4.10), 376 (4.23), 397 (4.17), 506 (4.74). HRMS (ESI): *m/z* found 520.1941, calcd for M^+ $C_{35}H_{23}BF_2N_2$ 520.1933.	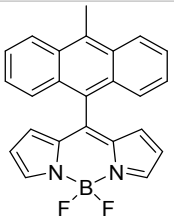
8-(10-Phenylanthracen-9-yl)-4,4-difluoro-4-bora-3a,4a-diaza-s-indacene (3). Obtained in 41% yield. Green powder, m.p. > 300 °C. R_f: 0.45 (DCM-hexane, 1:1). ^{1}H NMR (400 MHz, $CDCl_3$): δ 8.03 (s, 2H), 7.88 – 7.85 (m, 2H), 7.73 – 7.70 (m, 2H), 7.66 – 7.56 (m, 3H), 7.53 – 7.47 (m, 2H), 7.43 – 7.33 (m, 4H), 6.49 (d, J = 4.1 Hz, 2H), 6.42 (d, J = 3.1 Hz, 2H). ^{13}C NMR (100 MHz, CDCl3): δ 146.04, 144.82, 139.96, 138.37, 137.25, 131.53, 131.22, 130.61, 129.60, 128.69, 128.03, 127.23, 126.63, 126.60, 126.32, 125.60, 119.07. UV–vis (DCM): λ_{max} [nm] (log ε) = 356 (4.21), 374 (4.35), 394 (4.29), 506 (4.84). HRMS (ESI): *m/z* found 444.1630, calcd for M^+ $C_{29}H_{19}BF_2N_2$ 444.1609.	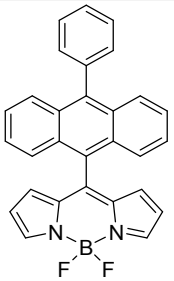
8-(4-(10-Phenylanthracen-9-yl)phenyl)-4,4-difluoro-4-bora-3a,4a-diaza-s-indacene (4). Obtained in 11% yield, m.p. > 300 °C. R_f: 0.39 (DCM-hexane, 1:1). ^{1}H NMR (400 MHz, $CDCl_3$): δ 8.02 (s, 2H), 7.84 (d, J = 8.0 Hz, 2H), 7.72 (ddd, J = 10.1, 8.0, 4.8 Hz, 5H), 7.66 – 7.55 (m, 4H), 7.53 – 7.48 (m, 2H), 7.44 – 7.34 (m, 4H), 7.23 – 7.18 (m, 2H), 6.65 (dd, J = 5.5, 4.2 Hz, 2H). ^{13}C NMR (100 MHz, $CDCl_3$): δ 144.24, 142.22, 138.77, 137.90 , 135.31, 131.63, 131.20, 130.66, 129.86, 129.64, 128.44, 127.93, 127.60, 127.21, 126.34, 125.48, 125.12, 118.64. UV-vis (DCM): λ_{max} [nm] (log *ε*) = 356 (4.32), 374 (4.35), 394 (4.23), 502 nm (4.72). HRMS (ESI): *m/z* found 520.1941, calcd for M^+ $C_{35}H_{23}BN_2F_2$ 520.1934.	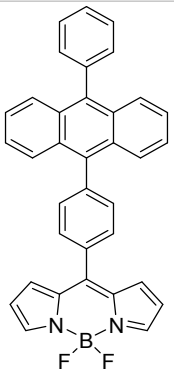
3,5-Dimethyl-8-(anthracen-9-yl)-4,4-difluoro-4-bora-3a,4a-diaza-s-indacene (5). Obtained in 37% yield. Red powder, m.p. > 300 °C. R_f: 0.47 (DCM-hexane, 1:1). ^{1}H NMR (400 MHz, $CDCl_3$): δ 8.57 (s, 1H), 8.03 (d, *J* = 8.5 Hz, 2H), 7.86 (dd, *J* = 8.8, 0.8 Hz, 2H), 7.50 – 7.42 (m, 2H), 7.41 – 7.34 (m, 2H), 6.12 (dd, *J* = 16.3, 4.1 Hz, 4H), 2.70 (s, 6H). ^{13}C NMR (100 MHz, $CDCl_3$): δ 158.08, 139.94, 136.34, 130.96, 130.86, 130.11, 128.61, 128.27, 127.11, 126.50, 126.30, 125.51, 119.84, 15.04. UV–vis (DCM): λ_{max} [nm] (log ε) = 349 (4.07), 366 (4.19), 386 (4.11), 506 (4.92). HRMS (ESI): m/z found 397.1701, calcd for $[M+H]^+$ $C_{25}H_{20}BN_2F_2$ 397.1686.	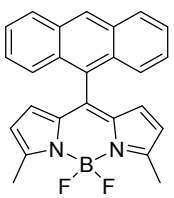

3,5-Dimethyl-8-(methylanthracen-9-yl)-4,4-difluoro-4-bora-3a,4a-diaza-s-indacene (6). Obtained in 20% yield. Analytical data are in accordance with previous reports.[5]	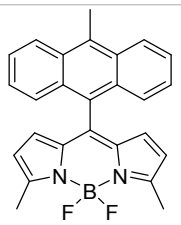
3,5-Dimethyl-8-(10-phenylanthracen-9-yl)-4,4-difluoro-4-bora-3a,4a-diaza-s-indacene (7). Obtained in 35% yield. Orange solid, m.p. > 300 °C. R_f: 0.48 (DCM-hexane, 1:1). ^{1}H NMR (400 MHz, $CDCl_3$): δ 7.92 (dd, *J* = 7.9, 1.2 Hz, 2H), 7.69 (dd, *J* = 7.7, 1.1 Hz, 2H), 7.65 – 7.55 (m, 3H), 7.51 – 7.44 (m, 2H), 7.36 (dddd, *J* = 10.0, 7.9, 6.5, 1.4 Hz, 4H), 6.26 (d, *J* = 4.1 Hz, 2H), 6.15 (d, *J* = 4.1 Hz, 2H), 2.72 (s, 6H). ^{13}C NMR (100 MHz, $CDCl_3$): δ 158.04, 140.26, 139.21, 138.38, 136.46, 131.09, 130.59, 130.16, 129.43, 128.47, 127.75, 127.04, 126.43, 126.11, 125.32, 119.82, 15.01. UV–vis (DCM): λ_{max} [nm] (log ε) = 356 (4.09), 374 (4.22), 395 (4.14), 518 (4.90). HRMS (ESI): m/z found 473.2016, calcd for $[M+H]^+$ $C_{31}H_{24}BF_2N_2$ 473.2000.	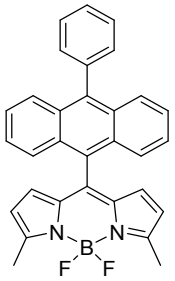
3,5-Dimethyl-8-(4-(10-phenylanthracen-9-yl)phenyl)-4,4-difluoro-4-bora-3a,4a-diaza-s-indacene (8). Obtained in 17% yield, Orange solid, m.p. > 300 °C; R_f : 0.45 (DCM-hexane 1:1). ^{1}H NMR (400 MHz, $CDCl_3$): δ 7.78 – 7.69 (m, 6H), 7.65 – 7.56 (m, 5H), 7.52 – 7.48 (m, 2H), 7.42 – 7.34 (m, 4H), 6.98 (d, *J* = 4.1 Hz, 2H), 6.37 (d, *J* = 4.1 Hz, 2H), 2.71 (s, 6H). ^{13}C NMR (100 MHz, $CDCl_3$): δ 157.73, 142.33, 141.19, 138.84, 137.71, 135.68, 134.57, 133.36, 131.23, 130.51, 129.78, 128.43, 127.56, 127.15, 126.48, 125.37, 125.10, 119.51, 14.97. UV–vis (DCM): λ_{max} [nm] (log ε) = 356 (4.30), 374 (4.33), 395 (4.25), 513 (4.89). HRMS (ESI): *m/z* found 549.2284, calcd for $[M+H]^+$ $C_{37}H_{28}BF_2N_2$ 549.2314.	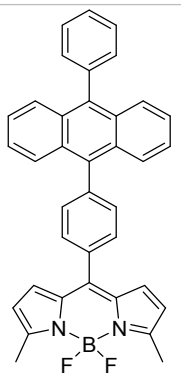
1,3,5,7-Tetramethyl-8-(anthracen-9-yl)-4,4-difluoro-4-bora-3a,4a-diaza-s-indacene (9). Obtained in 34% yield. Orange powder, m.p. > 300 °C. R_f: 0.26 (DCM-hexane, 1:1). ^{1}H NMR (400 MHz, $CDCl_3$): δ 8.58 (s, 1H), 7.97 (d, *J* = 48.3 Hz, 4H), 7.46 (d, *J* = 24.0 Hz, 4H), 5.90 (s, 2H), 2.63 (s, 6H), 0.65 (s, 6H). ^{13}C NMR (100 MHz, $CDCl_3$): δ 155.93, 143.05, 139.11, 131.47, 129.85, 128.49, 128.41, 127.11, 125.90, 125.28, 121.32, 14.86, 13.48. UV–vis (DCM): λ_{max} [nm] (log ε) = 350 (4.04), 367 (4.16), 387 (4.12), 506 (4.93). HRMS (ESI): *m/z* found 405.1944, calcd for $[M-F]^+$ $C_{27}H_{23}BN_2F$, 405.1937.	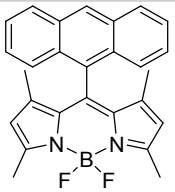
1,3,5,7-Tetramethyl-8-(methylanthracen-9-yl)-4,4-difluoro-4-bora-3a,4a-diaza-s-indacene (10). Obtained in 38% yield. Analytical data are in accordance with previous reports.[5]	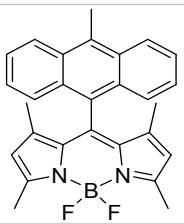
1,3,5,7-Tetramethyl-8-(10-phenylanthracen-9-yl)-4,4-difluoro-4-bora-3a,4a-diaza-s-indacene (11). Obtained in 50% yield. Orange powder, m.p. > 300 °C. R_f: 0.2 (DCM-hexane, 1:1). ^{1}H NMR (400 MHz $CDCl_3$): δ 7.96 (d, *J* = 8.3 Hz, 2H), 7.68 (d, *J* = 8.5 Hz, 2H), 7.64 – 7.55 (m, 3H), 7.49 – 7.45 (m, 2H), 7.38 (dddd, *J* = 9.9, 7.8, 6.5, 1.2 Hz, 4H), 5.93 (s, 2H), 2.65 (s, 6H), 0.75 (s, 6H). ^{13}C NMR (100 MHz, $CDCl_3$): δ 155.94, 143.08, 138.47, 131.47, 130.05, 129.48, 128.59, 127.92, 127.18, 126.77, 125.75, 125.38, 121.36, 121.34, 14.89, 13.57. UV–vis (DCM): λ_{max} [nm] (log ε) = 356 (4.15), 375 (4.30), 396 (4.24), 507 (4.98). HRMS (ESI): *m/z* found 500.3986, calcd for M^+ $C_{33}H_{27}BN_2F_2$ 500.3998.	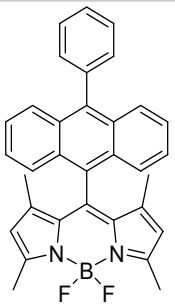

1,3,5,7-Tetramethyl-8-(4-(10-phenylanthracen-9-yl)phenyl)-4,4-difluoro-4-bora-3a,4a-diaza-s-indacene (12). Obtained in 57% yield. Orange powder, m.p. > 300 °C. R_f: 0.18 (DCM-hexane, 1:1). ^{1}H NMR (400 MHz, $CDCl_3$) δ 7.75 – 7.70 (m, 2H), 7.68 – 7.54 (m, 9H), 7.52 – 7.48 (m, 2H), 7.39 – 7.33 (m, 4H), 6.10 (s, 2H), 2.62 (s, 6H), 1.75 (s, 6H). ^{13}C NMR (100 MHz, $CDCl_3$) δ 155.80, 143.13, 141.69, 140.03, 139.00, 137.83, 136.01, 134.52, 132.39, 131.72, 131.41, 130.04, 129.80, 128.60, 128.43, 127.74, 127.37, 126.39, 125.55, 125.21, 121.61, 14.79. UV–vis (DCM): λ_{max} [nm] (log ε) = 357 (4.12), 375 (4.26), 396 (4.20), 502 (4.89). HRMS (ESI): *m/z* found 557.2563, calcd for $[M\text{-}F]^+$ $C_{39}H_{31}BN_2F$ 557.2565.	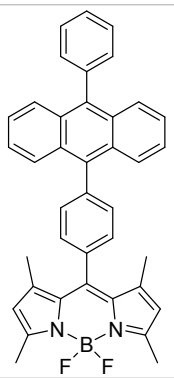
2,6-Diethyl-1,3,5,7-tetramethyl-8-(anthracen-9-yl)-4,4-difluoro-4-bora-3a,4a-diaza-s-indacene (13). Obtained in 74% yield. Brown powder, m.p. > 300 °C. R_f: 0.29 (DCM-hexane, 1:1). ^{1}H NMR (400 MHz, $CDCl_3$): δ 8.58 (s, 1H), 8.04 (d, *J* = 8.4 Hz, 2H), 7.95 (d, *J* = 8.7 Hz, 2H), 7.52 – 7.46 (m, 2H), 7.45 – 7.38 (m, 2H), 2.61 (s, 6H), 2.22 – 2.14 (m, 4H), 0.89 (t, *J* = 7.6 Hz, 6H), 0.56 (s, 6H). ^{13}C NMR (100 MHz, $CDCl_3$): δ 153.97, 138.09, 137.19, 132.66, 131.69, 131.31, 129.89, 129.21, 128.25, 128.00, 126.73, 125.66, 125.45, 16.98, 14.54, 12.63, 10.40. UV–vis (DCM): λ_{max} [nm] (log ε) = 351 (4.05), 368 (4.22), 387 (4.23), 531 (4.92). HRMS (ESI): *m/z* found 461.2582, calcd for $[M\text{-}F]^+$ $C_{31}H_{31}BN_2F$ 461.2564.	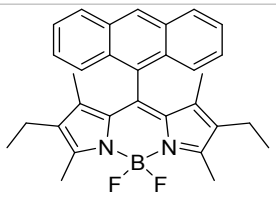
2,6-Diethyl-1,3,5,7-tetramethyl-8-(10-methylanthracen-9-yl)-4,4-difluoro-4-bora-3a,4a-diaza-s-indacene (14). Obtained in 74% yield. Brown powder, m.p. > 300 °C. R_f: 0.48 (DCM-hexane, 1:1). ^{1}H NMR (400 MHz, $CDCl_3$): δ 8.34 (d, *J* = 8.9 Hz, 2H), 7.96 (d, *J* = 8.7 Hz, 2H), 7.57 – 7.49 (m, 2H), 7.44 – 7.36 (m, 2H), 3.21 (s, 3H), 2.60 (s, 6H), 2.18 (q, *J* = 7.5 Hz, 4H), 0.88 (t, *J* = 7.6 Hz, 6H), 0.54 (s, 6H). ^{13}C NMR (100 MHz, $CDCl_3$): δ 154.16, 138.55, 138.26, 132.91, 132.42, 132.26, 130.19, 129.92, 128.09, 126.57, 126.50, 125.86, 125.04, 17.33, 14.92, 14.74, 12.97, 10.94. UV–vis (DCM): λ_{max} [nm] (log ε) = 358 (4.10), 377 (4.28), 398 (4.25), 531 (4.89). HRMS (ESI): *m/z* found 494.2716, calcd for M^+ $C_{32}H_{33}BN_2F_2$ 494.2705.	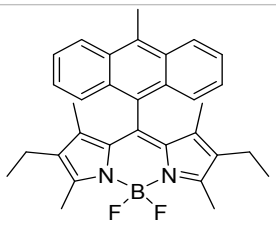
2,6-Diethyl-1,3,5,7-tetramethyl-8-(10-phenylanthracen-9-yl)-4,4-difluoro-4-bora-3a,4a-diaza-s-indacene (15). Obtained in a 22% yield. Brown solid, m.p. > 300 °C. R_f: 0.56 (DCM-hexane, 1:1). ^{1}H NMR (400 MHz, $CDCl_3$): δ 8.01 – 7.94 (m, 2H), 7.69 – 7.64 (m, 2H), 7.64 – 7.53 (m, 3H), 7.49 – 7.43 (m, 2H), 7.36 (dddd, *J* = 10.0, 7.8, 6.5, 1.3 Hz, 4H), 2.60 (s, 6H), 2.25 – 2.16 (m, 4H), 0.92 – 0.78 (m, 6H), 0.64 (s, 6H). ^{13}C NMR (100 MHz, $CDCl_3$): δ 153.98, 139.08, 138.42, 138.15, 132.68, 131.81, 131.32, 129.87, 129.51, 128.40, 127.69, 126.91, 126.38, 125.53, 17.02, 14.56, 12.63, 10.61. UV–vis (DCM): λ_{max} [nm] (log ε) = 359 (4.14), 375 (4.31), 396 (4.29), 532 (4.90). HRMS (ESI): *m/z* found 556.2861, calcd for M^+ $C_{32}H_{33}BN_2F_2$ 556.2861.	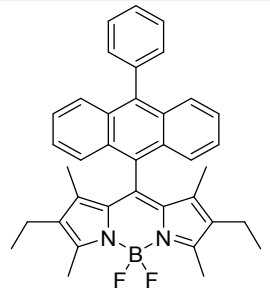
2,6-Diethyl-1,3,5,7-tetramethyl-8-(4-(10-phenylanthracen-9-yl)phenyl)-4,4-difluoro-4-bora-3a,4a-diaza-s-indacene (16). Obtained in 12% yield. Orange solid, m.p. > 300 °C. R_f: 0.55 (DCM-hexane, 1:1). ^{1}H NMR (400 MHz, $CDCl_3$): δ 7.76 – 7.46 (m, 13H), 7.40 – 7.31 (m, 4H), 2.58 (s, 6H), 2.43 – 2.32 (m, 4H), 1.64 (s, 6H), 1.05 (t, *J* = 7.6 Hz, 6H). ^{13}C NMR (100 MHz, $CDCl_3$): δ 153.85, 139.95, 139.58, 138.86, 138.23, 137.58, 136.00, 135.16, 132.97, 132.09, 131.24, 130.89, 129.86, 129.65, 128.49, 127.55, 127.17, 126.28, 125.34, 125.03, 17.15, 14.68, 12.55, 11.95. UV–vis (DCM): λ_{max} [nm] (log ε) = 358 (4.20), 376 (4.37), 396 (4.34), 527 (4.90). HRMS (ESI): *m/z* found 631.3108, calcd for M^+ $C_{43}H_{40}BN_2F_2$ 631.3108.	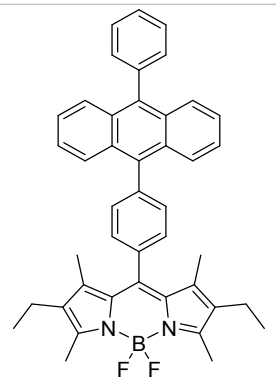

H. NMR spectroscopy Data

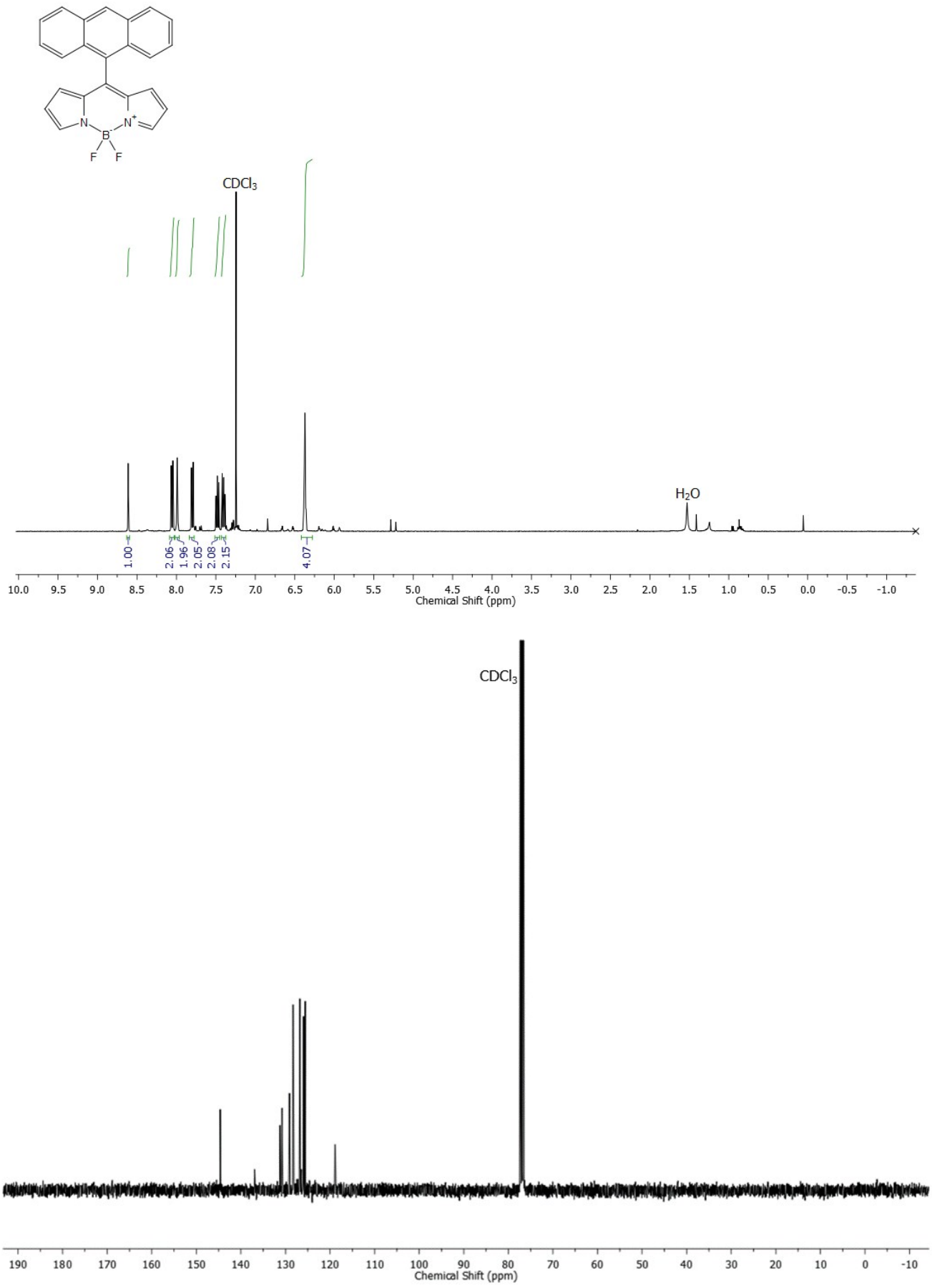

Figure S37: ^{1}H and ^{13}C NMR spectra of compound **1**.

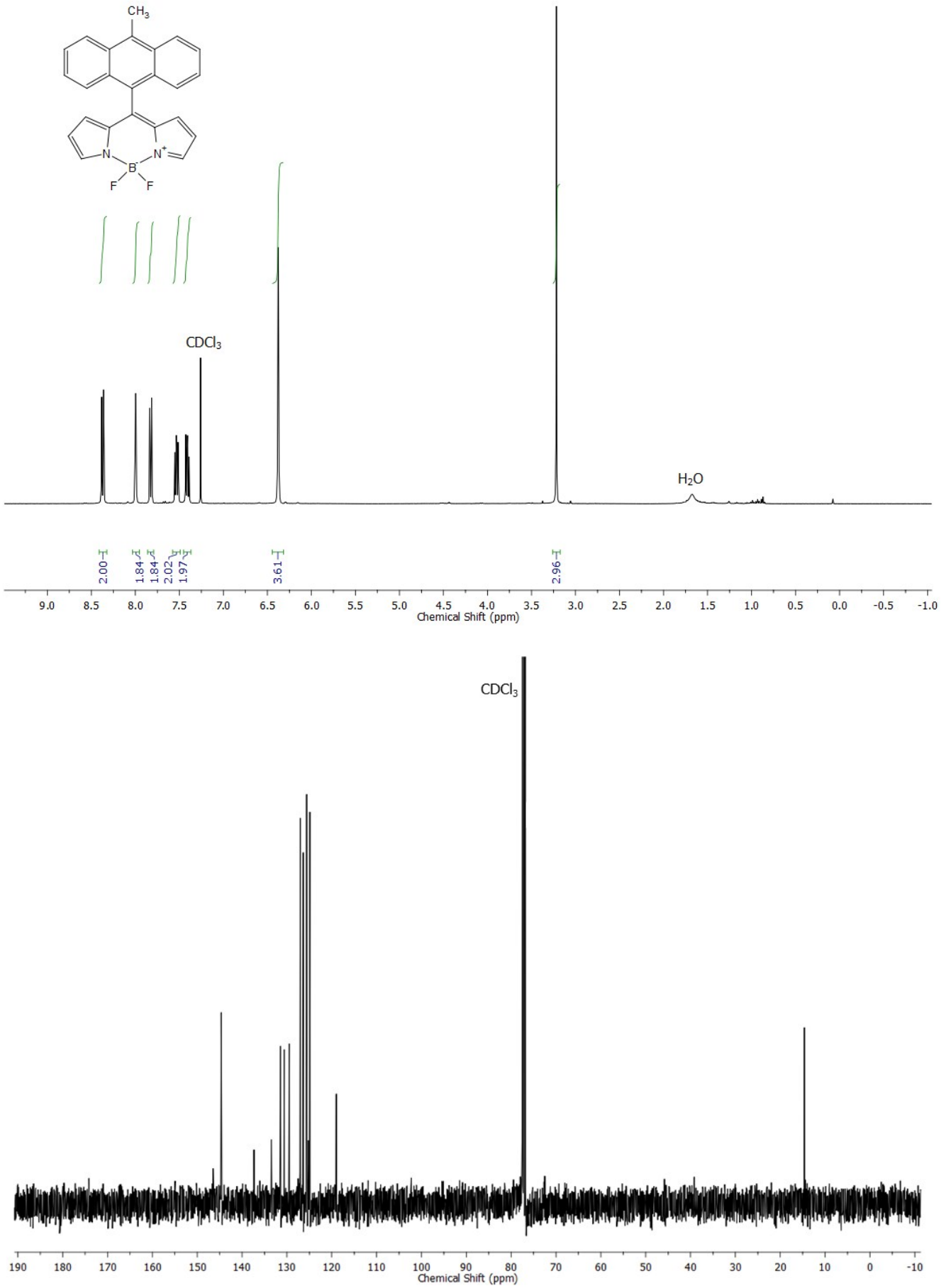

Figure S38: ^{1}H and ^{13}C NMR spectra of compound **2**.

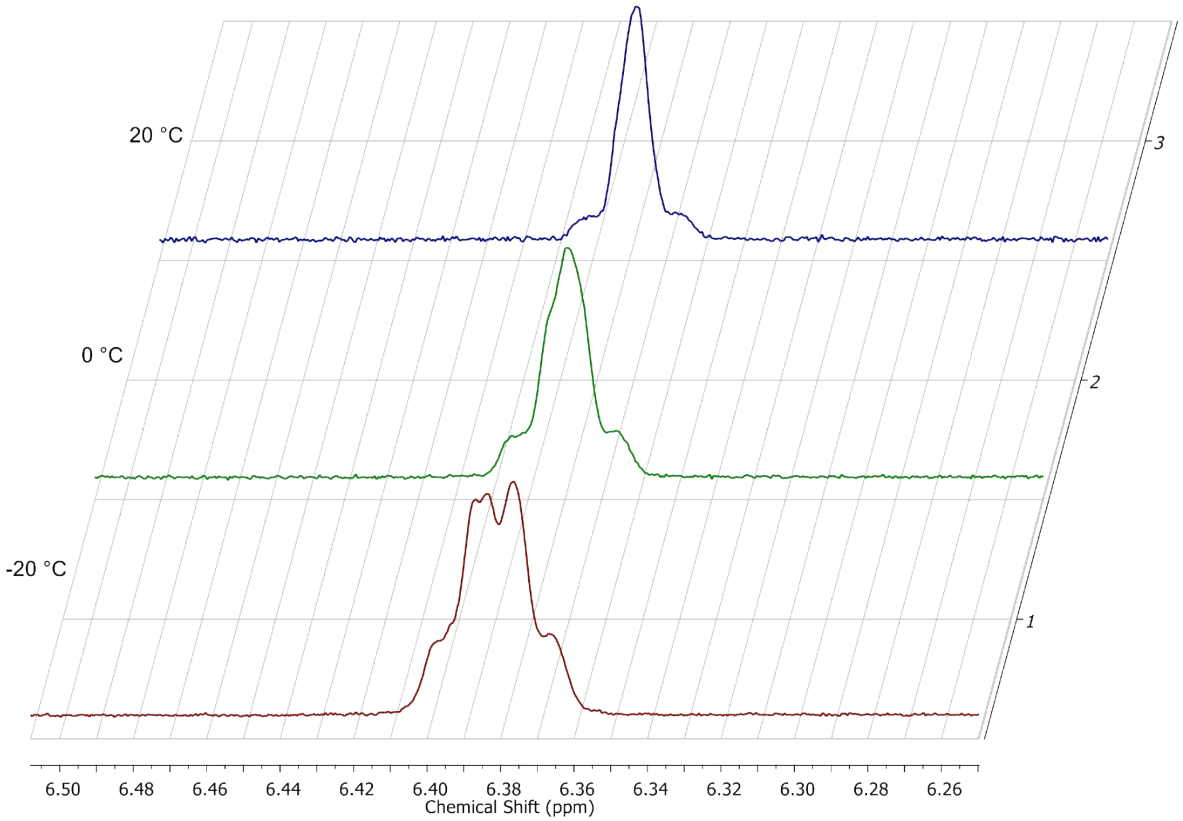

Figure S39: Part of VT-^{1}H NMR spectra of compound **2**. Splitting of pyrrolic protons signals in position 1 and 7 of the BODIPY core is due to the restriction of rotation of anthracene ring.

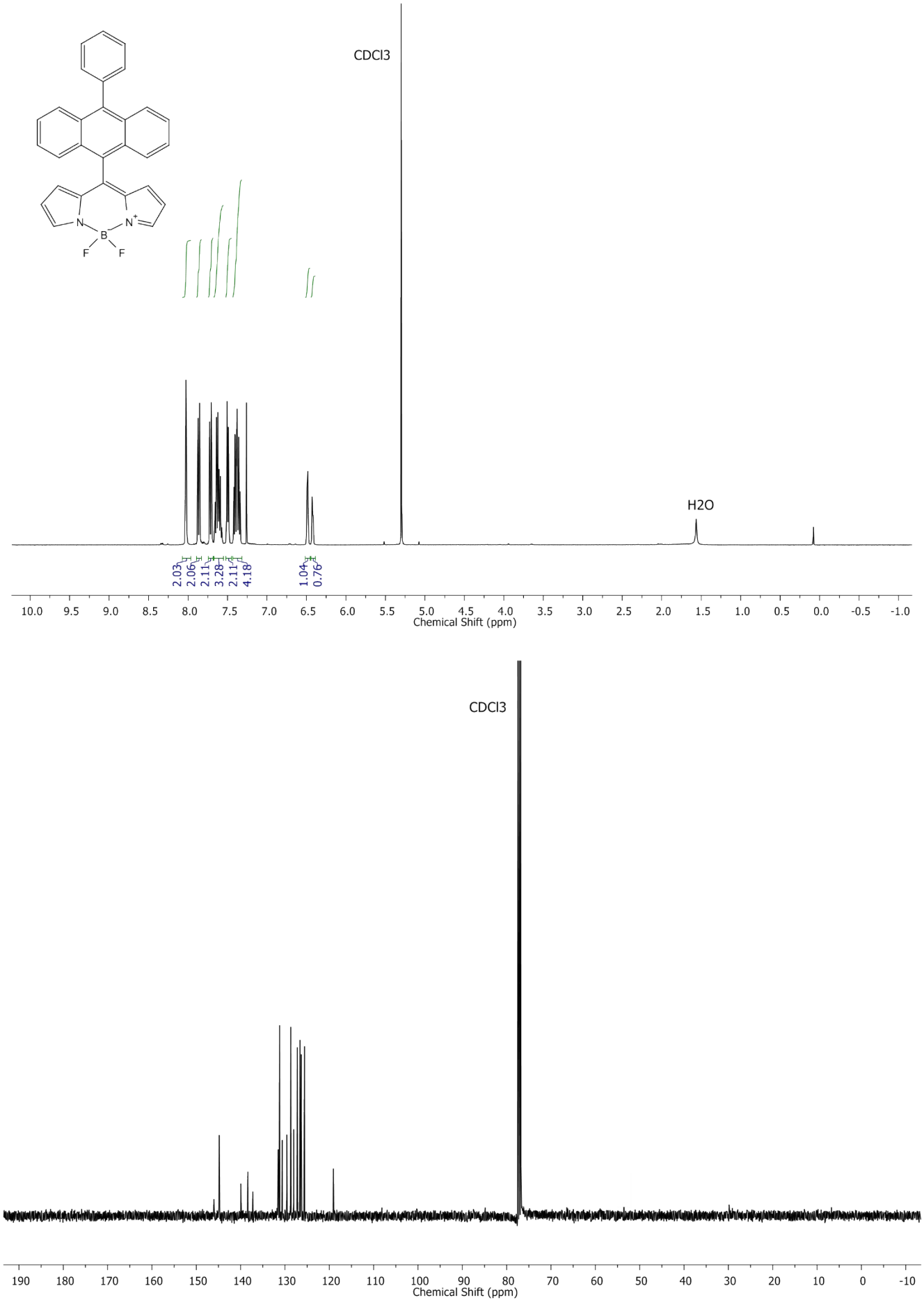

Figure S40: ^{1}H and ^{13}C NMR spectra of compound **3**.

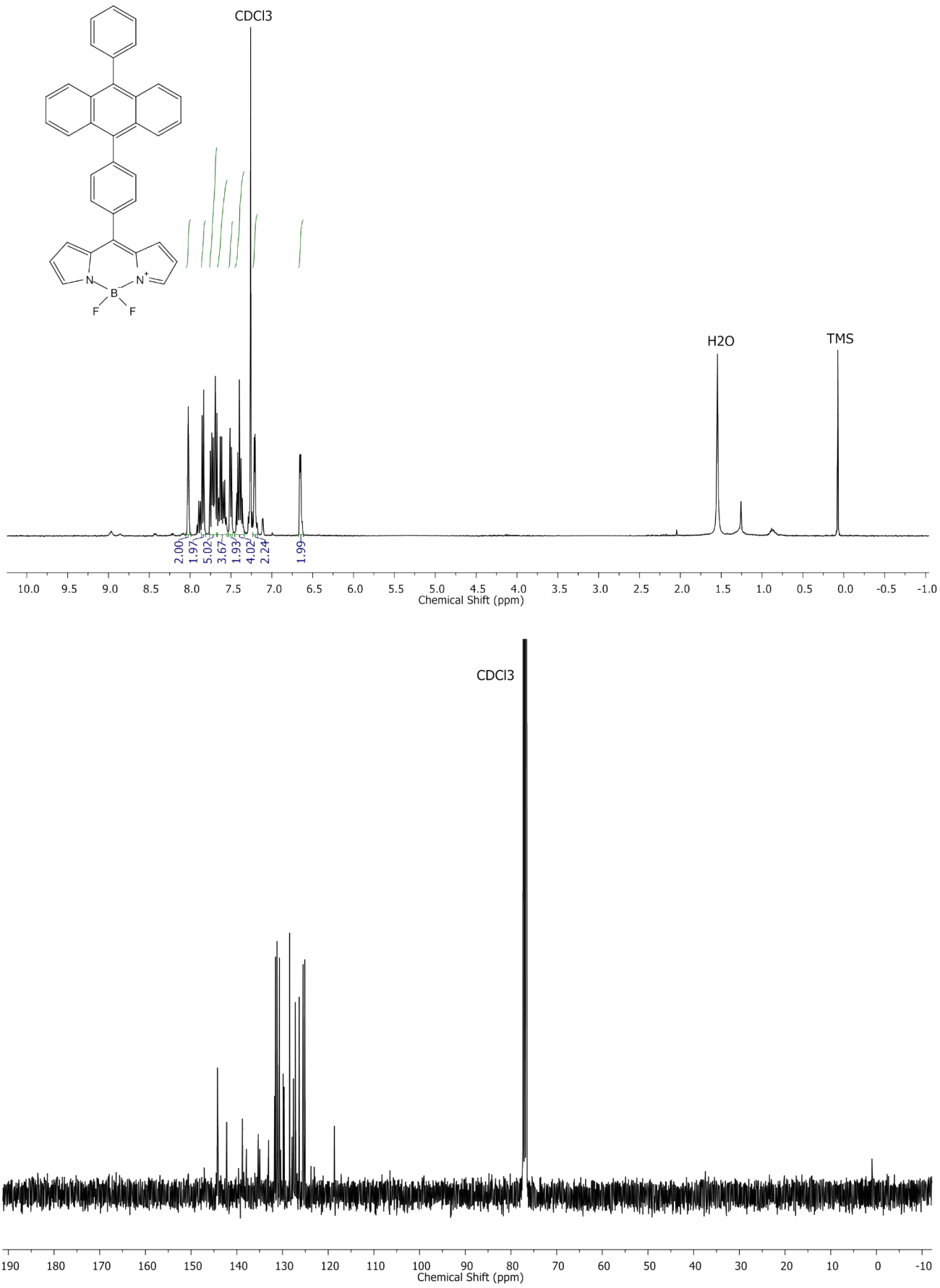

Figure S41: ^{1}H and ^{13}C NMR spectra of compound **4**.

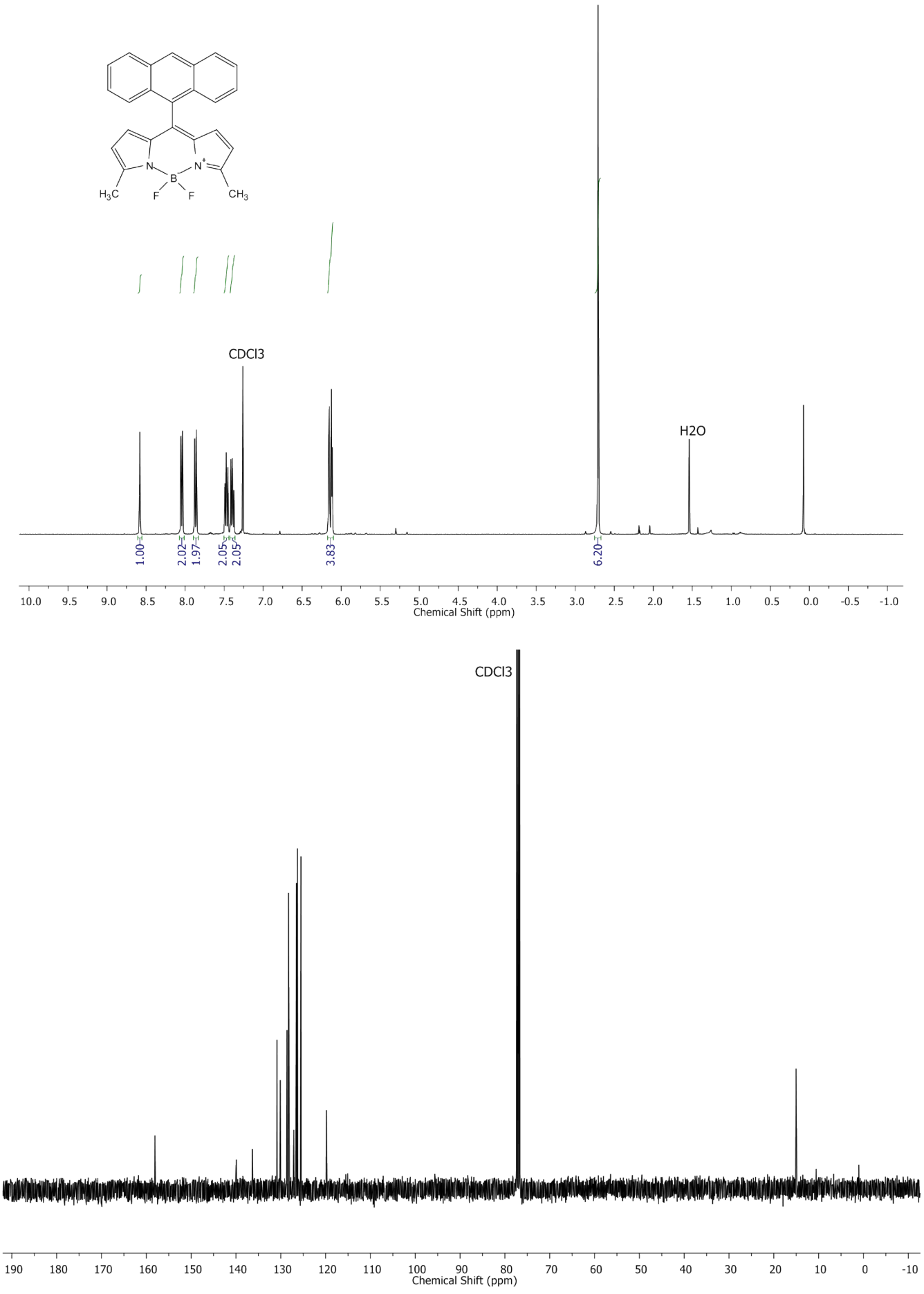

Figure S42: ^{1}H and ^{13}C NMR spectra of compound **5**.

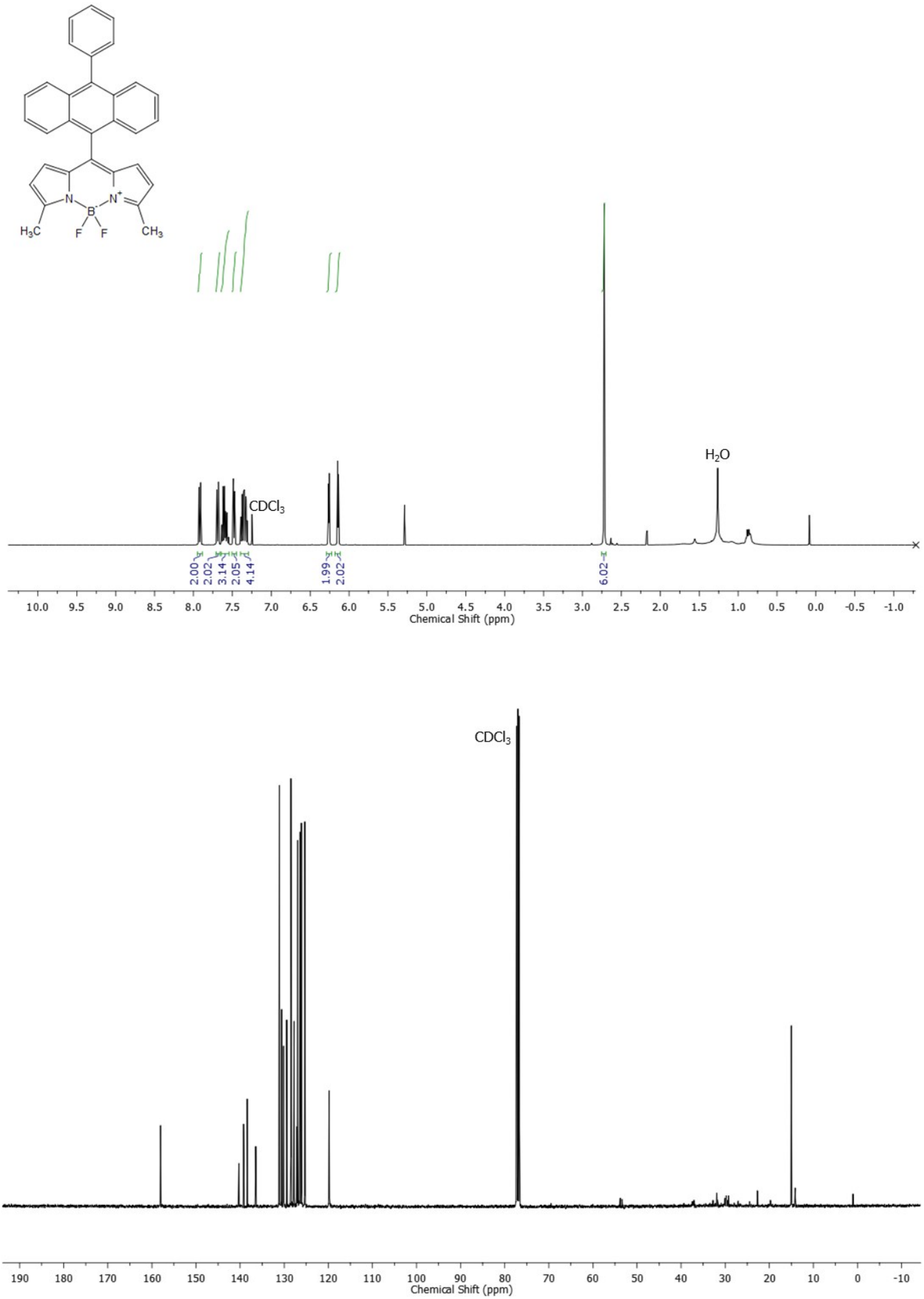

Figure S43: ^{1}H and ^{13}C NMR spectra of compound **7**.

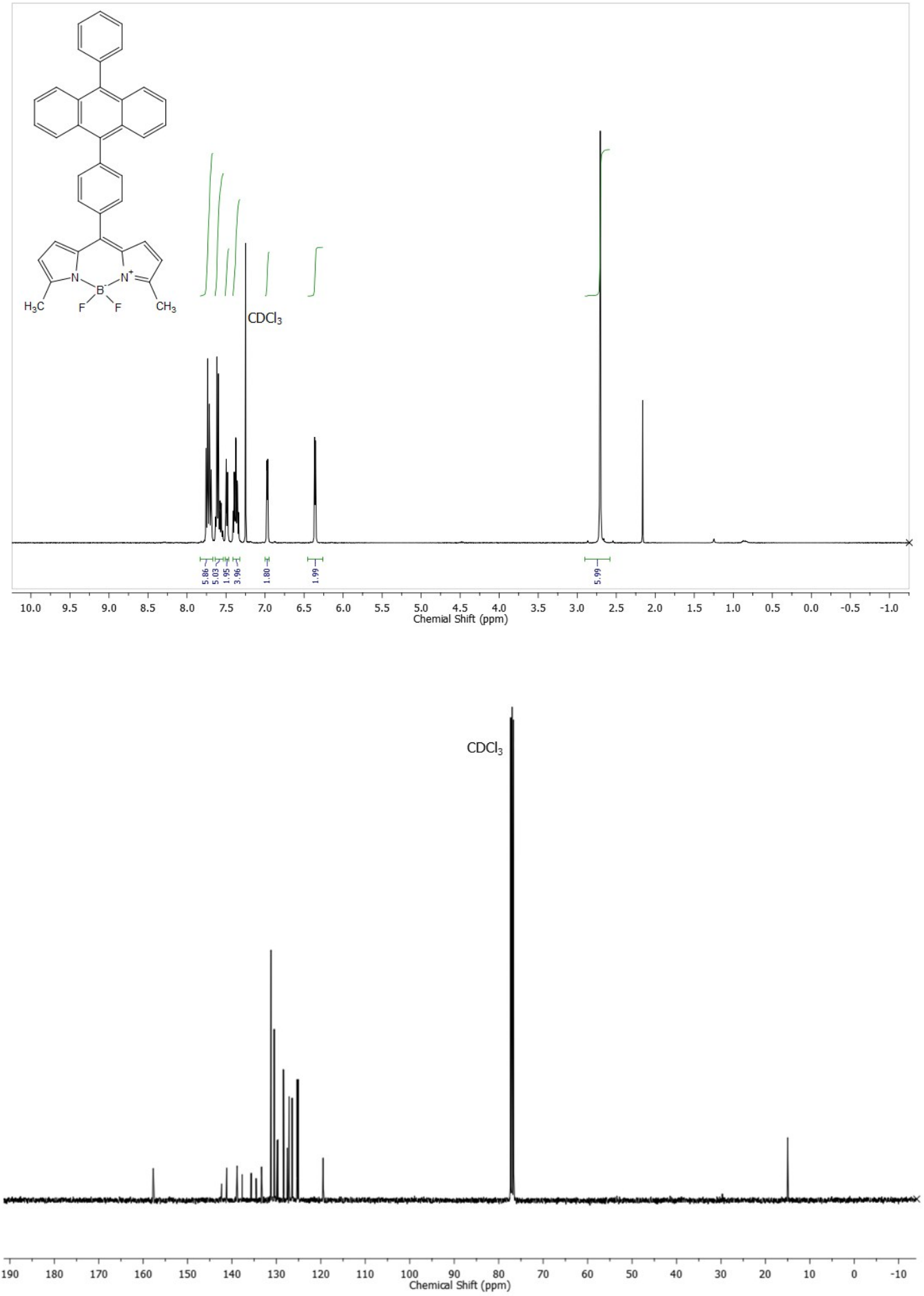

Figure S44: ^{1}H and ^{13}C NMR spectra of compound **8**.

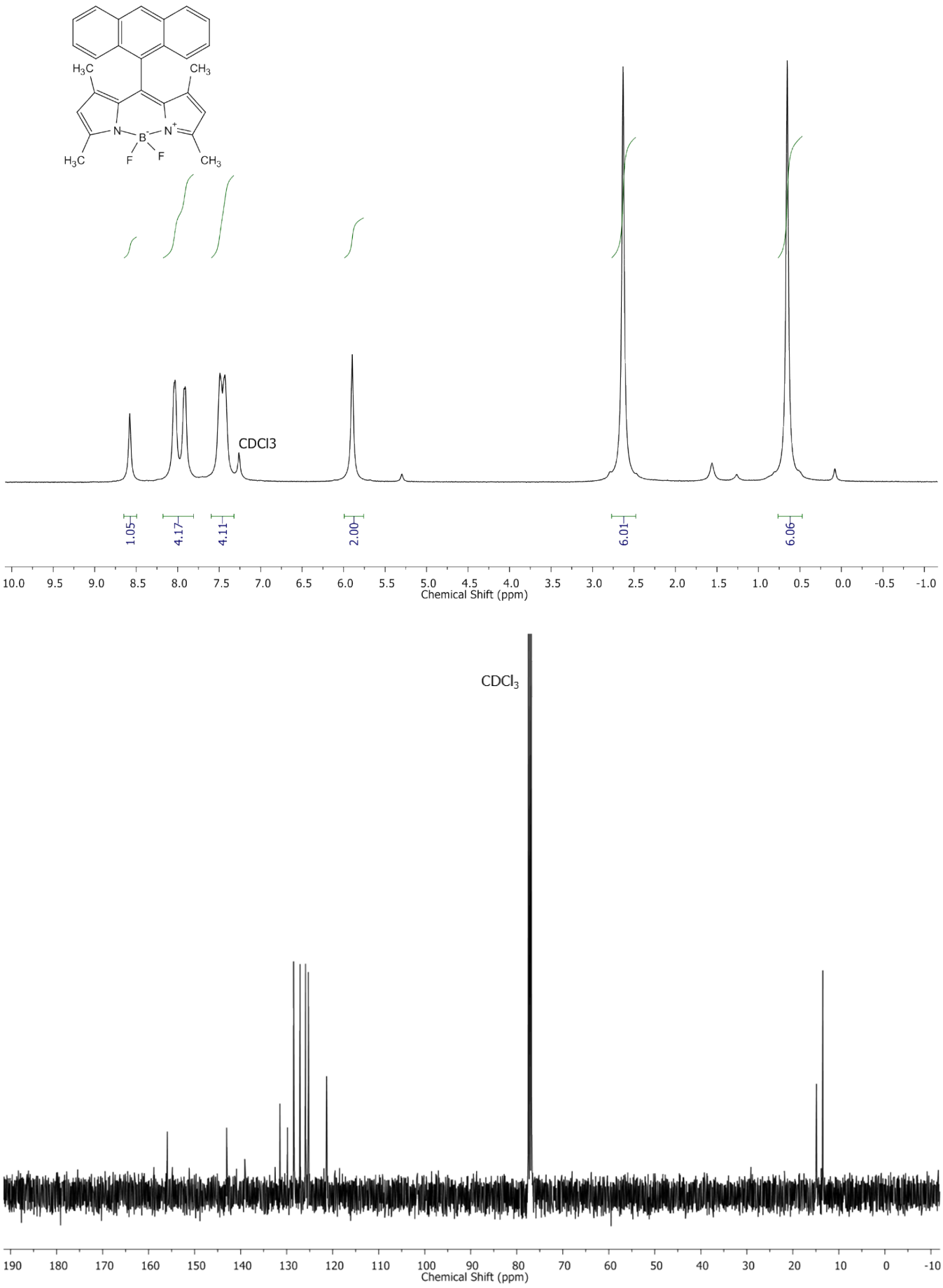

Figure S45: ^{1}H and ^{13}C NMR spectra of compound **9**.

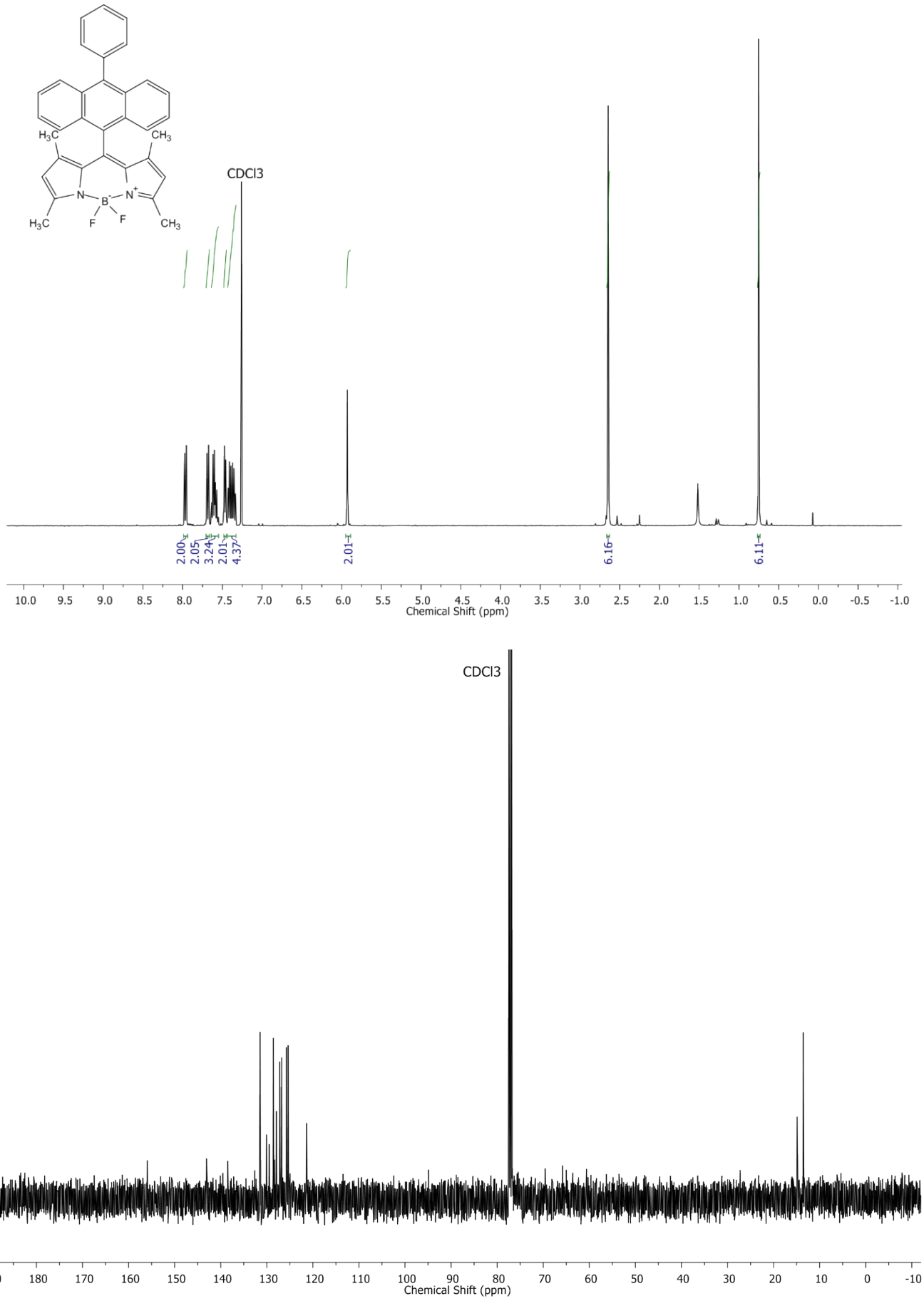

Figure S46: ^{1}H and ^{13}C NMR spectra of compound **11**.

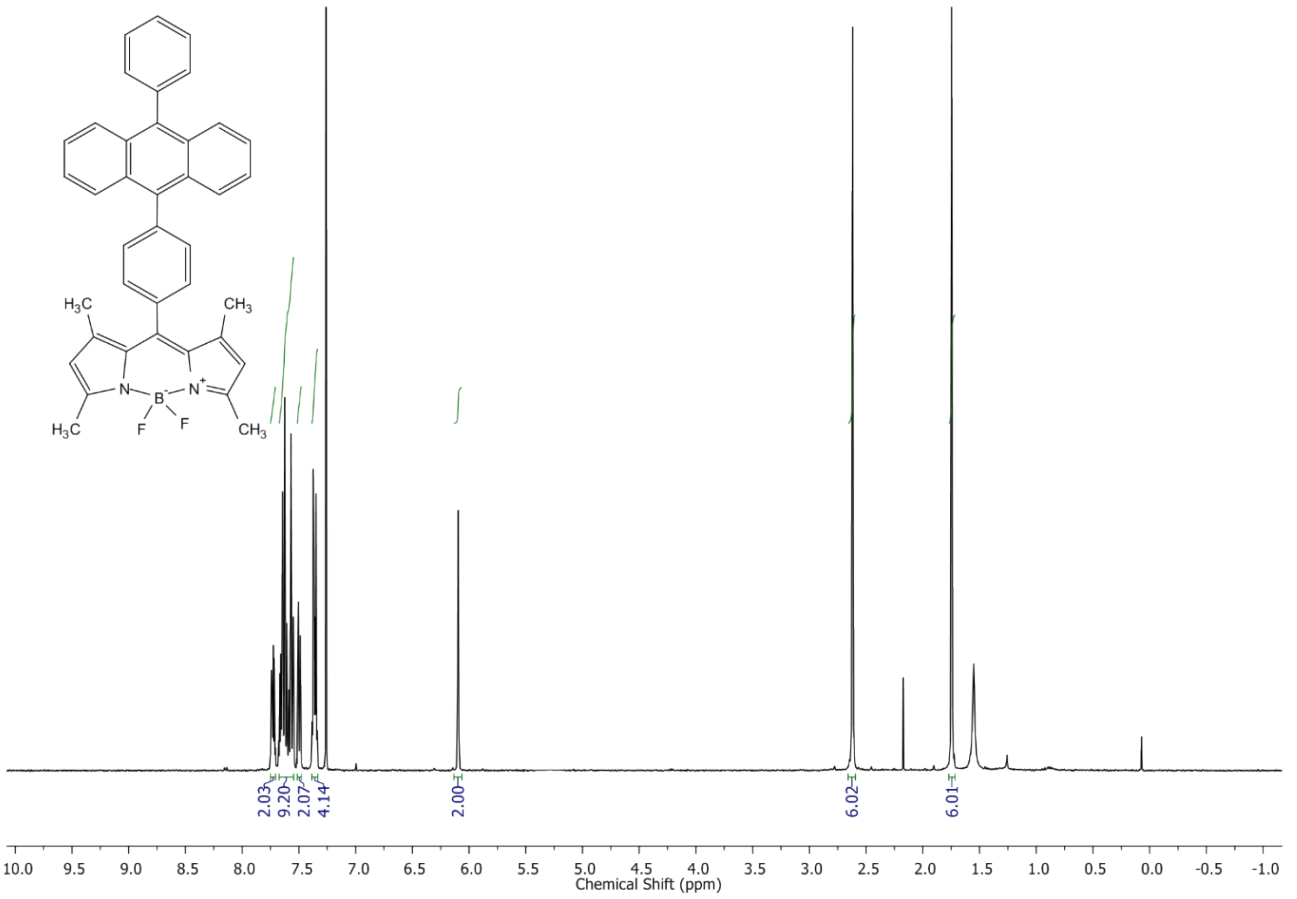

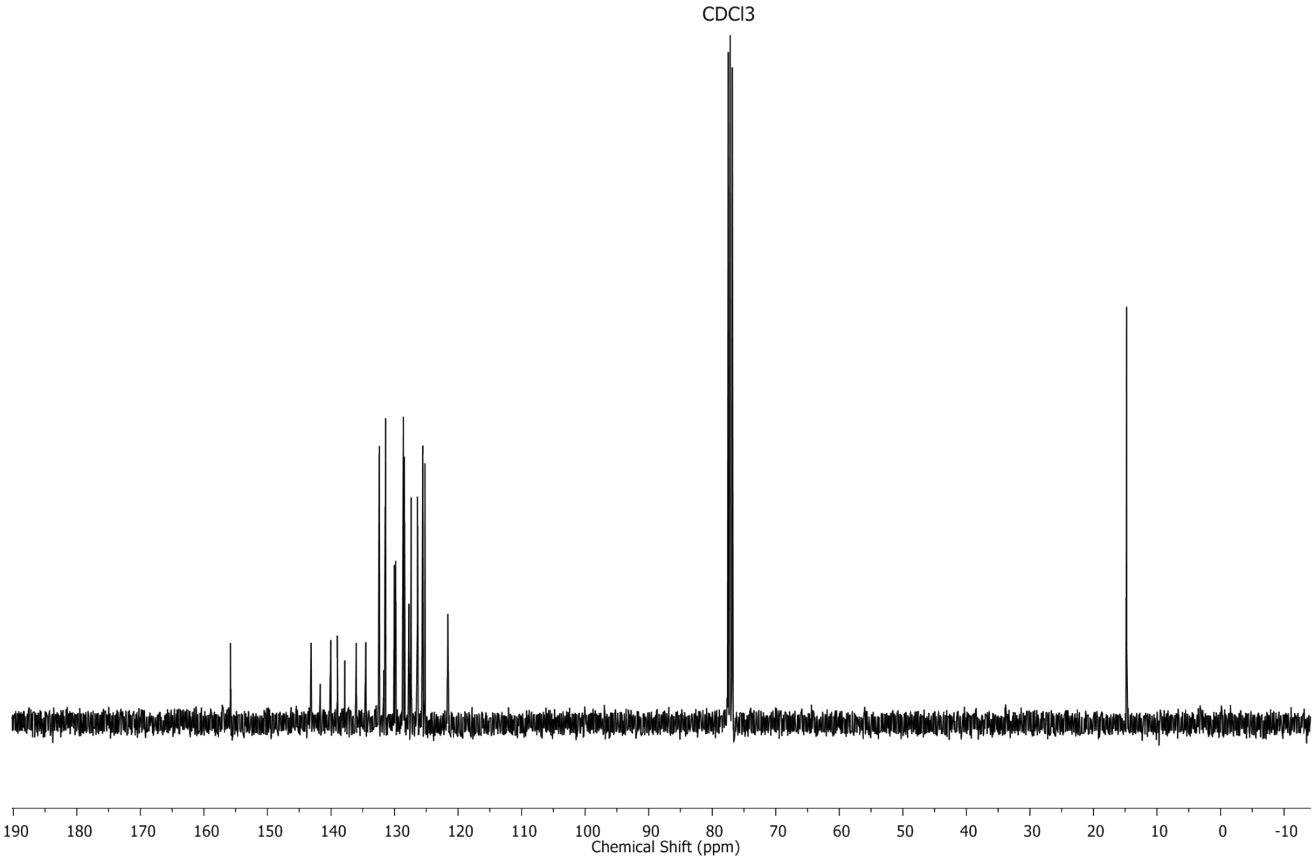

Figure S47: ^{1}H and ^{13}C NMR spectra of compound **12**.

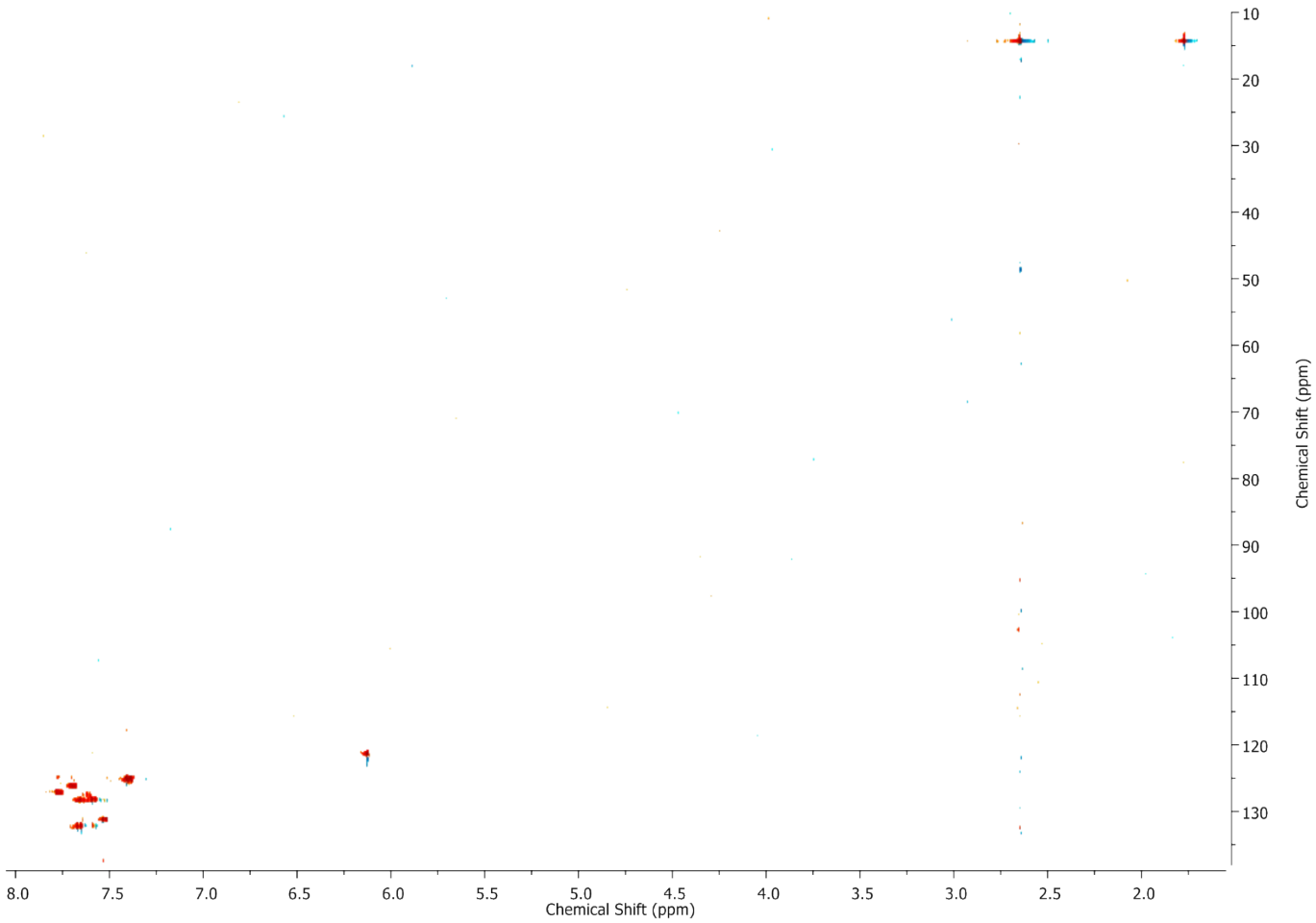

Figure S48: ^{1}H - ^{13}C HSQC NMR spectrum of compound **12**.

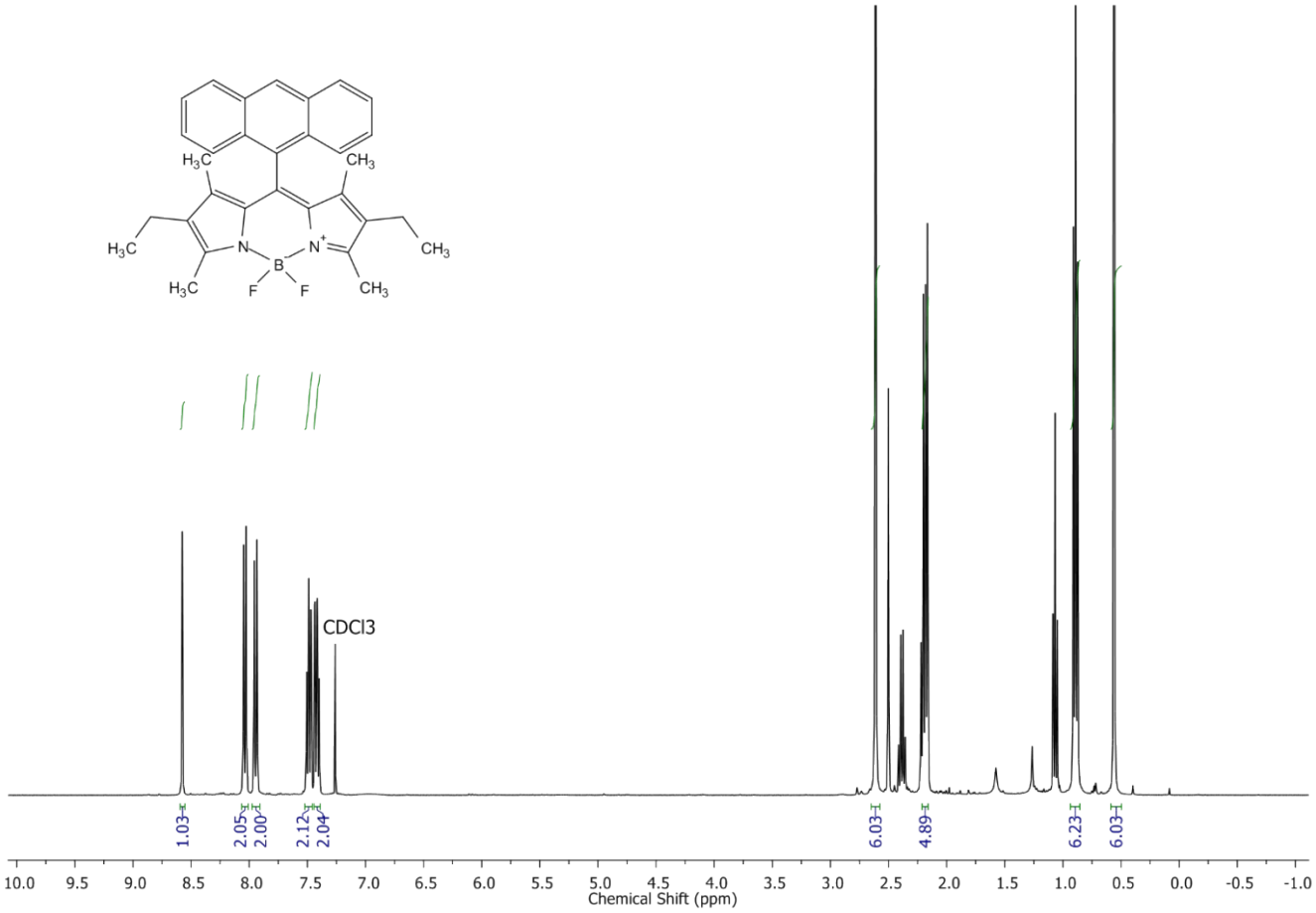

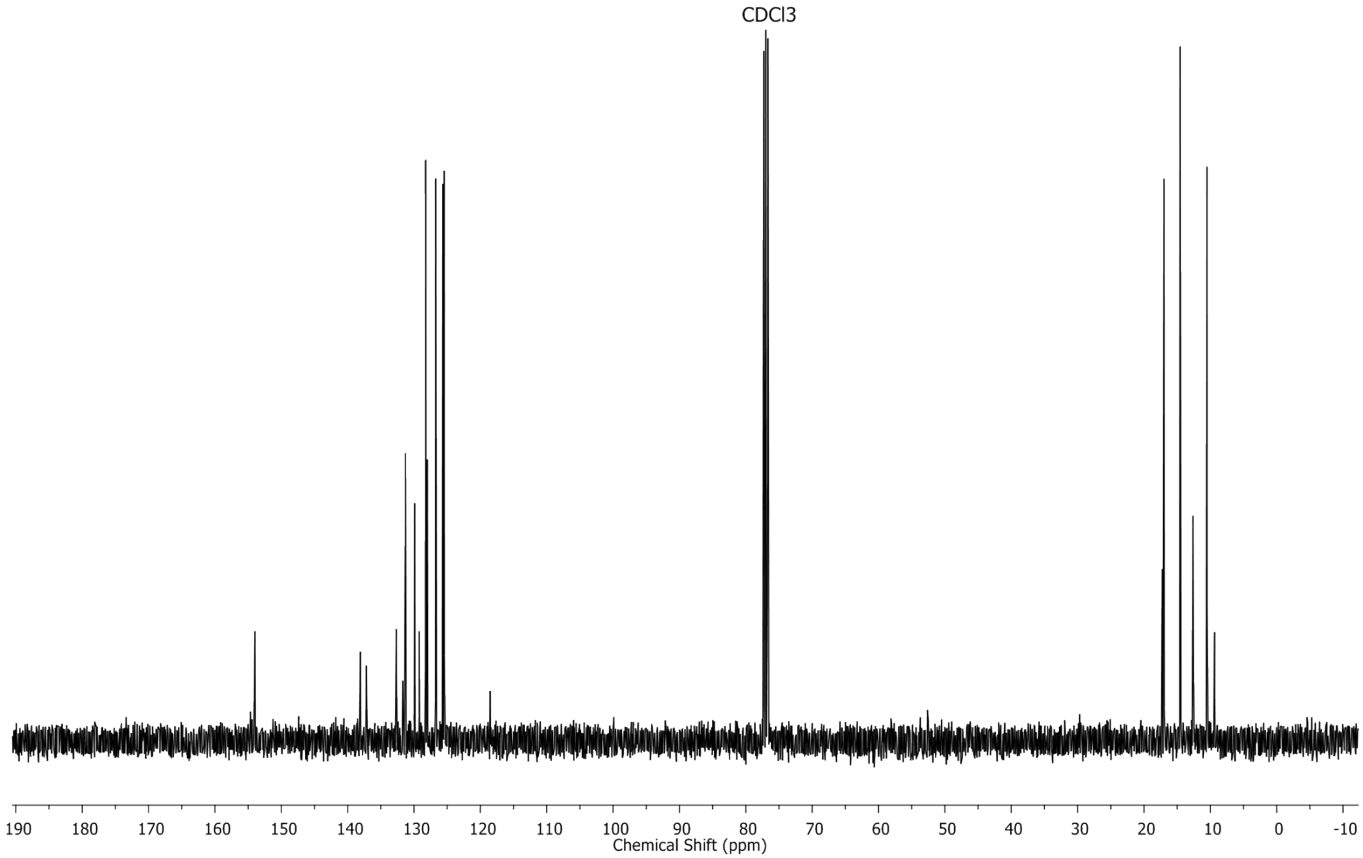

Figure S49: ^{1}H and ^{13}C NMR spectra of compound **13**.

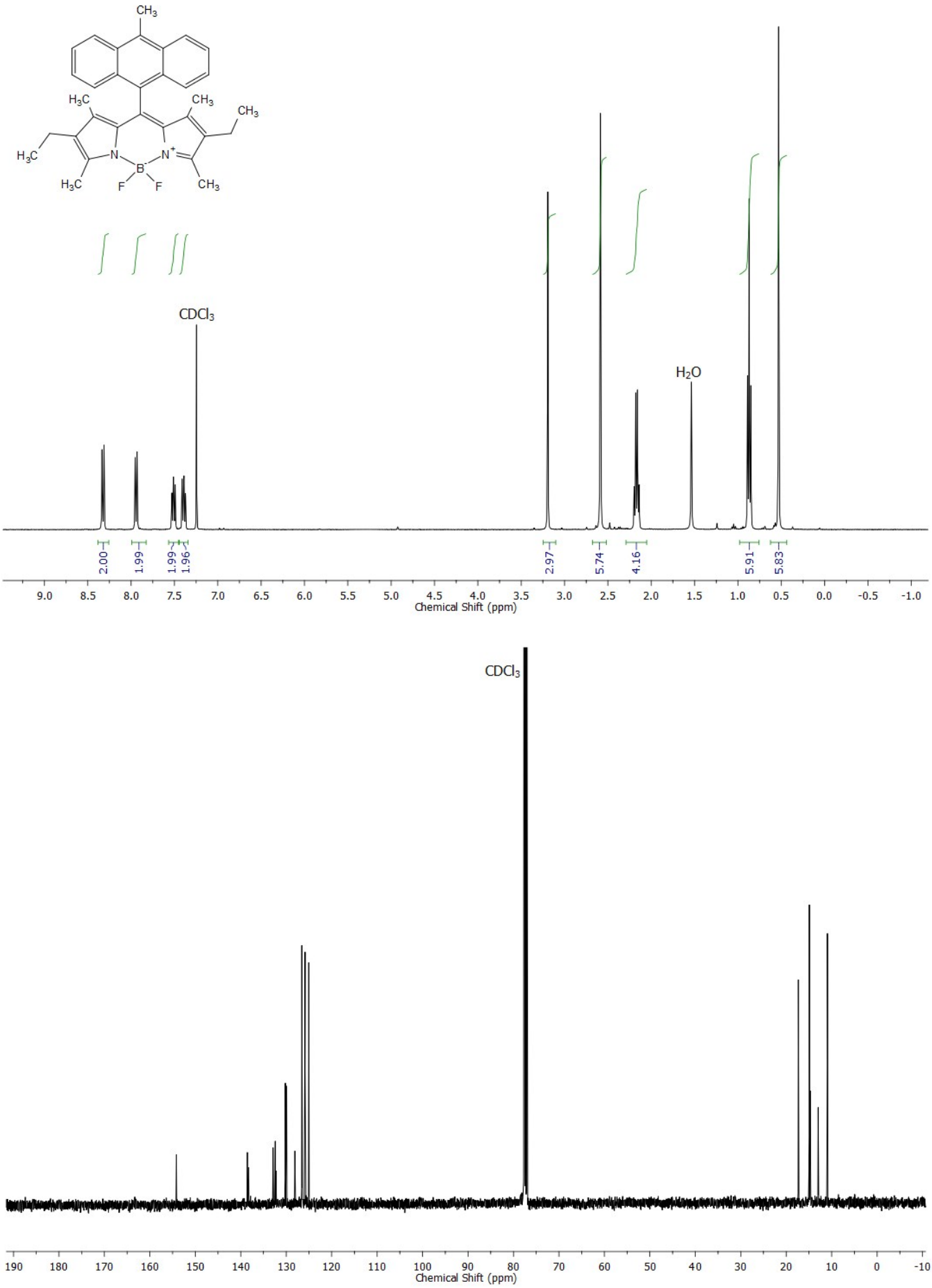

Figure S50: ^{1}H and ^{13}C NMR spectra of compound **14**.

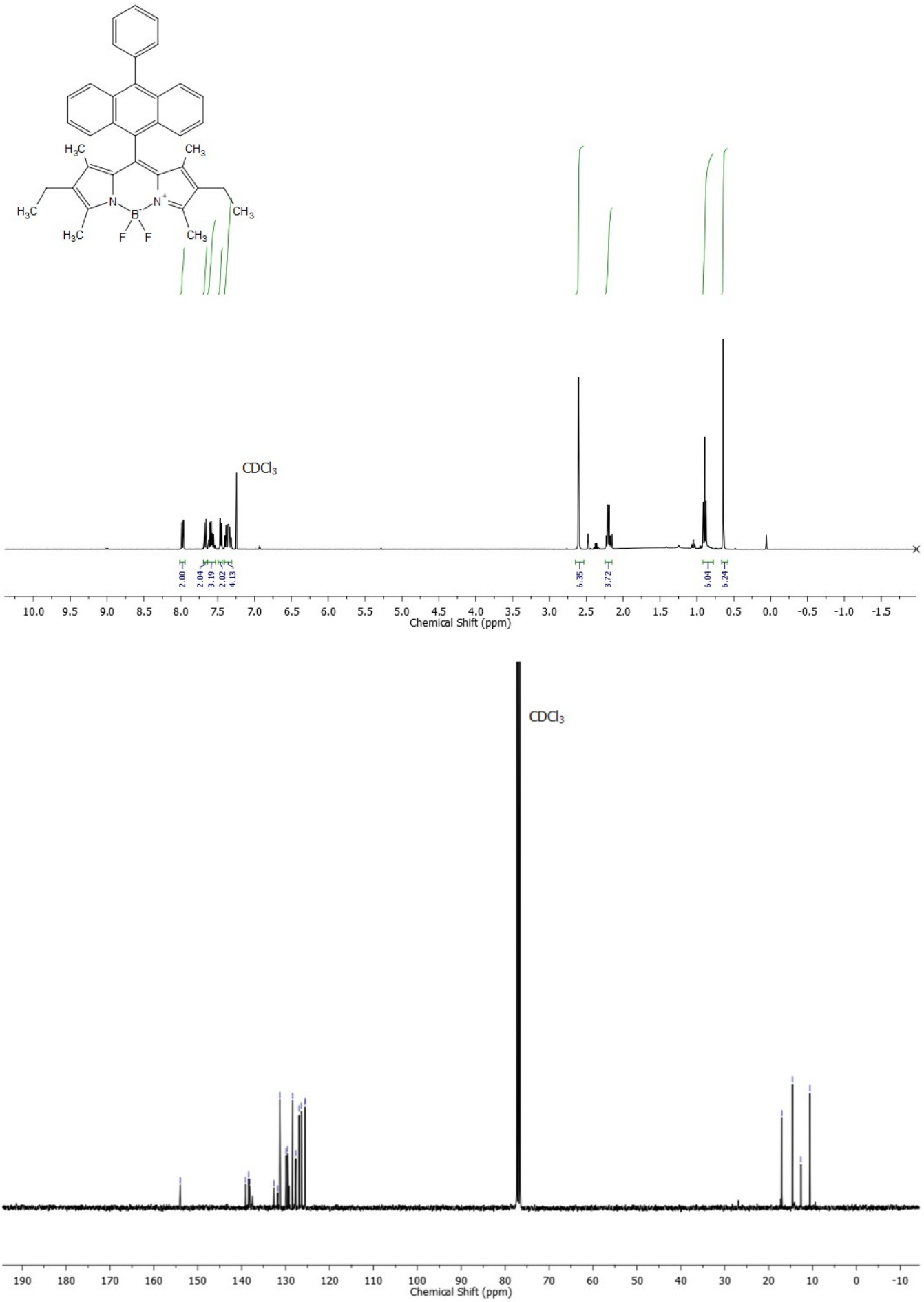

Figure S51: ^{1}H and ^{13}C NMR spectra of compound **15**.

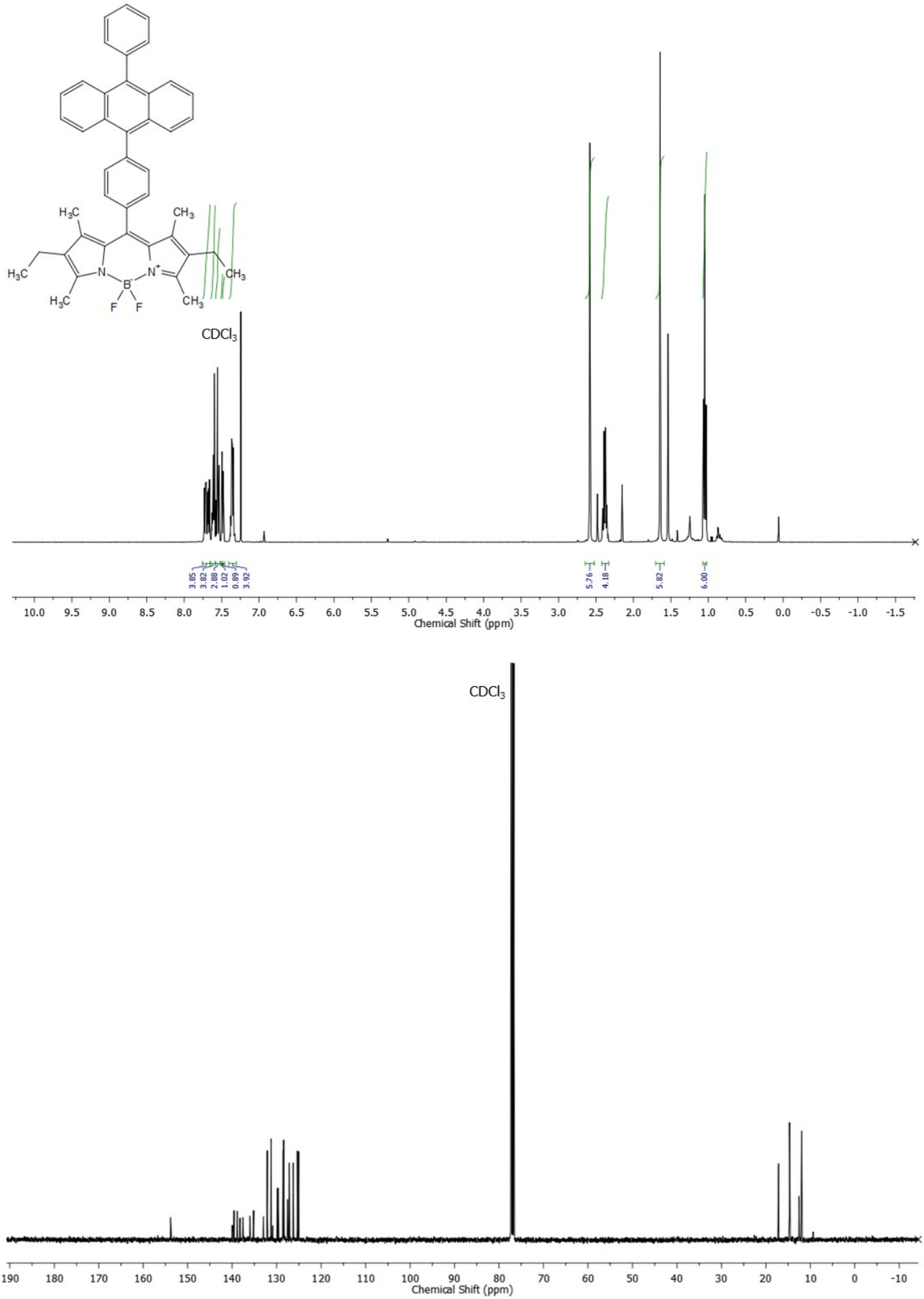

Figure S52: ^{1}H and ^{13}C NMR spectra of compound **16**.

I. References

[1] J.R. Lakowicz, Principles of Fluorescence Spectroscopy, 2nd Ed., Kluwer Academic/Plenum Publishers, New York, London, Moscow, Dordrecht, 1999.

[2] M. A. Filatov, S. Karuthedath, P. M. Polestshuk, H. Savoie, K. J. Flanagan, C. Sy, E. Sitte, M. Telitchko, F. Laquai, R. W. Boyle and M. O. Senge, *J. Am. Chem. Soc*., 2017, **139**, 6282.

[3] (a) *SAINT*, version 8.34a, Bruker AXS, Inc.; Madison, WI, 2013; (b) *SADABS*, version 2014/5, Bruker AXS, Inc.; Madison, WI, 2014; (c) *APEX2*, version 2014.11-0, Bruker AXS, Inc.; Madison, WI, 2014.

[4] (a) O. V. Dolomanov, L. J. Bourhis, R. J. Gildea, J. A. K. Howard and H. Puschmann, *J. Appl. Cryst.*, 2009, **42**, 339; (b) G. M. Sheldrick, *Acta Cryst. Sect. A*, 2015, **71**, 3.

[5] M. W. Schmidt, K. K. Baldridge, J. A. Boatz, S. T. Elbert, M. S. Gordon, J.H. Jensen, S. Koseki, N. Matsunaga, K. A. Nguyen, S. Su, T.L. Windus, M. Dupuis and J. A. Montgomery, *J. Comput. Chem.*, 1993, **14**, 1347.

[6] Y. Zhao and D. G. Truhlar, *Theor. Chem. Acc.*, 2006, **120**, 215.

[7] A. Schäfer, H. Horn and R. Ahlrichs, *J. Chem. Phys.*, 1992, **97**, 2571.

[8] H. Li, C. S. Pomelli, and J. H. Jensen, *Theor. Chem. Acc.*, 2003, **109**, 71.

[9] H. Nakano, *J. Chem. Phys.*, 1993, **99**, 7983.

[10] H. Nakano, R. Uchiyama and K. Hirao, *J. Comput Chem.*, 2002, **23**, 1166.

[11] P. A. Liddell, T. P. Forsyth, M. O. Senge and K. M. Smith, *Tetrahedron*, 1993, **49**, 1343.

[12] M. A. Filatov, R. Guilard and P. D. Harvey, *Org. Lett.*, 2010, **12**, 196.

[13] M. A. Filatov, E. Heinrich, D. Busko, I. Z. Ilieva, K. Landfester and S. Baluschev, *Phys. Chem. Chem. Phys.*, 2015, **17**, 6501.

[14] C. Caltagirone, M. Arca, A. M. Falchi, V. Lippolis, V. Meli, M. Monduzzi, T. Nylander, A. Rosa, J. Schmidt, Y. Talmon and S. Murgia, *RSC Adv.*, 2015, **5**, 23443.

[7] W. Wu, H. Guo, W. Wu, S. Ji and J. Zhao, *J. Org. Chem.*, 2011, **76**, 7056.